Award Number: W81XWH-15-1-0565

TITLE: Therapeutic Strategies against Cyclin E1-Amplified Ovarian Cancers

PRINCIPAL INVESTIGATOR: Rugang Zhang, Ph.D.

CONTRACTING ORGANIZATION: The Wistar Institute of Anatomy & Biology
Philadelphia, PA 19104

REPORT DATE: October 2016

TYPE OF REPORT: Annual

PREPARED FOR: U.S. Army Medical Research and Materiel Command
Fort Detrick, Maryland 21702-5012

REPORT DOCUMENTATION PAGE

Form Approved
OMB No. 0704-0188

1. REPORT DATE	2. REPORT TYPE	3. DATES COVERED
October 2016	Annual	30 Sep 2015 - 29 Sep 2016

4. TITLE AND SUBTITLE

Therapeutic Strategies against Cyclin E1-Amplified Ovarian Cancers

5a. CONTRACT NUMBER

5b. GRANT NUMBER
W81XWH-15-1-0565

5c. PROGRAM ELEMENT NUMBER

6. AUTHOR(S)
Rugang Zhang

E-Mail: rzhang@wistar.org

5d. PROJECT NUMBER

5e. TASK NUMBER

5f. WORK UNIT NUMBER

7. PERFORMING ORGANIZATION NAME(S) AND ADDRESS(ES)

The Wistar Institute of Anatomy & Biology
3601 Spruce Street Philadelphia, PA 19104-4265

8. PERFORMING ORGANIZATION REPORT NUMBER

9. SPONSORING / MONITORING AGENCY NAME(S) AND ADDRESS(ES)

U.S. Army Medical Research and Materiel Command
Fort Detrick, Maryland 21702-5012

10. SPONSOR/MONITOR'S ACRONYM(S)

11. SPONSOR/MONITOR'S REPORT NUMBER(S)

12. DISTRIBUTION / AVAILABILITY STATEMENT

Approved for Public Release; Distribution Unlimited

13. SUPPLEMENTARY NOTES

14. ABSTRACT

For Aim 1, we demonstrated 1)The HSP90-inhibitors 17-AAG and AT13387 has single agent activity against CCNE1-amplified cell lines; 2)HSP90-inhibition downregulates homologous recombination (HR) DNA repair and downregulates expression of HR pathway genes; 3)The HSP90-inhibitor AT13387 synergizes with platinum against CCNE1-amplified cell lines.
For Aim 2, we demonstrated 1)FOXM1 is necessary for the survival of CCNE1 amplified epithelial ovarian cancer cells. 2)FOXM1 interacts with Rb in CCNE1 amplified epithelial ovarian cancer cells. 3)Characterized small molecule inhibitor that disrupts the interaction between FOXM1 and Rb in CCNE1 amplified epithelial ovarian cancer cells.
For Aim 3, we demonstrated 1) Certain miRNAs including miR-1255b, miR-148b*, and miR-193b* inhibit HR DNA repair 2) These miRNAs synergize with platinum against CCNE1-amplified cell lines, that is expression of these miRNAs sensitizes cells to platinum.

15. SUBJECT TERMS
Epithelial Ovarian Cancer, CCNE1 amplification, Homologous Recombination DNA Repair, Platinum analogues, MicroRNAs, Heat shock protein 90 (HSP90) inhibitors, Forkhead box protein M1 (FOXM1), Retinoblastoma (RB), Poly-ADP Ribose Polymerase Inhibitors (PARP-inhibitors)

16. SECURITY CLASSIFICATION OF:			17. LIMITATION OF ABSTRACT	18. NUMBER OF PAGES	19a. NAME OF RESPONSIBLE PERSON
a. REPORT	b. ABSTRACT	c. THIS PAGE			19b. TELEPHONE NUMBER *(include area code)*
U	U	U	UU	103	USAMRMC

Table of Contents

Page

1. INTRODUCTION:

Approximately 20% of high grade serous ovarian cancers harbor Cyclin E1 (CCNE1) amplification and are associated with poor outcome and inferior responsiveness to standard platinum chemotherapy. Given their intrinsic resistance to platinum, management of CCNE1-amplified ovarian cancers is challenging. In this research, we evaluate three novel strategies against CCNE1-amplified ovarian cancers that address different aspects of CCNE1 biology. In the first aim, based on our preliminary data, we hypothesize that HSP90-inhibitors may be effective against CCNE1-amplified ovarian tumors because they suppress HR, downregulate BRCA1, and downregulate CCNE1. In the second aim, based on our preliminary data and the fact that RB functions downstream of cyclin E, we hypothesize that inhibition of FOXM1 and RB interaction is an effective approach for targeting CCNE1-amplified ovarian tumors. Specifically, suppression of FOXM1/RB interaction will lead to enhancement of RB/E2F interaction and suppression of E2F-dependent oncogenic activity resulting in activity against CCNE1-amplified cells. In the third aim, we hypothesize that miR-1255b, miR-148b*, and miR-193b* may be effective against CCNE1-amplified ovarian tumors in combination with platinum and PARPis. Potential mechanisms for this effect include suppression of HR and downregulation of BRCA1, RAD51 and BRCA2 that are relevant for CCNE1-amplified ovarian tumors which are dependent on hyperactive HR and are sensitive to suppression of BRCA1.

2. KEYWORDS:

Epithelial Ovarian Cancer, CCNE1 amplification, Homologous Recombination DNA Repair, Platinum analogues, MicroRNAs, Heat shock protein 90 (HSP90) inhibitors, Forkhead box protein M1 (FOXM1), Retinoblastoma (RB), Poly-ADP Ribose Polymerase Inhibitors (PARP-inhibitors)

3. ACCOMPLISHMENTS:

What were the major goals and objectives of the project?

The major goal for Aim 1 is to determine the activity of HSP90 inhibitors in CCNE1-amplified ovarian tumors.

The major goal for Aim 2 is to inhibit FOXM1 and RB interaction to suppress CCNE1-amplified ovarian tumors.

The major goal for Aim 3 is to determine the activity of certain miRNA mimics in combination with PARP-inhibitors or platinum against CCNE1-amplified ovarian tumors.

What was accomplished under these goals?

Since the starting of the award, substantial progress has been made toward achieving the goals as outline in the application.

For AIM 1:

During the first year of the award we were able to achieve the following goals:

1) The HSP90-inhibitor 17-AAG has single agent activity against a number of CCNE1-amplified cell lines

As proposed in Aim 1, we evaluated the activity of HSP90-inhibitor 17-AAG in various CCNE1-amplified ovarian cancer lines (1), including OVCAR3, COV318 and in the OVCAR4 cell line which harbors CCNE1 overexpression. To that end, cells were plated at 1000 cells per well on a 96- well plate in sextuplicate and treated with 17-AAG at indicated concentrations on the next day. After 5 days, cell viability was quantified by Celltiter Glo.

As shown in Figure 1A, we noted significant activity of 17-AAG in OVCAR3 and OVCAR4 cell lines with IC50 of 0.07 and 0.08uM respectively. 17-AAG was also active in COV381 with an IC50 of 0.14uM, albeit less than OVCAR3 and OVCAR4. This is consistent with our hypothesis that HSP90 inhibitors may have good single agent activity against CCNE1 amplified and overexpressing lines.

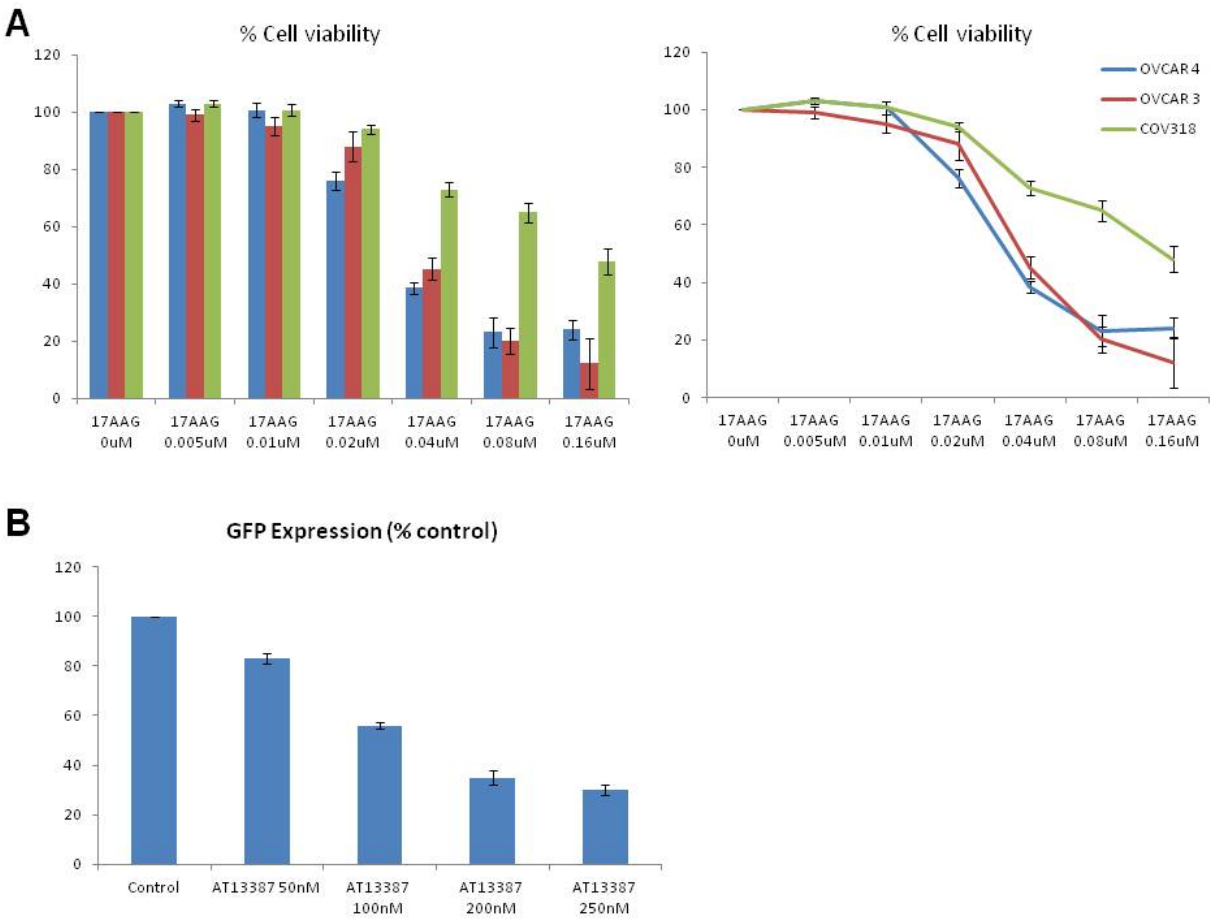

Figure 1. **A)** Activity of 17-AAG in OVCAR3, COV318 CCNE1 amplified and OVCAR4 CCNE1 overexpressing ovarian cancer lines. **B)** HSP90 inhibitor AT13387 suppresses HR as assessed by the Direct Repeat-GFP (DR-GFP) reporter assay.

The inferior activity may be related to inherent resistance to 17-AAG which may relate to mutations in HSP90 that affects the interaction with 17-AAG or overexpression of drug efflux pump MDR1 or elevated baseline HSP70 levels. We are currently assessing whether these mechanisms may contribute to this differential sensitivity of CCNE1-amplified lines to 17-AAG.

2) HSP90-inhibition downregulates homologous recombination (HR) DNA repair

One of our hypothesis of how HSP90 may have activity against CCNE1 amplified cells is based on the fact that CCNE1 amplified cells are hyperdependent on an intact HR (2). Therefore, by downregulating HR, HSP90 inhibitors may induce lethality in CCNE1 amplified cells. In this regard, during this funding period, we assessed whether the HSP90 inhibitor AT13387 suppresses HR using the Direct Repeat-GFP (DR-GFP) reporter assay (3).

In this assay, there is measurement of HR-mediated repair of an I-SceI induced site specific DSB. Specifically, 0.1 X 106 U2OS cells carrying DR-GFP reporter were plated on a 12-well plate overnight, treated with 17 AAG at indicated concentrations for 24 hrs, and transfected with 500 ng of I-SceI expression plasmid or control vector using Lipofectamine 2000. After 48 h, GFP-positive cells were assayed by FACScan.

As shown in Figure 1B, increasing concentrations of AT13387 reduced the efficacy of HR DNA repair by approximately 70%, down to plateau of 30%. This is also being confirmed using the RAD51 foci formation after ionizing radiation (IR) assay.

3) <u>The HSP90-inhibitor AT13387 synergizes with DNA damage inducing agents such as PARP-inhibitors against CCNE1-amplified cell lines</u>

One of the key goals of Aim 1 was to also assess the activity of HSP90 inhibitors in combination with platinum and PARP inhibitors in CCNE1-amplified cell lines. During this funding period we assessed the combination of the novel PARP inhibitor BMN673 (talazoparib) (4) in combination with the HSP90 inhibitor AT13387.

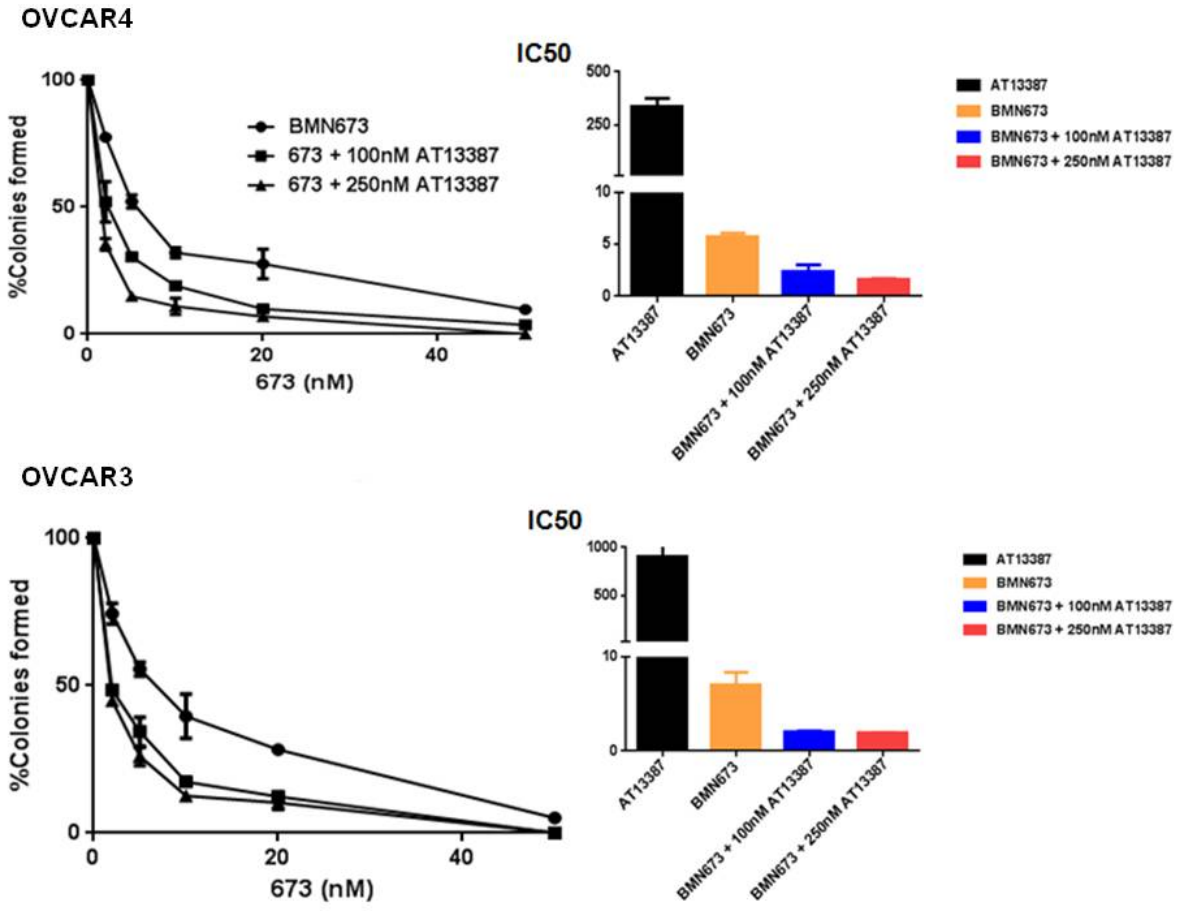

Figure 2. In vitro synergism between HSP90 inhibitor AT13387 and the PARP inhibitor BMN673 in OVCAR4 and OVCAR3.

We have now assessed the combination talazoparib and AT13387 in OVCAR4 and OVCAR3 which exhibit CCNE1 overexpression and amplification respectively using colony formation assay. Cells were treated with the indicated (Figure 2) BMN673 and AT13387 concentrations. As shown in Figure 2, in both cell lines, addition of small concentrations of AT13387 enhanced the cytotoxicity of BMN673, indicating synergism between BMN673 and AT13387. We plan to assess other PARPis as well, including olaparib.

For AIM 2:

The retinoblastoma protein (RB) is a tumor suppressor that functions downstream of cyclin E1 (encoded by the *CCNE1* gene) to regulate cell cycle, apoptosis and differentiation through its direct binding to and inhibition of the E2F transcription factor (5, 6). Disruption of RB and E2F interaction by viral oncogenic proteins such as HPV-E7 leads to neoplastic transformation (7). HPV-E7 inhibits RB function through a conserved LxCxE motif for high affinity RB binding (7, 8). Although RB pathway including its upstream regulator cyclin E is often deregulated in EOC (9), genetic alterations of the RB gene itself are relative rare in EOC (10-12). Notably, RB physically interacts with FOXM1 (13, 14), a transcription factor with oncogenic activity in EOC (9). Interestingly, the FOXM1 transcriptional network is significantly upregulated in EOC as well (9). Thus, we sought to determine whether the interaction between RB and FOXM1 can be targeted in EOC. Since RB functions downstream of cyclin E, we expect that this approach will be especially effective in *CCNE1* amplified EOCs.

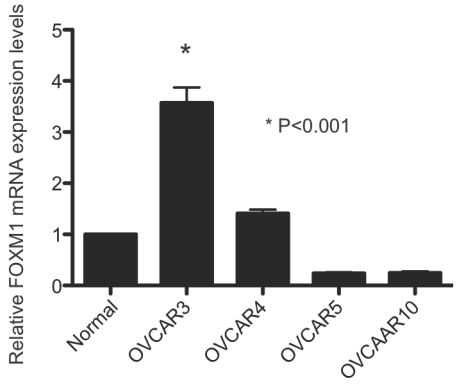

Figure 3. Expression of FOXM1 mRNA in a panel of EOC cell lines and normal fallopian tube epithelial cells determined by qRT-PCR.

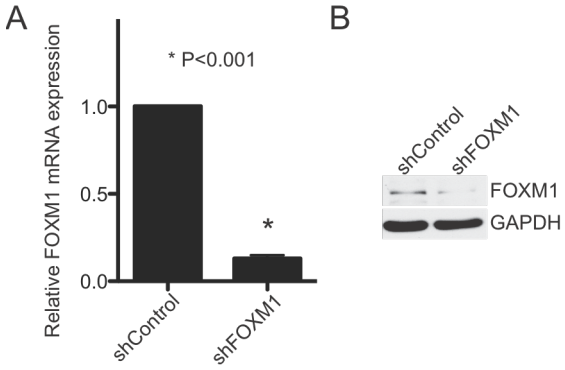

Figure 4. shRNA mediated knockdown of FOXM1 in OVCAR3 cells. Expression of FOXM1 in OVCAR3 expressing shFOXM1 or controls was determined by qRT-PCR (A) or immunoblotting (B).

Toward this goal, we first examined the expression of *FOXM1* mRNA in a panel of EOC cell lines by qRT-PCR. We used normal fallopian tube epithelial cells as a control. Notably, OVCAR3, a cell lines with known CCNE1 amplification showed the highest levels of FOXM1 expression (**Figure 3**). Thus, we used OVCAR3 cells to perform the subsequent functional studies. To determine the role of FOXM1 in OVCAR3 cells, we

developed a shRNA targeting the human FOXM1 gene. We validated the knockdown efficiency fo shFOXM1 by both qRT-PCR and immunoblotting (**Figure 4**).
Supporting the notion FOXM1 is required for the proliferation of CCNE1 amplified EOC cells. FOXM1 knockdown significantly suppressed the growth of OVCAR3 cells as determined by both cell growth curve and colony formation assays (**Figure 5**).

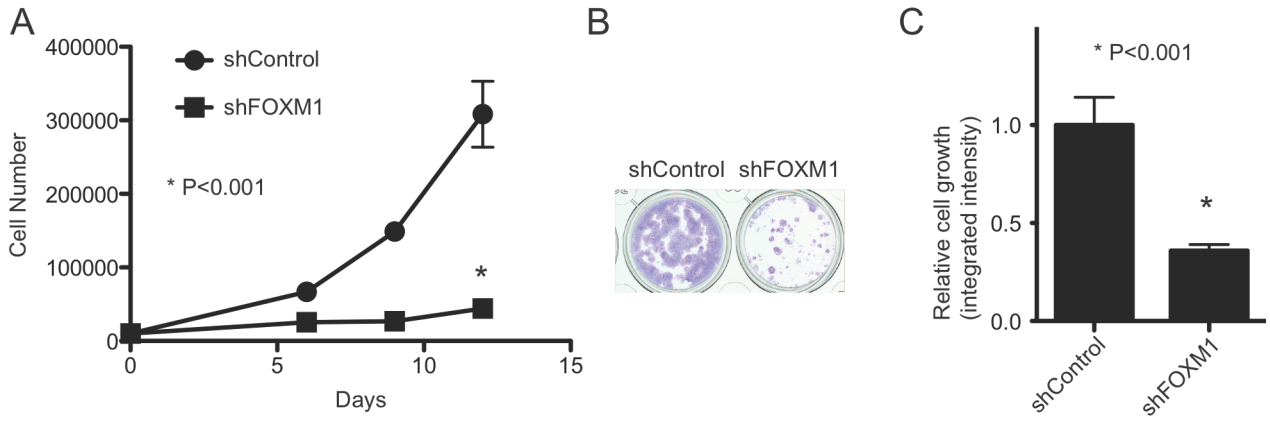

Figure 5. FOXM1 knockdown suppresses the growth of OVCAR3 cells. (A) Growth curves of OVCAR3 cells expressing shFOXM1 or controls. Mean of three independent experiments with SD. (B) Same as (A) but for colony formation assay. (C) Quantification of (B). Mean of three independent experiments with SD.

The binding between FOXM1 and RB depends upon a LxCxE motif on FOXM1 (13, 14). Notably, a class of thiadiazolidinedione compounds have previously been identified that disrupt the LxCxE motif mediated interaction between HPV-E7 and RB (15). These compounds are selectively cytotoxic in HPV-positive cells *in intro* and *in vivo* in mouse models (15). The observed effects correlate with its ability to suppress the disruption of RB/E2F complex by HPV-E7. This leads to a restoration of RB/E2F interaction and suppression of E2F dependent oncogenic activity. Since FOXM1's interaction with RB is also dependent upon the LxCxE motif (7, 8), we examined the effects of the RB/HPV-E7 disruption compound 478166 (or inhibitor 478726) on the interaction between FOXM1 and RB in EOC cells. In *CCNE1* amplified NIH-OVCAR3 cells (16), the interaction between FOXM1 and RB is readily detectable (**Figure 6A**). Co-immunoprecipitation analysis revealed that the interaction between FOXM1 and RB is substantially suppressed by inhibitor 478726

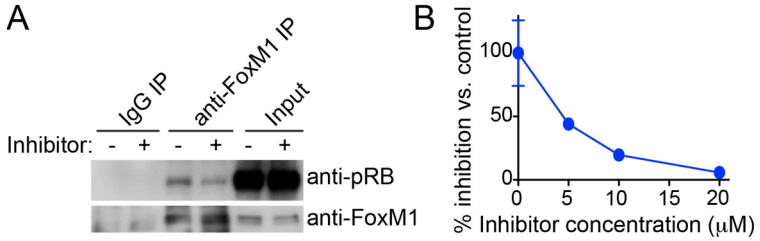

Figure 6. An inhibitor of FOXM1 and RB interaction that inhibits the growth of CCNE1 amplified NIH-OVCAR3 EOC cells. A) CCNE1 amplified NIH –OVCAR3 cells were treated with 5 mM inhibitor 478726 or control inactive compound 77333 for 48 h. The indicated cells were used for co-immunoprecipitation assay using an anti-FOXM1 antibody or a control IgG. The IPed product were examined by immunoblotting using the indicated antibodies. B) Same as A) but examined cell growth using the indicated concentration of inhibitor or control compound for 72 hours. Curves represent cell numbers normalized to control treatment.

(**Figure 6A**). Since the disruption of interaction between HPV-E7 and RB by the inhibitor leads to cell growth arrest in HPV positive human cancer cells (15), we examined whether disruption of FOXM1 and RB also inhibits the growth of *CCNE1* amplified NIH-OVCAR3 cells. Indeed, we observed a dose dependent suppression of cell growth by the inhibitor 478726 in these cells (**Figure 6B**). In summary, our preliminary data identified a small molecule inhibitor that can disrupt the interaction between FOXM1 and RB, which correlates with a dose-dependent growth inhibition in *CCNE1* amplified EOC cells.

In summary, we have demonstrated in Aim 2:

1) FOXM1 is necessary for the proliferation of CCNE1 amplified epithelial ovarian cancer cells.
2) FOXM1 interacts with Rb in CCNE1 amplified epithelial ovarian cancer cells.
3) Characterized small molecule inhibitor that disrupts the interaction between FOXM1 and Rb in CCNE1 amplified epithelial ovarian cancer cells.

For AIM 3:

During the first year of the award we were able to achieve the following goals:

1) Certain miRNAs including miR-1255b, miR-148b*, and miR-193b* inhibit HR DNA repair

As proposed in Aim 3, we evaluated whether certain miRNAs may inhibit HR repair in CCNE1 amplified cell lines. To achieve this we assessed the effects of miRNA mimics for miR-1255b, miR-148b*, and miR-193b* and miR-182 in CCNE1 amplified OVCAR3 cells using the RAD51 foci formation after ionizing radiation (IR) assay. Specifically, OVCAR3 cells were transfected with control miRNA mimic and the indicated (Figure 7) miRNA mimics stained for RAD51 (green) and 4′,6-diamidino-2-phenylindole (DAPI) (blue) 6 h after exposure to IR. The images were captured by fluorescence microscopy and RAD51 focus-positive cells (with > 5 foci) were quantified by comparing 100 cells.

As shown in Figure 7, treatment with miRNA mimics for miR-1255b, miR-148b*, and miR-193b* and miR-182, significantly reduced RAD51 foci formation after IR compared to control miRNA mimic, suggesting that these miRNA mimics can indeed inhibit HR repair in these CCNE1 amplified cells.

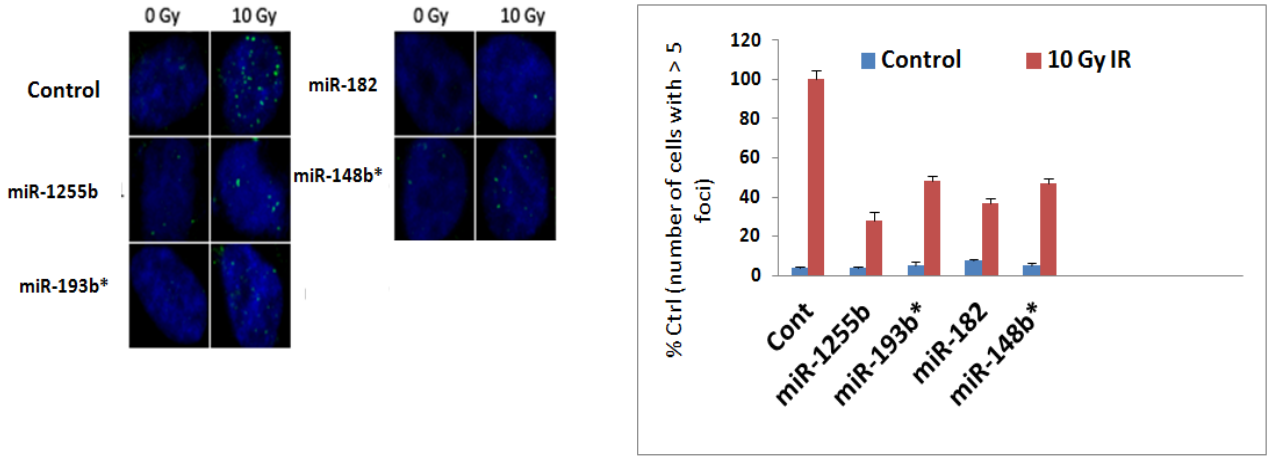

Figure 7. miRNA mimics for miR-1255b, miR-148b*, and miR-193b* and miR-182 inhibit HR repair in CCNE1 amplified OVCAR3 cells

2) These miRNAs synergize with platinum and PARP-inhibitors against CCNE1-amplified cell lines, that is expression of these miRNAs sensitizes CCNE1-amplified cells to platinum and PARP-inhibitors.

Another important goal of Aim 3, was to assess whether these miRNAs may synergize with platinum and PARPis in CCNE1-amplified cells.
To achieve this, luminescence based viability assay was performed in OVCAR3 and OVCAR4 ovarian cells. Cells were transfected with control miRNA, miRNA mimics for miR-1255b, miR-148b* and miR-193b* or BRCA1 siRNA (positive control). All cells were concomitantly treated with 1μM PARP inhibitor AZD2281 (Olaparib) and increasing concentrations of cisplatin for 5-6 days before ATP quantification.

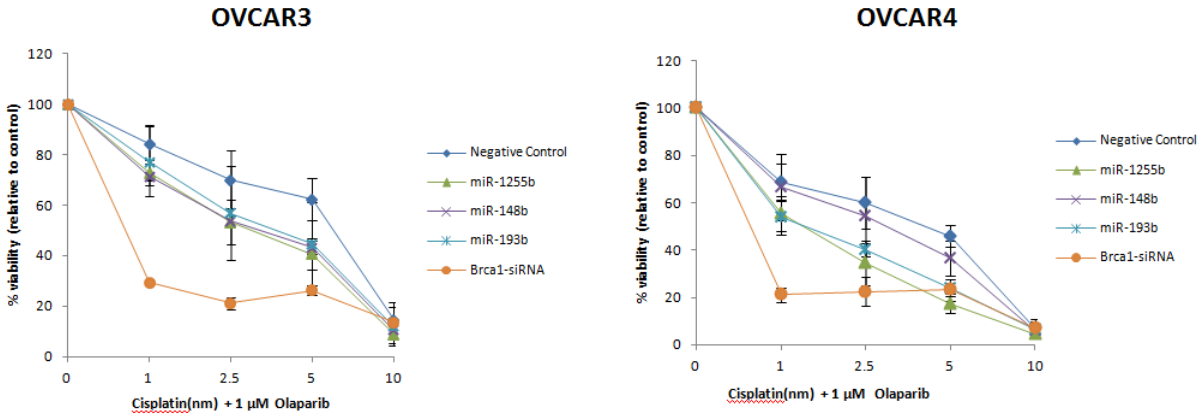

Figure 8. miRNA mimics for miR-1255b, miR-148b* and miR-193b* enhance cytotoxicity to cisplatin and olaparib.

As shown in Figure 8, miRNA mimics for miR-1255b, miR-148b* and miR-193b* enhanced sensitivity to cisplatin and olaparib, more than the negative control and less

than the positive control BRCA1 siRNA. These findings, together with our finding that these miRNA mimics inhibit HR in CCNE1 amplified cells, support our hypothesis and suggest a novel strategy for targeting CCNE1 amplified tumors. In the next funding period, we plan to perform studies of miRNA mimics with additional PARP-inhibitors and platinum agents, either alone or in combination, in CCNE1-amplified ovarian cancer cells.

REFERENCES

1. Domcke S, Sinha R, Levine DA, Sander C, Schultz N. Evaluating cell lines as tumour models by comparison of genomic profiles. Nat Commun. 2013;4:2126.
2. Etemadmoghadam D, Weir BA, Au-Yeung G, Alsop K, Mitchell G, George J, et al. Synthetic lethality between CCNE1 amplification and loss of BRCA1. Proc Natl Acad Sci U S A. 2013 Nov 26;110(48):19489-94.
3. Weinstock DM, Nakanishi K, Helgadottir HR, Jasin M. Assaying double-strand break repair pathway choice in mammalian cells using a targeted endonuclease or the RAG recombinase. Methods Enzymol. 2006;409:524-40.
4. Liu JF, Konstantinopoulos PA, Matulonis UA. PARP inhibitors in ovarian cancer: current status and future promise. Gynecol Oncol. 2014 May;133(2):362-9.
5. Harbour JW, Dean DC. The Rb/E2F pathway: expanding roles and emerging paradigms. Genes & development. 2000 Oct 1;14(19):2393-409.
6. Stevaux O, Dyson NJ. A revised picture of the E2F transcriptional network and RB function. Current opinion in cell biology. 2002 Dec;14(6):684-91.
7. Felsani A, Mileo AM, Paggi MG. Retinoblastoma family proteins as key targets of the small DNA virus oncoproteins. Oncogene. 2006 Aug 28;25(38):5277-85.
8. Lee JO, Russo AA, Pavletich NP. Structure of the retinoblastoma tumour-suppressor pocket domain bound to a peptide from HPV E7. Nature. 1998 Feb 26;391(6670):859-65.
9. Cancer Genome Atlas Research N. Integrated genomic analyses of ovarian carcinoma. Nature. 2011 Jun 30;474(7353):609-15.
10. Dodson MK, Cliby WA, Xu HJ, DeLacey KA, Hu SX, Keeney GL, et al. Evidence of functional RB protein in epithelial ovarian carcinomas despite loss of heterozygosity at the RB locus. Cancer research. 1994 Feb 1;54(3):610-3.
11. Hashiguchi Y, Tsuda H, Yamamoto K, Inoue T, Ishiko O, Ogita S. Combined analysis of p53 and RB pathways in epithelial ovarian cancer. Hum Pathol. 2001 Sep;32(9):988-96.
12. Kim TM, Benedict WF, Xu HJ, Hu SX, Gosewehr J, Velicescu M, et al. Loss of heterozygosity on chromosome 13 is common only in the biologically more aggressive subtypes of ovarian epithelial tumors and is associated with normal retinoblastoma gene expression. Cancer research. 1994 Feb 1;54(3):605-9.
13. Wierstra I, Alves J. Transcription factor FOXM1c is repressed by RB and activated by cyclin D1/Cdk4. Biological chemistry. 2006 Jul;387(7):949-62.
14. Major ML, Lepe R, Costa RH. Forkhead box M1B transcriptional activity requires binding of Cdk-cyclin complexes for phosphorylation-dependent recruitment of p300/CBP coactivators. Molecular and cellular biology. 2004 Apr;24(7):2649-61.

15. Fera D, Schultz DC, Hodawadekar S, Reichman M, Donover PS, Melvin J, et al. Identification and characterization of small molecule antagonists of pRb inactivation by viral oncoproteins. Chemistry & biology. 2012 Apr 20;19(4):518-28.
16. Etemadmoghadam D, Weir BA, Au-Yeung G, Alsop K, Mitchell G, George J, et al. Synthetic lethality between CCNE1 amplification and loss of BRCA1. Proceedings of the National Academy of Sciences of the United States of America. 2013 Nov 26;110(48):19489-94.

What opportunities for training and professional development did the project provide?

"Nothing to Report."

How were the results disseminated to communities of interest?

"Nothing to Report."

What do you plan to do during the next reporting period to accomplish the goals and objectives?

In the next reporting period:

For Aim 1, we plan to perform synergism studies of HSP90-inhibitors with additional PARP-inhibitors and with platinum agents in CCNE1-amplified ovarian cancer cells. We also intend to initiate tolerability studies of these agents in patient-derived xenografts (PDX) models of CCNE1-amplified ovarian cancer.
For Aim 2, we plan to accomplish whether and how the inhibitor of FOXM1 and RB interaction affects the growth of CCNE1-amplified epithelial ovarian cancer cells.
For Aim 3, we plan to perform synergism studies of miRNA mimics with additional PARP-inhibitors and platinum agents in CCNE1-amplified ovarian cancer cells. We also intend to evaluate possible targets of these miRNAs which explain their action of suppressing HR DNA repair.

4. IMPACT:

"Nothing to Report."

What was the impact on the development of the principal discipline(s) of the project?

"Nothing to Report."

What was the impact on other disciplines?

"Nothing to Report."

What was the impact on technology transfer?

"Nothing to Report."

What was the impact on society beyond science and technology?

"Nothing to Report."

5. CHANGES/PROBLEMS:

"Nothing to Report."

Changes in approach and reasons for change

"Nothing to Report."

Actual or anticipated problems or delays and actions or plans to resolve them

"Nothing to Report."

Changes that had a significant impact on expenditures

"Nothing to Report."

Significant changes in use or care of human subjects, vertebrate animals, biohazards, and/or select agents

"Nothing to Report."

6. PRODUCTS:

Identify for each publication: Author(s); title; journal; volume: year; page numbers; status of publication (published; accepted, awaiting publication; submitted, under review; other); acknowledgement of federal support (yes/no).

1. Zhu H, Bengsch F, Svoronons N, Rutkowski MR, Bitler BG, Allegrezza MJ, Yokoyama Y, Bradner JE, Conejo-Garcia JR, **Zhang R**. BET bromodomain inhibition promotes anti-tumor immunity by suppressing PD-L1 expression. **Cell Reports**, 16:2829-37, 2016.
2. Yokoyama Y, Zhu H, Lee JH, Kossenkov AV, Wu S, Wickramasinghe JM, Yin X, Palozola KC, Gardini A, Showe LC, Zaret KS, Liu Q, Speicher D, Conejo-Garcia JR, Bradner JE, Zhang Z, Sood AK, Ordog T, Bitler BG, **Zhang R**. BET inhibitors suppress ALDH activity by targeting ALDH1A1 super-enhancer in ovarian cancer. **Cancer Research**, in press
3. **Konstantinopoulos PA**, Ceccaldi R, Shapiro GI, D'Andrea AD. Homologous Recombination Deficiency: Exploiting the Fundamental Vulnerability of Ovarian Cancer. (2015) Cancer Discovery 5(11):1137-54.
4. Strickland KC, Howitt BE, Shukla SA, Rodig S, Ritterhouse LL, Liu JF, Garber JE, **Chowdhury D**, Wu CJ, D'Andrea AD, Matulonis UA, **Konstantinopoulos PA**. Association and prognostic significance of BRCA1/2-mutation status with neoantigen load, number of tumor-infiltrating lymphocytes and expression of PD-1/PD-L1 in high grade serous ovarian cancer. (2016) Oncotarget 22;7(12):13587-98.
5. Choi YE, Meghani K, Brault ME, Leclerc L, He YJ, Day TA, Elias KM, Drapkin R, Weinstock DM, Dao F, Shih KK, Matulonis U, Levine DA, **Konstantinopoulos PA, Chowdhury D**. Platinum and PARP Inhibitor Resistance Due to Overexpression of MicroRNA-622 in BRCA1-Mutant Ovarian Cancer. (2016) Cell Reports 14(3):429-39.

Books or other non-periodical, one-time publications.

"Nothing to Report."

Other publications, conference papers, and presentations.

"Nothing to Report."

- **Website(s) or other Internet site(s)**

"Nothing to Report."

- **Technologies or techniques**

"Nothing to Report."

- **Inventions, patent applications, and/or licenses**

"Nothing to Report."

- **Other Products**

"Nothing to Report."

7. PARTICIPANTS & OTHER COLLABORATING ORGANIZATIONS:

What individuals have worked on the project?

Name:	*Rugang Zhang*
Project Role:	*Principal Investigator*
Researcher Identifier (e.g. ORCID ID):	N/A
Nearest person month worked:	1
Contribution to Project:	Supervised the study.
Funding Support:	This award

Name:	*Sergey Karakashev*
Project Role:	*Postdoctoral Fellow*
Researcher Identifier (e.g. ORCID ID):	N/A
Nearest person month worked:	*5*
Contribution to Project:	Performed the study.
Funding Support:	This award

Has there been a change in the active other support of the PD/PI(s) or senior/key personnel since the last reporting period?

"Nothing to Report."

What other organizations were involved as partners?

"Nothing to Report."

8. SPECIAL REPORTING REQUIREMENTS: None

9. APPENDICES:

Cell Reports

Report

BET Bromodomain Inhibition Promotes Anti-tumor Immunity by Suppressing PD-L1 Expression

Graphical Abstract

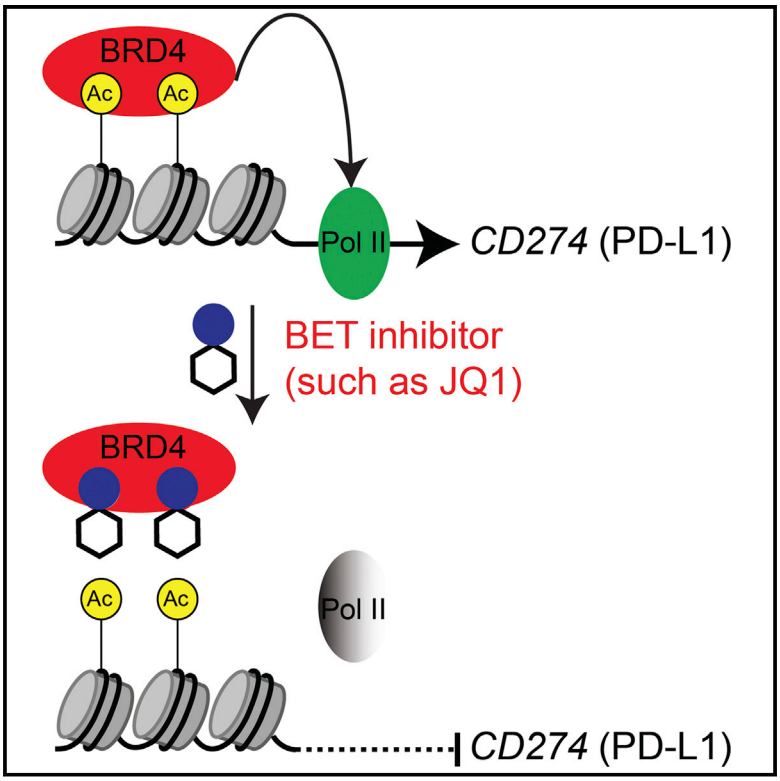

Authors

Hengrui Zhu, Fee Bengsch, Nikolaos Svoronos, ..., James E. Bradner, Jose R. Conejo-Garcia, Rugang Zhang

Correspondence

jrconejo@wistar.org (J.R.C.-G.), rzhang@wistar.org (R.Z.)

In Brief

Zhu et al. find that BET bromodomain inhibition suppresses PD-L1 expression and limits tumor progression in ovarian cancer in mice. *CD274* (encoding PD-L1) is a direct target of BRD4-mediated gene transcription. Together, these data suggest a small-molecule approach to blocking PD-L1 signaling.

Highlights

- BET inhibitors suppress PD-L1 expression in both immune cells and tumor cells
- *CD274* is a direct target gene of BRD4
- BET inhibitors increase cytotoxic T cell activity to limit tumor progression in mice

Accession Numbers

GSE81698

Zhu et al., 2016, Cell Reports *16*, 2829–2837
September 13, 2016
http://dx.doi.org/10.1016/j.celrep.2016.08.032

CellPress

Cell Reports
Report

BET Bromodomain Inhibition Promotes Anti-tumor Immunity by Suppressing PD-L1 Expression

Hengrui Zhu,[1] Fee Bengsch,[1] Nikolaos Svoronos,[2] Melanie R. Rutkowski,[2] Benjamin G. Bitler,[1] Michael J. Allegrezza,[2] Yuhki Yokoyama,[1] Andrew V. Kossenkov,[3] James E. Bradner,[4] Jose R. Conejo-Garcia,[2,*] and Rugang Zhang[1,5,*]
[1]Gene Expression and Regulation Program
[2]Tumor Microenvironment and Metastasis Program
[3]Center for Systems and Computational Biology
The Wistar Institute, Philadelphia, PA 19104, USA
[4]Dana-Farber Cancer Institute, Harvard Medical School, Boston, MA 02215, USA
[5]Lead Contact
*Correspondence: jrconejo@wistar.org (J.R.C.-G.), rzhang@wistar.org (R.Z.)
http://dx.doi.org/10.1016/j.celrep.2016.08.032

SUMMARY

Restoration of anti-tumor immunity by blocking PD-L1 signaling through the use of antibodies has proven to be beneficial in cancer therapy. Here, we show that BET bromodomain inhibition suppresses PD-L1 expression and limits tumor progression in ovarian cancer. *CD274* (encoding PD-L1) is a direct target of BRD4-mediated gene transcription. In mouse models, treatment with the BET inhibitor JQ1 significantly reduced PD-L1 expression on tumor cells and tumor-associated dendritic cells and macrophages, which correlated with an increase in the activity of anti-tumor cytotoxic T cells. The BET inhibitor limited tumor progression in a cytotoxic T-cell-dependent manner. Together, these data demonstrate a small-molecule approach to block PD-L1 signaling. Given the fact that BET inhibitors have been proven to be safe with manageable reversible toxicity in clinical trials, our findings indicate that pharmacological BET inhibitors represent a treatment strategy for targeting PD-L1 expression.

INTRODUCTION

Tumors evade anti-tumor immunity by inhibitory pathways that regulate the function of T lymphocytes, known as immune checkpoints (Topalian et al., 2015). Programmed cell death (PD)-1 protein is predominantly expressed on the surface of T cells, while its ligands, such as PD-L1, are expressed on the surface of both cancer cells and immune cells (Zou et al., 2016). Interaction between PD-1 and PD-L1 inhibits T cell activity, which reduces T cell-mediated cytolysis. Therefore, inhibiting this interaction could result in increased anti-tumor immunity. Indeed, blockade of immune checkpoints by antibodies has demonstrated remarkable activity in several cancer types (Mahoney et al., 2015). For example, antibody-based blockage of PD-1 and PD-L1 signaling is therapeutically beneficial in an expanding list of malignancies (Zou et al., 2016). Despite these anti-tumor benefits, checkpoint blockade using these antibodies is associated with unique adverse effects known as immune-related adverse events (irAEs) due to nonspecific immunologic activation (Naidoo et al., 2015). Prolonged immunosuppression, often required to treat irAEs, predisposes patients to infections.

PD-L1 is associated with prognosis in several cancer types. PD-L1 expression predicts a better prognosis in ovarian cancer (Webb et al., 2016), which remains the most lethal gynecological malignancy in the developed world. Blockade of PD-1/PD-L1 signaling enhances the amplitude of anti-tumor immunity in ovarian cancer (Abiko et al., 2013; Cubillos-Ruiz et al., 2009). PD-L1 expression correlates with clinical response to anti-PD-1/L1 therapy (Zou et al., 2016). Despite the importance of PD-L1 in tumor immunity, the regulation of PD-L1 expression remains poorly understood. DNA hypomethylating agents such as azacytidine increase PD-L1 expression in non-small-cell lung cancer (Wrangle et al., 2013). This suggests that chromatin modifiers, including writers, readers, and erasers (i.e., epigenetic mechanisms), play a critical role in regulating PD-L1 expression. Whether agents that target epigenetic regulators could be used to inhibit PD-L1 signaling remains to be explored.

The bromodomain and extraterminal (BET) protein BRD4 directly binds to acetylated lysine on histone tails and other nuclear proteins to promote gene transcription by RNA polymerase II (Pol II) (Filippakopoulos and Knapp, 2014). Specific BET inhibitors have been developed. Clinical trials in hematopoietic malignancies have demonstrated the anti-tumor activity of BET inhibitors with a manageable toxicity prolife (Filippakopoulos and Knapp, 2014). Here, we show that inhibition of BRD4 suppresses PD-L1 expression and increases cytotoxic T cell activity to limit tumor progression in vivo in ovarian cancer models. Our findings establish an immune checkpoint targeting approach by repurposing existing pharmacological BET inhibitors.

RESULTS

BET Inhibitors Suppress PD-L1 Expression

Given the importance of targeting PD-L1 in anti-tumor immunity and the poorly understood nature of its regulation, we evaluated a panel of 24 small-molecule inhibitors known to target epigenetic regulators (obtained from The Structure Genomics Consortium) to

identify "hits" that suppress the expression of PD-L1. As upregulation of PD-L1 is known to play a critical role in ovarian cancer (Abiko et al., 2013), we focused on epithelial ovarian cancer (EOC) cell lines. To identify suitable cell models for the small-molecule screen, we examined PD-L1 expression in a panel of EOC cell lines: PEO1, OVCAR3, OVCAR10, PEO4, and Kuramochi. PEO1 and OVCAR3 cells express high levels of PD-L1 (Figures S1A and S1B) and were used for the screen. To limit the potential bias introduced by variation in growth inhibition induced by the small-molecule inhibitors, we established a growth inhibition curve for each small-molecule inhibitor. We used the established IC_{20} (inhibitory concentration 20%) value of each small-molecule inhibitor (Table S1). The highest dose tested (20 μM) was used for those inhibitors whose IC_{20} was not achieved (Figure 1A; Table S1). Using flow-cytometric (fluorescence-activated cell sorting; FACS) analysis, we measured the fold change in PD-L1 expression based on mean fluorescence intensity for each of the 24 inhibitors (Figure 1B). This analysis identified a list of five inhibitors that significantly suppressed PD-L1 expression in PEO1 cells. Similar analyses in OVCAR3 cells revealed a list of four inhibitors that significantly suppressed PD-L1 expression (Figure S1C). The top three "hits" for reducing PD-L1 expression in both cell lines are BET inhibitors: JQ1, Bromosporine, and PFI-1 (Figures 1B and S1C). Inhibition of PD-L1 was specific to BET inhibitors, but not bromodomain inhibitors in general, because other bromodomain inhibitors such as SGC-CBP30 did not significantly reduce PD-L1 expression (Figure 1C).

Interferon-gamma (IFNγ) induces PD-L1 expression. As a secondary screen, we determined the effects of the same panel of epigenetic inhibitors on PD-L1 expression in cells treated with IFNγ (Figure 1D). This screen revealed that only the same three BET inhibitors significantly suppressed PD-L1 expression in the presence of IFNγ stimulation (Figures 1D–1F). BET-inhibitor-induced suppression of PD-L1 was not due to changes in IFNγ secretion because EOC cell lines did not secrete detectable levels of IFNγ, and JQ1 did not affect the secretion of IFNγ (data not shown). Thus, we identified BET inhibitors as suppressors of PD-L1 expression.

BET Inhibition Reduces PD-L1 Expression at the Transcriptional Level in a Dose- and Time-Dependent Manner

As JQ1 is clinically applicable (known as TEN-010 in clinical trials), we performed further validation on this inhibitor. We demonstrated that JQ1 treatment decreased PD-L1 expression with or without IFNγ stimulation (Figures 2A and S2A). JQ1 reduced PD-L1 expression in a dose-dependent manner (Figure 2B). Similar dose-dependent suppression of PD-L1 expression was also observed in IFNγ-stimulated cells (Figure 2B). We also observed a time-dependent suppression of PD-L1 expression by JQ1, where suppression of PD-L1 expression was observed 24 hr post-treatment (Figures 2C and S2B). Notably, expression of *CD274*, the gene encoding PD-L1, was reduced in a dose- and time-dependent manner that mirrors PD-L1 downregulation induced by JQ1 (Figures 2D, 2E, and S2C). This indicates that suppression of PD-L1 expression by JQ1 occurs at the transcriptional level. Notably, JQ1 reduced PD-L1 expression at a dose (e.g., 20 nM) that did not affect the growth of treated cells (Figures S2D and S2E). This suggests that the observed reduction in PD-L1 expression is not a consequence of growth inhibition induced by JQ1 (Figures 2B and 2E; Figures S2D and S2E). Therefore, we conclude that JQ1 reduces PD-L1 expression at the transcriptional level in a dose- and time-dependent manner.

CD274 Is a Direct Target Gene of BRD4

BRD4 is often amplified in ovarian cancer and is a major target of JQ1 (Baratta et al., 2015; Goundiam et al., 2015). To determine whether genetic knockdown of BRD4 directly regulates PD-L1 expression, BRD4 was knocked down using three individual shRNAs (short hairpin RNAs), termed shBRD4s (Figures 3A and 3B). All three shBRD4s efficiently knocked down BRD4 expression and decreased PD-L1 expression (Figures 3A–3D). Similar results were observed in multiple EOC cell lines (Figures S3A–S3C). The observed decrease in PD-L1 expression was rescued by the expression of a shBRD4-resistant wild-type BRD4 (Figures 3E and 3F). In addition, BRD4 knockdown also reduced PD-L1 expression in IFNγ-stimulated cells (Figure 3G).

Next, we profiled the global changes in mRNA expression induced by JQ1 or shBRD4 in PEO1 cells by QuantSeq (GEO: GSE81698). Notably, *CD274* expression was downregulated ~4-fold by both JQ1 and shBRD4 in this analysis (Figure S3D). Pathway enrichment analysis on significantly changed genes revealed biological processes, including lymphocyte chemotaxis and inflammatory response (Table S2).

We next determined whether BRD4 correlates with PD-L1 expression in EOC. Using a panel of EOC cell lines, we observed a trend toward a positive correlation between BRD4 and PD-L1 expression (Figure 3H). We examined whether *BRD4* and *CD274* expression is positively correlated in EOC specimens. We used a published database that profiled gene expression in 53 cases of laser capture and microdissected (LCM) high-grade serous EOCs (Mok et al., 2009). Indeed, there was a significant, positive correlation between *BRD4* and *CD274* in EOCs (Figure 3I, $p < 0.0001$).

Next, we determined whether *CD274* is a direct target gene of BRD4. BRD4 chromatin immunoprecipitation (ChIP) followed by next-generation sequencing (ChIP-seq) in OVCAR3 cells revealed that BRD4 is enriched at the *CD274* gene promoter (Figure S3E). ChIP analysis showed a significant association of BRD4 with the *CD274* promoter, which was decreased with JQ1 treatment (Figures 3J and S3F). Notably, JQ1 treatment did not significantly reduce acetylated H3 levels at the *CD274* promoter (Figure 3K). The observed JQ1-mediated suppression of PD-L1 correlated with decreased association of RNA Pol II with the *CD274* promoter (Figure 3L). Next, we determined whether upregulation of PD-L1 expression by IFNγ correlates with increased association of BRD4 at the *CD274* promoter. Indeed, IFNγ treatment enhanced the association of BRD4 with the *CD274* promoter, which was reduced by JQ1 treatment (Figure 3M). This was not due to the upregulation of BRD4 by IFNγ, because we did not observe an increase in BRD4 protein expression in cells treated with IFNγ (Figure 3N). Together, these data support the notion that *CD274* is a direct target gene of BRD4, which is subject to JQ1-mediated repression at the transcriptional level (Figure 3O).

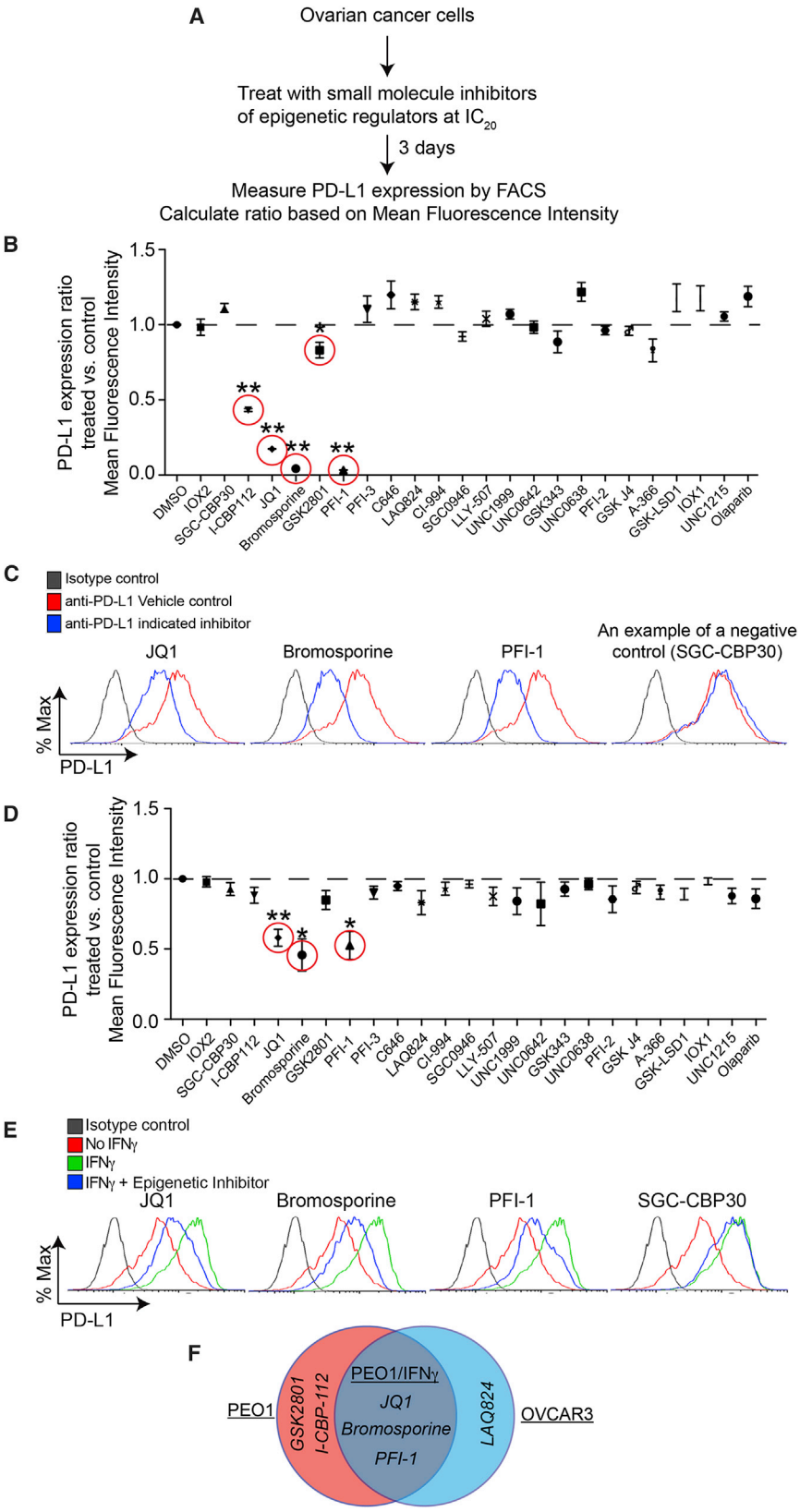

Figure 1. BET Inhibitors Suppress PD-L1 Expression in Ovarian Cancer Cells

(A) Flow diagram of experimental design.

(B) Plot of the ratio of PD-L1 expression on PEO1 cells treated with doses of the indicated epigenetic inhibitors or vehicle controls as detailed in Table S1. *$p < 0.04$; **$p < 0.0001$.

(C) Representative changes in PD-L1 expression determined by FACS on PEO1 cells treated with the indicated BET inhibitors. SGC-CBP30 was used as a negative control.

(D) Same as in (B) but for IFNγ-stimulated (20 ng/ml, 24 hr) PEO1 cells. *$p < 0.02$; **$p < 0.002$.

(E) Representative changes in PD-L1 expression determined by FACS on PEO1 cells stimulated with IFNγ (20 ng/ml, 24 hr) and treated with the indicated BET inhibitors. SGC-CBP30 was used as a negative control.

(F) Venn diagram of "hits" that suppress PD-L1 expression from the three indicated screens.

Error bars represent SEM of three independent experiments. See also Figure S1 and Table S1.

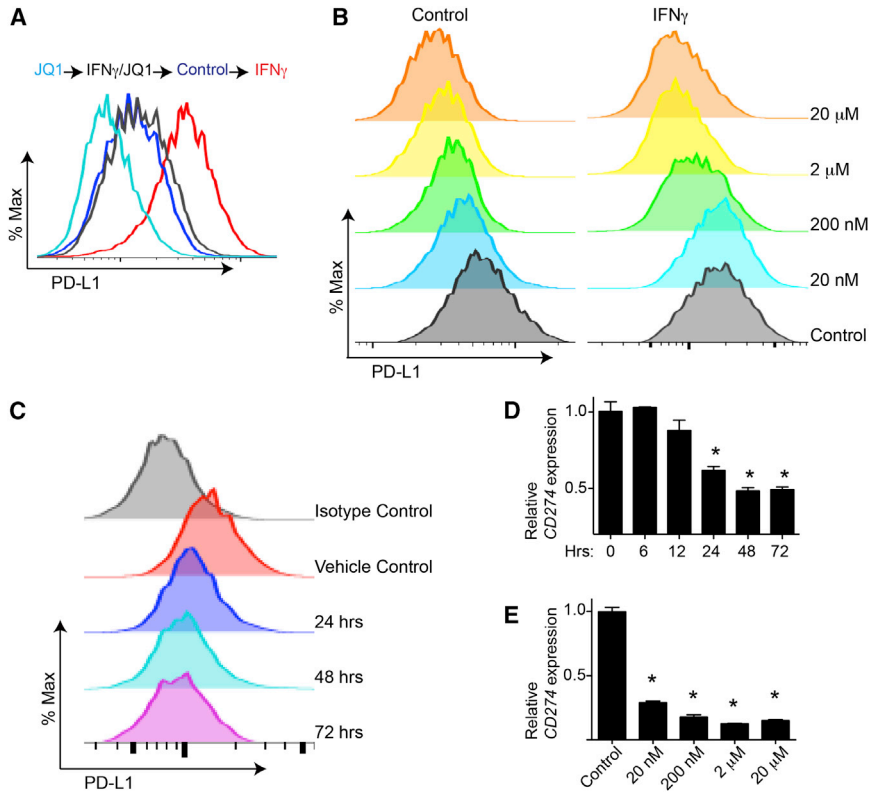

Figure 2. BET Inhibitor JQ1 Suppresses PD-L1 Expression at the Transcriptional Level

(A) PEO1 cells stimulated with or without IFNγ (20 ng/ml, 24 hr) were treated with or without 200 nM JQ1 for 72 hr. PD-L1 expression was determined by FACS.

(B) PEO1 cells with or without IFNγ (20 ng/ml, 24 hr) stimulation were treated with indicated doses of JQ1 for 72 hr. PD-L1 expression was determined by FACS.

(C) PEO1 cells were treated with 200 nM JQ1. PD-L1 expression was determined by FACS at the indicated time points.

(D) PEO1 cells were treated with 200 nM JQ1. mRNA expression of *CD274* (encoding PD-L1) was determined by qRT-PCR at the indicated time points. *$p < 0.05$.

(E) PEO1 cells were treated with the indicated doses of JQ1 for 72 hr, and *CD274* (encoding PD-L1) mRNA expression was determined by qRT-PCR. *$p < 0.05$.

Error bars represent SEM of three independent experiments. See also Figure S2.

The BET Inhibitor JQ1 Limits Tumor Progression in a Cytotoxic T Cell-Dependent Manner

Besides tumor cells, PD-L1 is expressed on tumor-associated immune cells, such as regulatory dendritic cells (DCs) and macrophages in ovarian cancer (Scarlett et al., 2012). Notably, PD-L1 expression on both DCs and macrophages and the tumor cells is important for evading anti-tumor immunity (Zou et al., 2016). Therefore, we determined that JQ1 decreased PD-L1 expression on mouse bone-marrow-derived DCs (BMDCs) (Figure S4A).

To determine the effects of BET inhibitors on PD-L1 expression and anti-tumor immunity in vivo, we utilized the ID8-*Defb29/Vegf-a* syngeneic mouse model. This model recapitulates the aggressive inflammatory microenvironment of human ovarian carcinomas, and PD-L1 signaling is critical for cancer progression in this model (Cubillos-Ruiz et al., 2009). For in vivo experiments, the injected mice were allowed to develop ascites for 7 days and treated with 50 mg/kg JQ1 or vehicle control twice weekly for 18 additional days (Figure 4A). PD-L1 expression on both immune and tumor cells from peritoneal washes was examined. Indeed, there was a significant decrease in PD-L1 expression on immune cells such as DCs and macrophages isolated from JQ1 treated mice compared with controls (Figures 4B and 4C). PD-L1 expression on the tumor cells was also significantly reduced by JQ1 treatment (Figures 4B and 4C). Notably, the observed JQ1-mediated reduction in PD-L1 expression on tumor cells was overcome by overexpressing *CD274* in tumor cells (Figures 4D and S4B). As a control, *CD274* overexpression in tumor cells did not affect the suppression of PD-L1 expression by JQ1 in DCs (Figure S4C). This indicates that the observed reduction in PD-L1 by JQ1 in vivo is due to its suppression of endogenous PD-L1 instead of an indirect effect. The dose of JQ1 used was significantly lower than those of previous studies (Filippakopoulos et al., 2010), which did not significantly reduce the percentage of $CD8^+$ cytotoxic T cells (Figures S4D and S4E). Therefore, we can achieve a dose of JQ1 that suppresses PD-L1 expression on both immune cells, such as DCs and macrophages, and tumor cells without affecting the survival of cytotoxic T cells.

Next, we determined the effects of JQ1 on $CD8^+$ cytotoxic T cell activity. We observed an increased number of tumor-associated T cells that secreted Granzyme B, as determined by enzyme-linked immunospot (ELISpot) analysis in JQ1-treated mice compared to controls (Figures 4E and 4F). Similar results were also obtained with an independent syngeneic mouse model using the UPK10 cell line (Figures S4G and S4H). Consistently, JQ1 treatment increased the percentage of IFNγ-producing $CD8^+$ cytotoxic T cells (Figures 4G and 4H). Together, these findings support the notion that JQ1 treatment suppresses PD-L1 expression on both immune and tumor cells in vivo and increases $CD8^+$ cytotoxic T activity.

We next determined the effects of JQ1 treatment on tumor growth in vivo. JQ1 significantly suppressed tumor growth in an orthotopic ID8-luciferase syngeneic mouse model (Figures 4I, 4J, and S4I). Significantly, the observed tumor-suppressive effects are $CD8^+$ T cell dependent because antibody-mediated depletion of $CD8^+$ T cells abrogated the therapeutic benefit of JQ1 treatment (Figures 4I and 4J). In addition, JQ1 treatment significantly improved the survival of mice receiving adoptively transferred tumor-reactive T cells in an orthotopic UPK10 syngeneic mouse model (Figure 4K). Together, these data support the notion that BET inhibition limits the progression of ovarian cancer in a $CD8^+$ cytotoxic T cell-dependent manner.

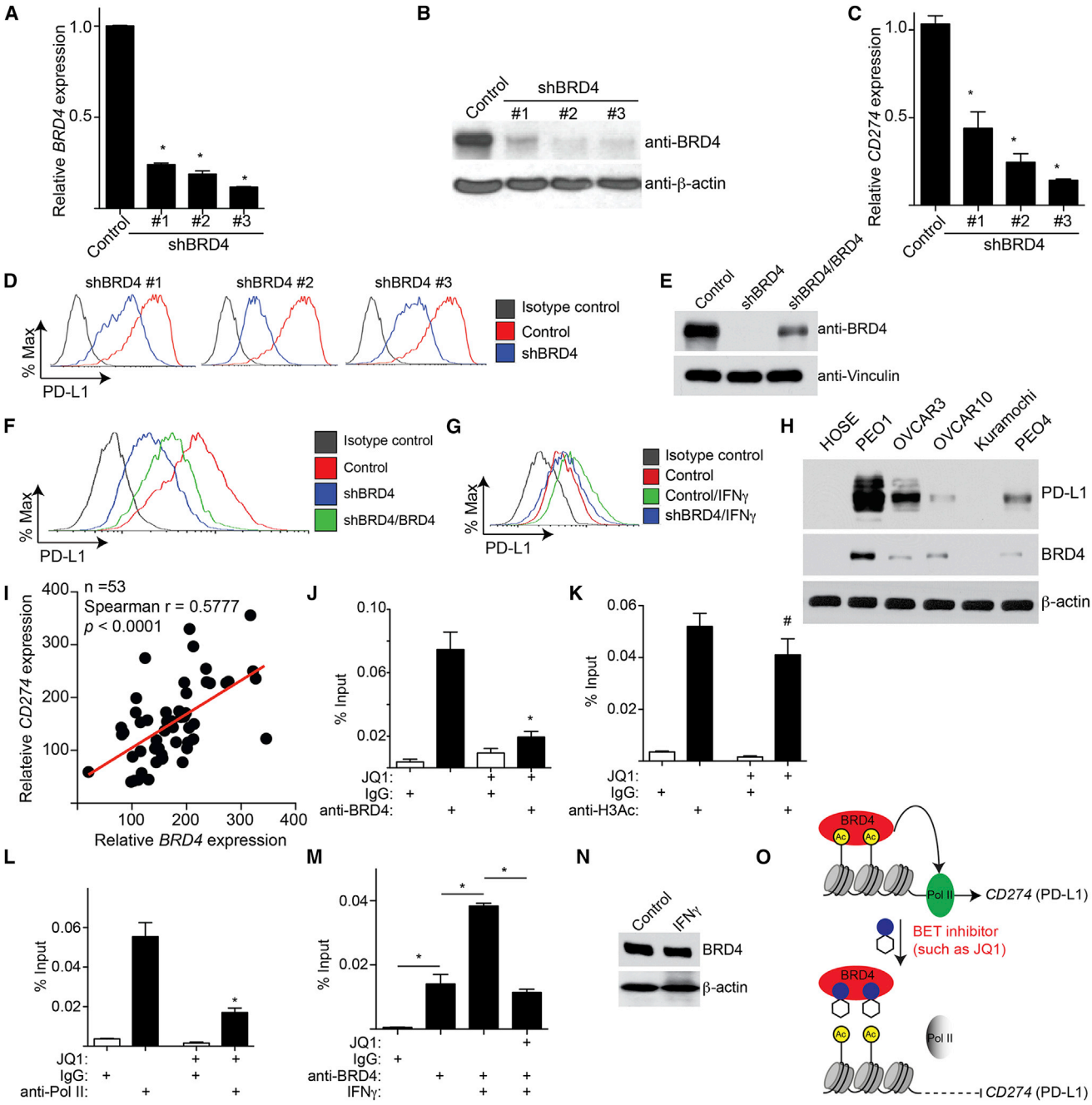

Figure 3. *CD274* Is a Direct Target Gene of BRD4

(A) PEO1 cells expressing shBRD4 or control were examined for *BRD4* expression by qRT-PCR. *p < 0.05.

(B) Same as in (A) but examined for the expression of BRD4 protein by immunoblotting.

(C) Same as in (A) but examined for *CD274* mRNA expression by qRT-PCR. *p < 0.05.

(D) Same as in (A). PD-L1 expression was determined by FACS.

(E) PEO1 cells expressing shBRD4 (#3) that targets the 3′ UTR region of the human *BRD4* gene with or without simultaneous expression of a wild-type *BRD4* open reading frame. BRD4 and Vinculin expression was determined by immunoblot.

(F) Same as in (E) but examined for PD-L1 expression by FACS.

(G) PEO1 cells expressing shBRD4 (#3) or control with or without IFNγ (20 ng/ml, 24 hr) stimulation were examined for PD-L1 expression by FACS.

(H) Expression of BRD4, PD-L1, and β-actin were examined in the indicated ovarian cancer cell lines or normal human ovarian surface epithelial (HOSE) cells by immunoblot.

(I) Correlation between *BRD4* and *CD274* expression was determined by Spearman statistical analysis in 53 cases of laser capture and microdissected high-grade serous ovarian cancer specimens.

(legend continued on next page)

DISCUSSION

Several BET inhibitors are now in clinical development for a number of cancer types (Filippakopoulos and Knapp, 2014). Although anti-PD-L1 antibody therapy is generally well tolerated, it is known to trigger irAEs—in particular, with prolonged treatment (Naidoo et al., 2015). Missing from immunotherapy are traditional small-molecule drugs that may offer several unique advantages (Adams et al., 2015). Our findings raise the possibility of targeting PD-L1 using BET inhibitors. BET inhibitors suppress macrophage inflammatory responses and attenuate systematic inflammatory processes (Belkina et al., 2013; Nicodeme et al., 2010). Thus, it is possible that BET inhibitors may quell the inflammatory response without eliminating the anti-tumor immune response.

PD-L1-positive myeloid cells play a key role in human ovarian cancer (Curiel et al., 2004). BET inhibitors affect PD-L1 expression in both tumor cells and in myeloid DCs and macrophages (Figures 4 and S4). Therefore, BET inhibitors suppress PD-L1 expression in both host antigen-presenting cells and tumor cells. Compared with immune-associated PD-L1, oncogenic PD-L1 and its role in tumor immunity remain poorly defined (Zou et al., 2016). Interestingly, BET inhibitors suppress PD-L1 expression in tumor cells with or without IFNγ stimulation (Figures 2 and S2). Thus, this mechanism may couple oncogenic and immune-associated PD-L1 regulation.

Identification of potential biomarkers that predict the response to anti-PD-L1 therapy in cancer remains a clinical challenge (Melero et al., 2015). In particular, patients who positively respond to anti-PD-L1 therapy despite a lack of PD-L1 expression highlight the complex regulation of PD-L1 in cancer (Brahmer et al., 2015). Our findings establish that BRD4 is a critical regulator of PD-L1 expression, as BRD4 inhibition blocks the IFNγ-induced upregulation of PD-L1 (Figures 2 and 3). This suggests that BRD4 expression may dictate how well PD-L1 can be induced in response to signals from the tumor microenvironment.

BRD4 is localized to 19p13.1. This *BRD4* locus is often amplified in ovarian cancer (Goundiam et al., 2015). In fact, ovarian cancer shows one of the highest *BRD4* amplification rates in all cancer types based on The Cancer Genome Atlas (TCGA) database (data not shown). BRD4 expression positively correlates with *CD274* expression in ovarian cancer specimens (Figure 3I). However, the existence of tumors with high BRD4 expression and low *CD274* expression suggests that additional cell-intrinsic or -extrinsic mechanisms may also regulate *CD274* expression. Nonetheless, it will be interesting to correlate the response to anti-PD-L1 blockade therapy with BRD4 amplification or expression. Notably, BRD4 also promotes survival and proliferation of ovarian cancer cells (Baratta et al., 2015). Therefore, BET inhibitors may have dual anti-tumor effects on both tumor cells as well as the tumor-promoting immune environment.

Our findings demonstrate that BET inhibitors suppress PD-L1 expression, which correlates with an increase in cytotoxic T cell activity. A limitation of the study is that BET inhibition affects the expression of other genes in addition to *CD274* (Figure S3; Table S2). Changes in the expression of other genes could also contribute to the observed anti-tumor effects. However, we previously demonstrated that decreased PD-L1 in myeloid cells, smaller than those elicited by JQ1, are sufficient to have anti-tumor immune responses (Cubillos-Ruiz et al., 2009). Therefore, our data support the notion that downregulation of PD-L1 plays a significant role in the observed anti-tumor immune response induced by JQ1. Given the demonstrated broad applicability of PD-L1 blockade therapy in human cancer, we anticipate our findings to have far-reaching implications for developing future combinatory cancer therapies.

EXPERIMENTAL PROCEDURES

In Vivo Syngeneic Mouse Model

All animal protocols described in this study were approved by the Institutional Animal Care and Use Committee (IACUC) at The Wistar Institute. Six- to eight-week-old female wild-type C57BL/6 mice were purchased from Charles River Laboratories. ID8 cells were provided by K. Roby (Department of Anatomy and Cell Biology, University of Kansas) and retrovirally transduced to express *Defb29* and *Vegf-a* (Conejo-Garcia et al., 2004). Mouse ovarian tumor UPK10 cells were described previously (Scarlett et al., 2012). The ID8-*Defb29/Vegf-a* intraperitoneal (i.p.) tumor model was generated as previously described (Conejo-Garcia et al., 2004). Briefly, 2×10^6 ~70% confluent ID8-*Defb29/Vegf-a* cells were injected into the peritoneal cavity of mice and allowed to establish tumors. After 1 week, mice were randomized into two groups and treated twice a week with 50 mg/kg JQ1 or vehicle control by i.p. injection for 3 weeks.

For anti-CD8 antibody treatment, 2×10^6 luciferase-expressing ID8 cells were orthotopically transplanted into C57BL/6 mice by i.p. injection. The transplanted tumors were allowed to establish for 22 days. The mice were then randomized and treated intraperitoneally with 50 mg/kg JQ1 twice a week with or without an anti-CD8 antibody, 500 μg per mouse, once a week. Tumor growth was followed by non-invasive imaging, as previously described (Bitler et al., 2015), using an IVIS Spectrum. Images were analyzed using Live Imaging 4.0 software.

Tumor-Reactive T Cell-Adoptive Immunotherapy

T cells from tumor-free mice were primed with tumor-antigen-pulsed BMDCs as described previously (Nesbeth et al., 2009). Briefly, BMDCs were pulsed overnight with γ-irradiated (10,000 rad) and UV-treated (30 min) UPK10 tumor cells at a ratio of 10:1 (dendritic cells:tumor cells). Tumor-antigen-pulsed BMDCs were then co-cultured with T cells at a 1:10 (BMDC:T cell) ratio in the presence of interleukin 2 (IL-2; 10 U/ml) and interleukin 7 (IL-7; 1 ng/ml) (both from PeproTech) for 7 days. Female C57BL/6 mice (6–8 weeks old) were intraperitoneally injected with 2×10^6 UPK10 tumor cells and treated intraperitoneally with JQ1 or vehicle control on day 5 and day 12. 1×10^6 tumor-antigen-primed T cells were transferred into tumor-bearing mice on day 7 and day 14 post-tumor challenge.

Statistical Analysis

GraphPad Prism Version 5.0 was used to perform statistical analyses. The Student's t test was used to determine p values of raw data. A p value <0.05 was considered as significant.

(J–L) PEO1 cells were treated with or without 200 nM JQ1 for 24 hr. The cells were subjected to ChIP analysis using antibodies against BRD4 (J), H3Ac (K), or Pol II (L). An isotype-matched IgG was used as a negative control. The association with the *CD274* gene promoter was quantified by qPCR. $^{\#}p > 0.05$; $^{*}p < 0.05$.
(M) Same as in (J), but for PEO1 cells with or without IFNγ (20 ng/ml, 24 hr) stimulation were treated with JQ1. $^{*}p < 0.05$.
(N) Same as in (M) but examined for BRD4 and β-actin protein expression by immunoblot.
(O) A model for BRD4-mediated regulation of PD-L1 expression.
Error bars represent SEM of three independent experiments. See also Figure S3 and Table S2.

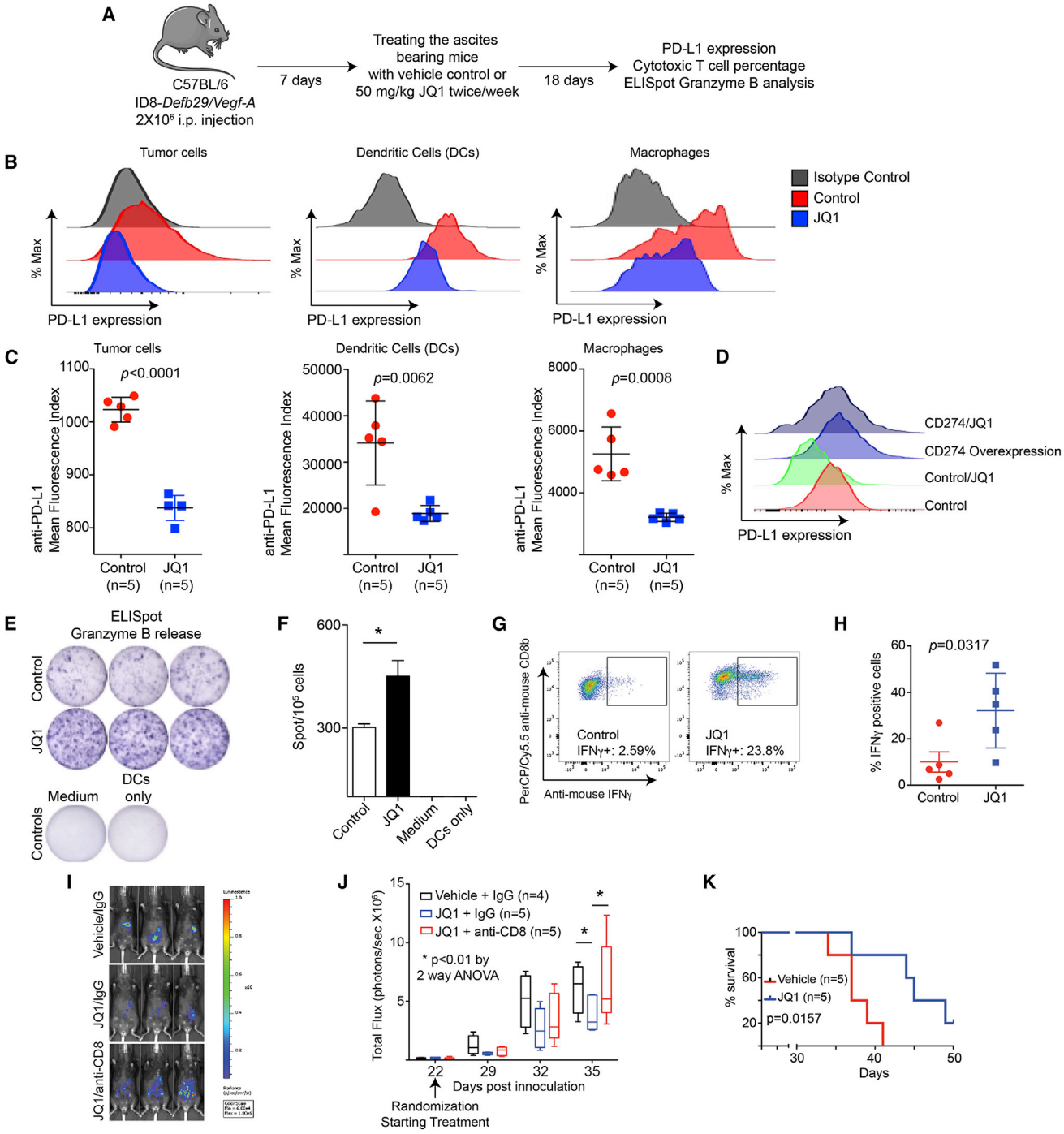

Figure 4. JQ1 Decreases PD-L1 Expression and Limits Tumor Progression in a Cytotoxic T Cell-Dependent Manner In Vivo

(A) Flow diagram of experimental design. These experiments were repeated three times.

(B) 2 × 10^6 total cells from peritoneal wash were subjected to staining using antibodies against CD45.2-PE/Cy7, CD11c-APC/Cy7, F4/80-PerCP/Cy5.5, MHCII-PE, and PDL1-APC. PD-L1 expression was determined by FACS. CD45.2-PE/Cy7-negative cells were gated as tumor cells. Among CD45.2-PE/Cy7-positive cells, MHCII and CD11c double-positive cells were gated as dendritic cells, while MHCII- and F4/80-positive cells were gated as macrophages.

(C) Quantification of PD-L1 expression in indicated cell populations.

(D) C57BL/6 mice were injected intraperitoneally with ID8-*Defb29/Vegf-a* cells with or without *CD274* overexpression. Mice were randomized and treated with 50 mg/kg JQ1 twice every week for 18 days or vehicle controls. Cells from peritoneal wash were subjected to analysis for PD-L1 expression using the same approach as detailed in (B). Shown is PD-L1 expression in tumor cells (CD45.2-PE/Cy7 negative) from the indicated groups. Due to low cell numbers, cells from five mice in each of the indicated groups were combined for FACS analysis.

(legend continued on next page)

ACCESSION NUMBERS

The accession number for the QuantSeq data reported in this paper is GEO: GSE81698.

SUPPLEMENTAL INFORMATION

Supplemental Information includes Supplemental Experimental Procedures, four figures, and two tables and can be found with this article online at http://dx.doi.org/10.1016/j.celrep.2016.08.032.

AUTHOR CONTRIBUTIONS

H.Z., F.B., N.S., and M.R.R. designed experiments. H.Z., F.B., N.S., M.R.R., B.G.B., M.J.A., Y.Y., and A.V.K. conducted experiments and analyzed data. J.E.B. provided key experimental materials. J.R.C.-G. and R.Z. supervised the study. R.Z. conceived the study. H.Z., M.R.R., B.G.B., J.R.C.-G., and R.Z. wrote the manuscript.

ACKNOWLEDGMENTS

We thank The Structure Genomics Consortium for providing the panel of small-molecule inhibitors that target epigenetic regulators. We thank members of the R.Z. lab for discussion and Dr. Katherine Aird for critical comments. This work was supported by NIH/National Cancer Institute R01 grants (CA160331, CA163377, and CA202919 to R.Z.), U.S. Department of Defense grants (OC140632P1 and OC150446 to R.Z.), an Ovarian Cancer Research Fund (OCRF) program project (to R.Z.), and The Jayne Koskinas & Ted Giovanis Breast Cancer Research Consortium at Wistar (to R.Z.). H.Z. is an OCRF Ann Schreiber Mentored Investigator. B.G.B. is supported by an NIH/National Cancer Institute grant (K99CA194318). Support of Core Facilities was provided by Cancer Center Support Grant (CCSG) CA010815 to The Wistar Institute.

For J.E.B, The Dana-Farber Cancer Institute has licensed intellectual property from the Bradner Laboratory concerning BET bromodomain inhibitors to Tensha Therapeutics, now owned by Roche Pharmaceuticals.

Received: February 16, 2016
Revised: July 21, 2016
Accepted: August 10, 2016
Published: September 13, 2016

REFERENCES

Abiko, K., Mandai, M., Hamanishi, J., Yoshioka, Y., Matsumura, N., Baba, T., Yamaguchi, K., Murakami, R., Yamamoto, A., Kharma, B., et al. (2013). PD-L1 on tumor cells is induced in ascites and promotes peritoneal dissemination of ovarian cancer through CTL dysfunction. Clin. Cancer Res. *19*, 1363–1374.

Adams, J.L., Smothers, J., Srinivasan, R., and Hoos, A. (2015). Big opportunities for small molecules in immuno-oncology. Nat. Rev. Drug Discov. *14*, 603–622.

Baratta, M.G., Schinzel, A.C., Zwang, Y., Bandopadhayay, P., Bowman-Colin, C., Kutt, J., Curtis, J., Piao, H., Wong, L.C., Kung, A.L., et al. (2015). An in-tumor genetic screen reveals that the BET bromodomain protein, BRD4, is a potential therapeutic target in ovarian carcinoma. Proc. Natl. Acad. Sci. USA *112*, 232–237.

Belkina, A.C., Nikolajczyk, B.S., and Denis, G.V. (2013). BET protein function is required for inflammation: Brd2 genetic disruption and BET inhibitor JQ1 impair mouse macrophage inflammatory responses. J. Immunol. *190*, 3670–3678.

Bitler, B.G., Aird, K.M., Garipov, A., Li, H., Amatangelo, M., Kossenkov, A.V., Schultz, D.C., Liu, Q., Shih, IeM., Conejo-Garcia, J.R., et al. (2015). Synthetic lethality by targeting EZH2 methyltransferase activity in ARID1A-mutated cancers. Nat. Med. *21*, 231–238.

Brahmer, J., Reckamp, K.L., Baas, P., Crinò, L., Eberhardt, W.E., Poddubskaya, E., Antonia, S., Pluzanski, A., Vokes, E.E., Holgado, E., et al. (2015). Nivolumab versus docetaxel in advanced squamous-cell non-small-cell lung cancer. N. Engl. J. Med. *373*, 123–135.

Conejo-Garcia, J.R., Benencia, F., Courreges, M.C., Kang, E., Mohamed-Hadley, A., Buckanovich, R.J., Holtz, D.O., Jenkins, A., Na, H., Zhang, L., et al. (2004). Tumor-infiltrating dendritic cell precursors recruited by a beta-defensin contribute to vasculogenesis under the influence of Vegf-A. Nat. Med. *10*, 950–958.

Cubillos-Ruiz, J.R., Engle, X., Scarlett, U.K., Martinez, D., Barber, A., Elgueta, R., Wang, L., Nesbeth, Y., Durant, Y., Gewirtz, A.T., et al. (2009). Polyethylenimine-based siRNA nanocomplexes reprogram tumor-associated dendritic cells via TLR5 to elicit therapeutic antitumor immunity. J. Clin. Invest. *119*, 2231–2244.

Curiel, T.J., Coukos, G., Zou, L., Alvarez, X., Cheng, P., Mottram, P., Evdemon-Hogan, M., Conejo-Garcia, J.R., Zhang, L., Burow, M., et al. (2004). Specific recruitment of regulatory T cells in ovarian carcinoma fosters immune privilege and predicts reduced survival. Nat. Med. *10*, 942–949.

Filippakopoulos, P., and Knapp, S. (2014). Targeting bromodomains: epigenetic readers of lysine acetylation. Nat. Rev. Drug Discov. *13*, 337–356.

Filippakopoulos, P., Qi, J., Picaud, S., Shen, Y., Smith, W.B., Fedorov, O., Morse, E.M., Keates, T., Hickman, T.T., Felletar, I., et al. (2010). Selective inhibition of BET bromodomains. Nature *468*, 1067–1073.

Goundiam, O., Gestraud, P., Popova, T., De la Motte Rouge, T., Fourchotte, V., Gentien, D., Hupé, P., Becette, V., Houdayer, C., Roman-Roman, S., et al. (2015). Histo-genomic stratification reveals the frequent amplification/overexpression of CCNE1 and BRD4 genes in non-BRCAness high grade ovarian carcinoma. Int. J. Cancer *137*, 1890–1900.

Mahoney, K.M., Rennert, P.D., and Freeman, G.J. (2015). Combination cancer immunotherapy and new immunomodulatory targets. Nat. Rev. Drug Discov. *14*, 561–584.

Melero, I., Berman, D.M., Aznar, M.A., Korman, A.J., Pérez Gracia, J.L., and Haanen, J. (2015). Evolving synergistic combinations of targeted immunotherapies to combat cancer. Nat. Rev. Cancer *15*, 457–472.

(E) Granzyme B ELISpot assay of total cells from peritoneal washes. 1×10^5 total cells obtained from peritoneal wash were subjected to analysis. Representative image of positive spot from the indicated groups is shown.
(F) Quantification of (E). $^*p < 0.05$.
(G) 2×10^6 luciferase-expressing ID8 cells were orthotopically transplanted into C57BL/6 mice by i.p. injection. The transplanted tumors were allowed to establish for 22 days. The mice were then randomized and treated with 50 mg/kg JQ1 twice a week with or without an anti-CD8 antibody (500 μg per mouse) once a week (vehicle controls, n = 4; JQ1/IgG, n = 5; and JQ1/anti-CD8, n = 5). The percentage of $IFN\gamma^+$ $CD8^+$ T cells was analyzed by intracellular staining. Shown are representative results of $IFN\gamma^+$ cells in live CD45+CD3+CD8+ in the indicated groups.
(H) Quantification of (G).
(I) Same as in (G). Tumor growth was monitored by luciferase imaging. Shown are representative images taken at the end of the experiment (day 35).
(J) Same as in (I). Tumor growth in the indicated groups was monitored by luciferase imaging, and total flux for each of the indicated groups is depicted as a box-and-whiskers plot that indicates the range of minimum to maximum total flux of individual mice from each of the indicated groups.
(K) 2×10^6 UPK10 cells were orthotopically transplanted into C57BL/6 mice by i.p. injection. The tumor-bearing mice received 1×10^6 tumor-antigen-primed T cells on days 7 and 14. The mice were randomized, treated on days 5 and 12 with or without 50 mg/kg JQ1, and followed for survival (n = 5). Kaplan-Meier survival curves of the indicated groups. The p value was calculated by log-rank Mantel-Cox test.
See also Figure S4.

Mok, S.C., Bonome, T., Vathipadiekal, V., Bell, A., Johnson, M.E., Wong, K.K., Park, D.C., Hao, K., Yip, D.K., Donninger, H., et al. (2009). A gene signature predictive for outcome in advanced ovarian cancer identifies a survival factor: microfibril-associated glycoprotein 2. Cancer Cell *16*, 521–532.

Naidoo, J., Page, D.B., Li, B.T., Connell, L.C., Schindler, K., Lacouture, M.E., Postow, M.A., and Wolchok, J.D. (2015). Toxicities of the anti-PD-1 and anti-PD-L1 immune checkpoint antibodies. Ann. Oncol. *26*, 2375–2391.

Nesbeth, Y., Scarlett, U., Cubillos-Ruiz, J., Martinez, D., Engle, X., Turk, M.J., and Conejo-Garcia, J.R. (2009). CCL5-mediated endogenous antitumor immunity elicited by adoptively transferred lymphocytes and dendritic cell depletion. Cancer Res. *69*, 6331–6338.

Nicodeme, E., Jeffrey, K.L., Schaefer, U., Beinke, S., Dewell, S., Chung, C.W., Chandwani, R., Marazzi, I., Wilson, P., Coste, H., et al. (2010). Suppression of inflammation by a synthetic histone mimic. Nature *468*, 1119–1123.

Scarlett, U.K., Rutkowski, M.R., Rauwerdink, A.M., Fields, J., Escovar-Fadul, X., Baird, J., Cubillos-Ruiz, J.R., Jacobs, A.C., Gonzalez, J.L., Weaver, J., et al. (2012). Ovarian cancer progression is controlled by phenotypic changes in dendritic cells. J. Exp. Med. *209*, 495–506.

Topalian, S.L., Drake, C.G., and Pardoll, D.M. (2015). Immune checkpoint blockade: a common denominator approach to cancer therapy. Cancer Cell *27*, 450–461.

Webb, J.R., Milne, K., Kroeger, D.R., and Nelson, B.H. (2016). PD-L1 expression is associated with tumor-infiltrating T cells and favorable prognosis in high-grade serous ovarian cancer. Gynecol. Oncol. *141*, 293–302.

Wrangle, J., Wang, W., Koch, A., Easwaran, H., Mohammad, H.P., Vendetti, F., Vancriekinge, W., Demeyer, T., Du, Z., Parsana, P., et al. (2013). Alterations of immune response of non-small cell lung cancer with azacytidine. Oncotarget *4*, 2067–2079.

Zou, W., Wolchok, J.D., and Chen, L. (2016). PD-L1 (B7-H1) and PD-1 pathway blockade for cancer therapy: mechanisms, response biomarkers, and combinations. Sci. Transl. Med. *8*, 328rv4.

Cancer Research

BET Inhibitors Suppress ALDH Activity by Targeting *ALDH1A1* Super-Enhancer in Ovarian Cancer

Yuhki Yokoyama[1], Hengrui Zhu[1], Jeong Heon Lee[2], Andrew V. Kossenkov[3], Sherry Y. Wu[4,5], Jayamanna M. Wickramasinghe[3], Xiangfan Yin[6], Katherine C. Palozola[7], Alessandro Gardini[1], Louise C. Showe[3,6], Kenneth S. Zaret[7], Qin Liu[6], David Speicher[6], Jose R. Conejo-Garcia[8], James E. Bradner[9], Zhiguo Zhang[2,10], Anil K. Sood[4,5,11], Tamas Ordog[10], Benjamin G. Bitler[1], and Rugang Zhang[1]

Abstract

The emergence of tumor cells with certain stem-like characteristics, such as high aldehyde dehydrogenase (ALDH) activity due to ALDH1A1 expression, contributes to chemotherapy resistance and tumor relapse. However, clinically applicable inhibitors of ALDH activity have not been reported. There is evidence to suggest that epigenetic regulation of stem-related genes contributes to chemotherapy efficacy. Here, we show that bromodomain and extraterminal (BET) inhibitors suppress ALDH activity by abrogating BRD4-mediated ALDH1A1 expression through a super-enhancer element and its associated enhancer RNA. The clinically applicable small-molecule BET inhibitor JQ1 suppressed the outgrowth of cisplatin-treated ovarian cancer cells both *in vitro* and *in vivo*. Combination of JQ1 and cisplatin improved the survival of ovarian cancer–bearing mice in an orthotopic model. These phenotypes correlate with inhibition of *ALDH1A1* expression through a super-enhancer element and other stem-related genes in promoter regions bound by BRD4. Thus, targeting the BET protein BRD4 using clinically applicable small-molecule inhibitors, such as JQ1, is a promising strategy for targeting ALDH activity in epithelial ovarian cancer. *Cancer Res; 76(21); 6320–30. ©2016 AACR.*

Introduction

Chemotherapeutic drugs, such as cisplatin, have had a major impact on the therapeutic management of many tumors, and in particular in epithelial ovarian cancer (EOC; ref. 1). However, chemotherapy resistance is a major cause of cancer morbidity and mortality. For example, although EOC, in particular high-grade serous carcinoma (HGSC), initially respond well to platinum-based chemotherapy, relapse often occurs with decreased chemotherapy sensitivity (2). The hypothesis that this occurs due to cancer stem-like cells (CSC) remains controversial. However, there is substantial evidence in the literature that cells with CSC characteristics contribute to chemotherapy resistance and tumor relapse (3). Putative EOC CSCs are typically characterized by increased aldehyde dehydrogenase (ALDH) activity with concomitant upregulation of ALDH1A1 (4–6). ALDH activity is functionally important in EOC, as suppressing ALDH activity by knocking down ALDH1A1 has been shown to sensitize EOC cells to chemotherapy (4). In addition, a population of normal ovarian stem cells also has increased ALDH activity (7), further supporting its functioning in putative ovarian CSCs. Despite the mounting evidence on the critical role of ALDH1A1 in regulating CSCs (8), the molecular mechanisms underlying its regulation remain poorly understood. Notably, clinically applicable inhibitors of ALDH activity or ALDH1A1-targeting approaches have not been reported.

Recent genome-wide next-generation sequencing studies in human cancers have revealed frequent alterations in genes and proteins that are critical in regulating the epigenetic landscape of chromatin (9, 10). This suggests that proteins encoded by these genes may be cancer therapeutic targets. Accordingly, small-molecule inhibitors targeting chromatin-regulating epigenetic enzymes have been developed (11). The bromodomain and extraterminal (BET) family of proteins recognize acetylated lysine on histones through their bromodomains (12). BET proteins control the transcription of their target genes either directly by

[1]Gene Expression and Regulation Program, The Wistar Institute, Philadelphia, Pennsylvania. [2]Department of Biochemistry and Molecular Biology, Mayo Clinic, Rochester, Minnesota. [3]Center for Systems and Computational Biology, The Wistar Institute, Philadelphia, Pennsylvania. [4]Department of Gynecologic Oncology, The University of Texas MD Anderson Cancer Center, Houston, Texas. [5]Center for RNAi and Non-Coding RNA, The University of Texas MD Anderson Cancer Center, Houston, Texas. [6]Molecular and Cellular Oncology Program, The Wistar Institute, Philadelphia, Pennsylvania. [7]Institute for Regenerative Medicine, Epigenetics Program, and Department of Cell and Developmental Biology, Perelman School of Medicine, University of Pennsylvania, Pennsylvania. [8]Tumor Microenvironment and Metastasis Program, The Wistar Institute, Philadelphia, Pennsylvania. [9]Department of Medical Oncology, Dana-Farber Cancer Institute, Harvard Medical School, Boston, Massachusetts. [10]Mayo Clinic, Rochester, Minnesota. [11]Department of Cancer Biology, The University of Texas MD Anderson Cancer Center, Houston, Texas.

Note: Supplementary data for this article are available at Cancer Research Online (http://cancerres.aacrjournals.org/).

Y. Yokoyama and H. Zhu contributed equally to this article.

Corresponding Author: Rugang Zhang, The Wistar Institute, 3601 Spruce Street, Philadelphia, PA 19104; E-mail: rzhang@wistar.org; and Benjamin G. Bitler, bbitler@wistar.org

doi: 10.1158/0008-5472.CAN-16-0854

recruiting transcriptional machinery or indirectly through involving enhancer elements in a lineage and context-specific manner (12). Highly specific BET inhibitors are in clinical trials (13). Pharmacologic inhibitors of BET proteins have shown efficacy in the clinic in a number of pathologies, most notably in cancer. There is evidence to suggest that epigenetic regulation of stem-related genes contributes to chemotherapy efficacy (14, 15). Using unbiased approaches, here, we have identified BET inhibitors as suppressors of ALDH activity that potentiate the antitumor effects of cisplatin in EOC.

Materials and Methods

Cell lines and epigenetic small-molecule screen

Human EOC cell lines were obtained from ATCC within 3 years and were reauthenticated by The Wistar Institute's Genomics Facility at the end of the experiments within last 3 months using short tandem repeat profiling using AmpFLSTR Identifiler PCR Amplification Kit (Life Technologies) and cultured as described previously (16). The Structural Genome Consortium generously provided the epigenetic compound library. OVCAR3 cells were plated in 384-well plates and treated with serial dilutions (0–20 μmol/L) of 24 epigenetic compounds with or without IC_{20} cisplatin. Data were analyzed with GraphPad (Prism).

In situ 3C assay

In situ chromosome conformation capture (3C) samples were prepared as described previously with modifications (17). Briefly, cells (5×10^6) were cross-linked with 1% formaldehyde and quenched by 2.5 mol/L glycine. Cells were collected and resuspended in Hi-C lysis buffer (10 mmol/L Tris-HCl pH 8.0, 10 mmol/L NaCl, 0.2% NP-40) with proteinase inhibitor (Sigma). The cell suspension was incubated on ice, washed with Hi-C buffer, resuspended in 0.5% SDS, and incubated at 65°C for 5 minutes. After quenching the SDS, chromatin was digested overnight by MboI and then ligated. Ligated DNA was purified using Wizard SV Gel and PCR Clean-Up System (Promega). Quantitative PCR was performed by using Quantitect Probe PCR Master Mix (Qiagen) with custom probe and primers as described previously (18). Probe and primer sequences are indicated in Supplementary Table S1.

Nascent RNA sequencing and chromatin immunoprecipitation sequencing

For nascent RNA sequencing (RNA-seq), cells were incubated with 0.5 mmol/L ethidium uridine (EU) and treated with 125 nmol/L JQ1 or vehicle control for 40 minutes. Total RNA was extracted with TRIzol reagent and RNeasy Mini Kit. The EU-labeled RNAs were biotinylated and precipitated by using the Click-it Nascent RNA Capture Kit (Life Technologies) following the manufacturer's instructions. Briefly, 5 μg EU-labeled RNA was biotinylated with 0.25 mmol/L biotin azide in Click-it Reaction Buffer. Biotinylated RNAs were ethanol precipitated and resuspended in ultrapure water. Biotinylated RNAs were incubated with Dynabeads MyOne Streptavidin T1 magnetic beads in Click-it RNA and subjected to library preparation. Libraries for RNA-seq were prepared with Ovation Human FFPE RNA-Seq Multiplex System 1–8 (NuGEN) and sequenced on an Illumina NextSeq 500.

For chromatin immunoprecipitation sequencing (ChIP-seq), cells were cross-linked with 1% formaldehyde for 10 minutes, followed by quenching with 125 mmol/L glycine for 5 minutes. Fixed cells were resuspended in cell lysis buffer (10 mmol/L Tris-HCl, pH 7.5, 10 mmol/L NaCl, 0.5% NP-40) and incubated on ice for 10 minutes. The lysates were washed with MNase digestion buffer (20 mmol/L Tris-HCl, pH 7.5, 15 mmol/L NaCl, 60 mmol/L KCl, 1 mmol/L $CaCl_2$) once and incubated for 20 minutes at 37°C in the presence of 1,000 gel units of MNase (NEB, M0247S) in 250 μL reaction volume. After adding the same volume of sonication buffer (100 mmol/L Tris-HCl, pH 8.1, 20 mmol/L EDTA, 200 mmol/L NaCl, 2% Triton X-100, 0.2% sodium deoxycholate), the lysates were sonicated for 5 minutes (30 seconds on/off) in a Diagenode Bioruptor and centrifuged at 15,000 rpm for 10 minutes. The cleared supernatant equivalent to $2–4 \times 10^6$ cells was incubated with 2 μg of anti-BRD4 antibody (Bethyl, A301-985A) on a rocker overnight. Bound chromatin was eluted and reverse cross-linked at 65°C overnight. For next-generation sequencing, ChIP-seq libraries were prepared from 10 ng of ChIP and input DNAs with the Ovation Ultralow DR Multiplex system (NuGEN). The ChIP-seq libraries were sequenced in a 51 base pairs paired end run using the Illumina HiSeq 2000.

In vivo orthotopic xenograft mouse model

The Institutional Animal Care and Use Committee (IACUC) at The Wistar Institute (Philadelphia, PA) approved all animal protocols described in this study. NOD/scid gamma (NSG) mice were injected intraperitoneally with OVCAR3 luciferase cells (5×10^6). Tumors were allowed to establish for 3 weeks and randomized into four groups: control ($n = 12$), JQ1 ($n = 11$), cisplatin ($n = 12$), and cisplatin/JQ1 ($n = 13$). Tumor growth was followed by noninvasive imaging as described previously (19). Briefly, tumors were visualized by injecting luciferin (4 mg/mice i.p.) resuspended in PBS, and imaged with an IVIS Spectrum. JQ1 was resuspended in 10% 2-hydroxypropyl-β-cyclodextrin solvent (Sigma-Aldrich) as described previously (20). Cisplatin was purchased from SelleckChem and dissolved in PBS. Mice were treated daily with intraperitoneal injections of vehicle controls and/or JQ1 (20 mg/kg) and/or biweekly with cisplatin (750 μg/kg). Tumor cells collected from peritoneal washes were incubated with ammonium chloride to lyse erythrocytes and then used for the ALDEFLUOR assay and stained with PE-anti-mouse CD45 (BD Biosciences) antibody to exclude mouse-derived hematopoietic cells. Survival of tumor-bearing mice was evaluated on the basis of IACUC criteria.

Analysis using primary human ovarian tumors

For analyzing ALDH activity, the protocol for using the primary human ovarian tumor specimen was approved by the Wistar Institute Institutional Review Board (IRB). For expression of enhancer RNA (eRNA), *BRD4* and *ALDH1A1*, the protocol using human ovarian tumor specimens was approved by the IRB at The M.D. Anderson Cancer Center (Houston, Texas). RNA was extracted from 26 high-grade serous ovarian tumors using the mirVana RNA Isolation Kit (Thermo Fisher Scientific) according to the manufacturer's protocol. Analysis of RNA levels was performed on a 7500 Fast Real-Time PCR System (Applied Biosystems) with SYBR Green–based real-time PCR using the primers as detailed in Supplementary Methods. Expression of β-actin was used as a housekeeping gene control. Analysis was performed using the 7500 Real-Time PCR software.

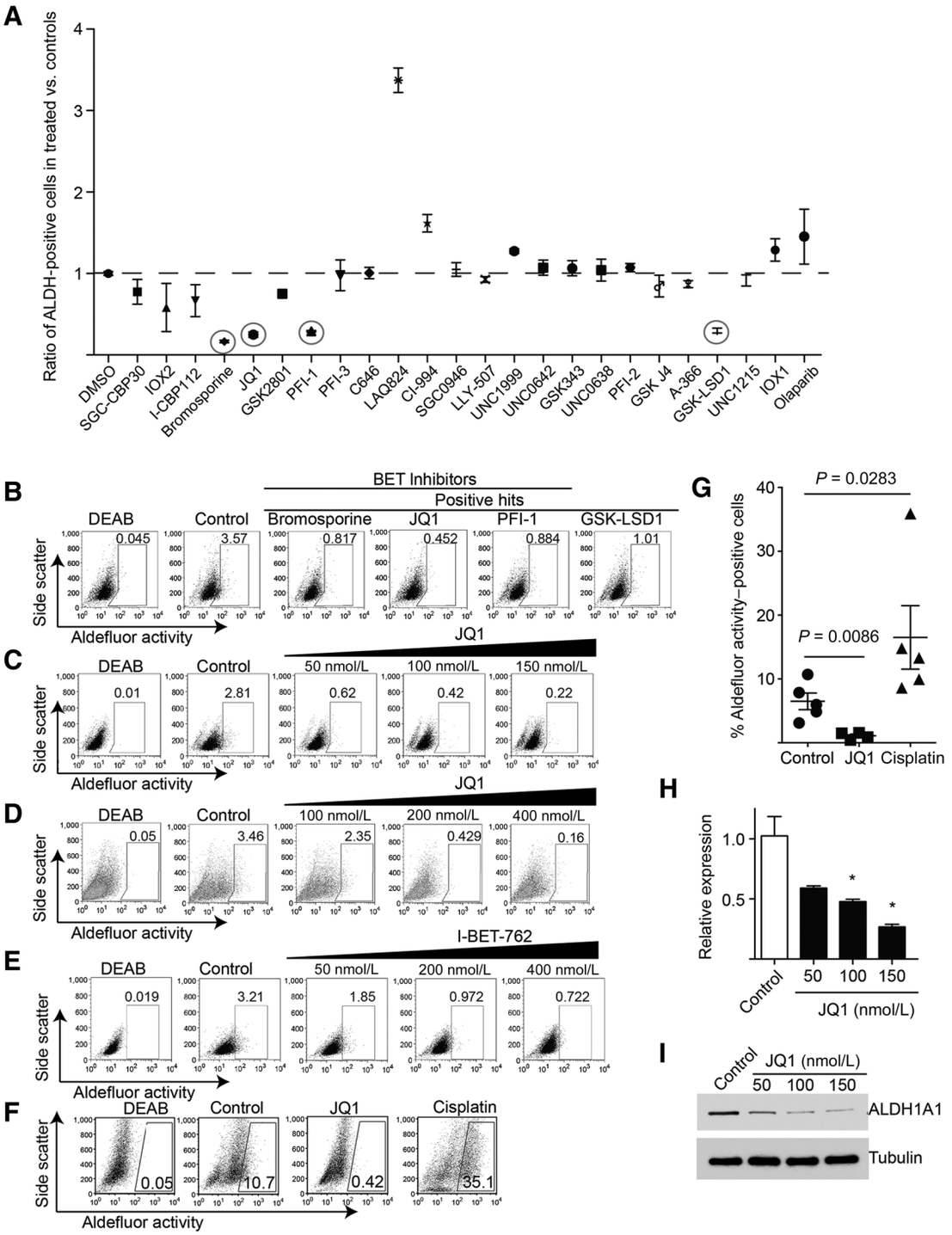

Figure 1.

BET inhibition decreases ALDH enzymatic activity and suppresses ALDH1A1 expression. **A,** plot of ratio of the quantified ALDH-positive cells OVCAR3 cells treated with the IC_{20} dose of the indicated epigenetic inhibitors or vehicle controls. For epigenetic inhibitors whose IC_{20} dose was not achieved, the highest dose tested (20 μmol/L) was used in the assay. Error bars, SEM of three independent experiments. **B,** representative changes in ALDH activity in OVCAR3 cells treated with the indicated positive "hits" identified in the evaluation. DEAB-treated cells were used as a negative control for ALDH activity. **C,** OVCAR3 cells were treated with the indicated doses of the BET inhibitor JQ1, and ALDH activity was measured by FACS. The percentages of positive cells are indicated. **D,** same as **C,** but for primary ovarian cancer cells isolated from a serous histosubtype ovarian tumor. **E,** same as **C,** but for the BET inhibitor I-BET-762. **F,** JQ1 inhibits ALDH activity *in vivo* in an intraperitoneal xenograft model using OVCAR3 cells. Percentages of ALDH activity–positive cells collected from peritoneal washes of the indicated treatment groups are indicated. Please see Materials and Methods for experimental details. **G,** quantification of **F**. Error bars, SEM. **H,** same as **C,** but examined for *ALDH1A1* mRNA expression by qRT-PCR. Mean of three independent experiments with SEM. *, $P < 0.03$. **I,** same as **C,** but examined for ALDH1A1 protein expression by immunoblotting.

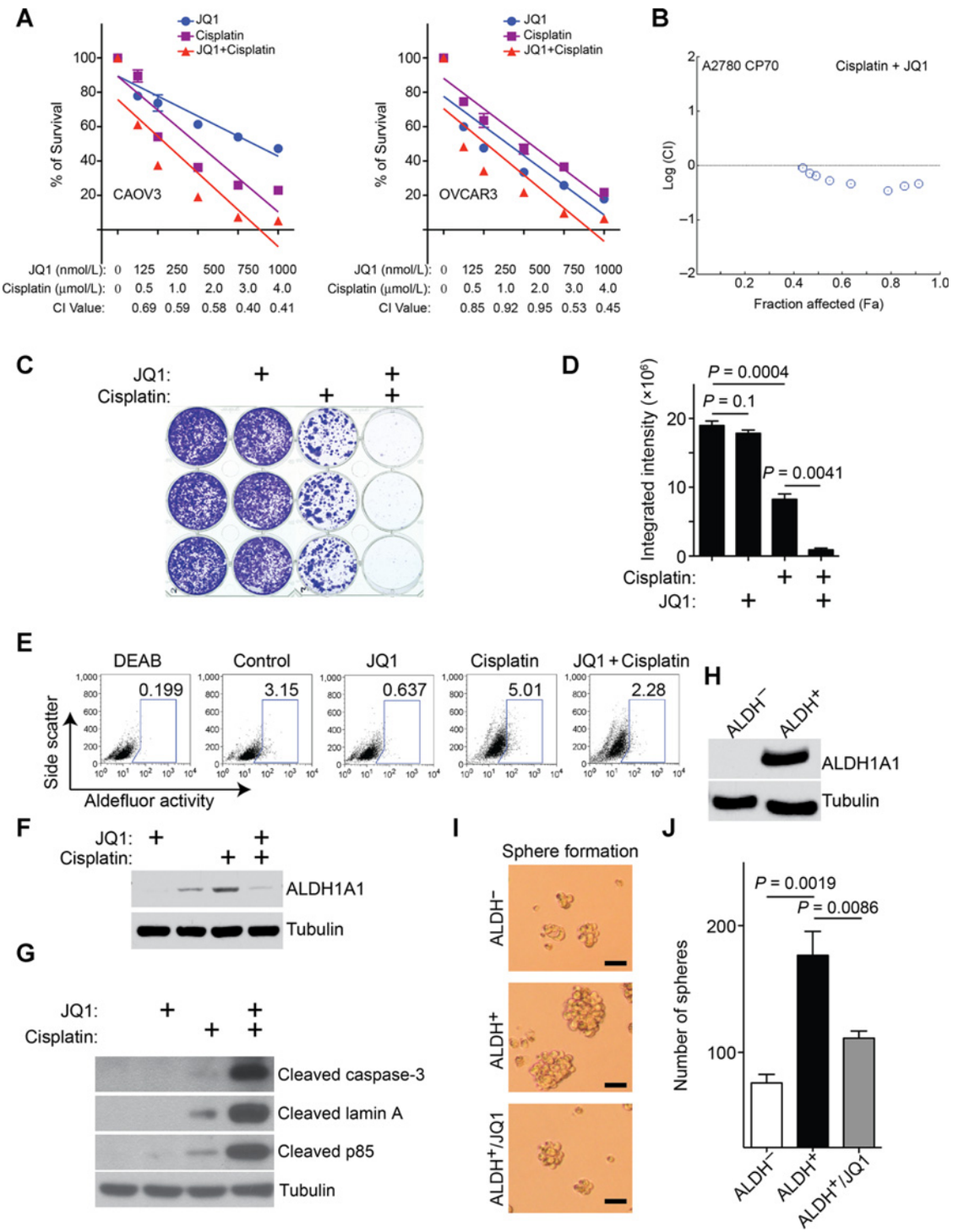

Figure 2.

JQ1 synergizes with cisplatin, which correlates with inhibition of ALDH activity. **A,** synergy analysis for JQ1 and cisplatin in the indicated ovarian cancer cell lines. Cells were treated with the indicated concentration of JQ1 and cisplatin for 72 hours. The combination index (CI) value was calculated. Combination index values: <1, synergism; 1, additive effect; >1, antagonism. Error bars, SEM and $n = 3$. **B,** logarithmic combination index plot of JQ1 (200 nmol/L) is generated in combination with cisplatin in cisplatin-resistant CP70 ovarian cancer cells. **C,** OVCAR3 cells treated with 125 nmol/L JQ1, 250 nmol/L cisplatin, or in combination for 12 days were assayed for colony formation. **D,** quantification of **C**. Mean of three independent experiments with SEM **E,** same as **C**, but cells were only treated for 72 hours and examined for the percentage of ALDH activity–positive cells by FACS. **F,** same as **E**, but examined for ALDH1A1 expression by immunoblotting. **G,** same as **E**, but examined for the indicated markers of apoptosis. **H,** ALDH1A1 protein expression in FACS-sorted ALDH activity–positive and negative cells determined by immunoblotting. **I,** sphere formation by the indicated ALDH activity–negative cells or ALDH activity–positive cells treated with or without JQ1. Scale bar, 40 μm. **J,** quantification of **I**. Mean of three independent experiments with SEM.

Bioinformatics and statistical analysis

For ChIP-seq, alignment was done versus hg19 version of human genome using bowtie algorithm. BRD4 ChIP-seq for vehicle control–treated cells was compared versus input and versus JQ1 using HOMER algorithm with "-histone" option. FDR <1% was set as a significance threshold. RNA-seq data were aligned using bowtie2 algorithm, and RSEM was used for estimating number of reads for each gene. EdgeR was used to test for differential expression and FDR <10% was used as a significance threshold unless stated otherwise. Ingenuity Pathway Analysis software was used to test gene sets for enrichment of cellular functions and canonical pathways, and Ingenuity Knowledge Base was used to create regulation and protein–protein interaction network for stem-related genes. Differences in percentage between different classes were tested using Fisher exact test, with $P < 0.05$ used as a significance threshold. H3K4Me1 and H3K27Ac broad peaks were downloaded from ENCODE for GM12878, H1-hESC, HSMM, HUVEC, K562, NHEK, and NHLF cell lines for overlap with BRD4 peaks. To determine the effect of combination treatment, CI (combination index) values were calculated by using Compusyn software (21). CIs <1, 1, and >1 represent synergism, additive effect, and antagonism, respectively.

Results

BET inhibitors suppress ALDH activity and inhibit *ALDH1A1* expression

As ALDH activity regulates the putative ovarian CSCs and stem-related genes are subjected to epigenetic regulation (4–6, 14, 15), we evaluated a panel of 24 small-molecule inhibitors known to target epigenetic regulators obtained from The Structure Genomics Consortium on their ability to suppress ALDH activity (Fig. 1A; Supplementary Table S2). We examined the expression of ALDH1A1, the major determinant of ALDH activity (4, 8), in a panel of high-grade serous EOC cell lines (Supplementary Fig. S1A and S1B; ref. 22). We performed the evaluation of ALDH activity in OVCAR3 cells because these cells have high ALDH1A1 expression (Supplementary Fig. S1B). To limit the potential bias introduced by different growth inhibition potential among the small-molecule inhibitors, we established a growth inhibition curve for each small-molecule inhibitor and based the dose of each small-molecule inhibitor on the established IC_{20} value (Supplementary Table S2). The highest tested dose (20 μmol/L) was used for those inhibitors whose IC_{20} was not achieved. Validating our experimental design, a previously reported positive regulator of ALDH activity, an HDAC inhibitor, was identified (23). We identified four small-molecule inhibitors that significantly suppressed ALDH activity (Fig. 1A and B). Notably, all three BET inhibitors in the panel scored as "hits" that significantly suppressed ALDH activity. As JQ1 is clinically applicable (known as TEN-010 in clinical trials), we performed further validation on this inhibitor. We validated that JQ1 decreased ALDH activity in a dose-dependent manner (Fig. 1C and Supplementary Fig. S1C) and in primary EOCs (Fig. 1D). Similar results were also obtained by using I-BET 762, another BET inhibitor that is now in clinical development (Fig. 1E). We further validated that JQ1 decreases ALDH activity of EOC cells *in vivo* in an orthotopic xenograft mouse model (Fig. 1F and G). As a positive control, cisplatin increased ALDH activity *in vivo* as reported previously (4). Notably, both *ALDH1A1* mRNA and ALDH1A1 protein levels were decreased by JQ1 treatment in a dose-dependent manner in multiple cell lines (Fig. 1H and I and Supplementary Fig. S1D and S1E). This suggests that JQ1 decreases ALDH activity by suppressing *ALDH1A1* expression at the transcriptional level.

BRD4 inhibition suppresses ALDH activity and inhibits ALDH1A1 expression

As high ALDH activity is implicated in chemotherapy response (8), we determined whether BET inhibitors synergize with cisplatin by inhibiting ALDH activity. Indeed, JQ1 displayed a synergistic effect with cisplatin in multiple EOC cell lines (Fig. 2A). In addition, JQ1 displayed a synergistic effect with

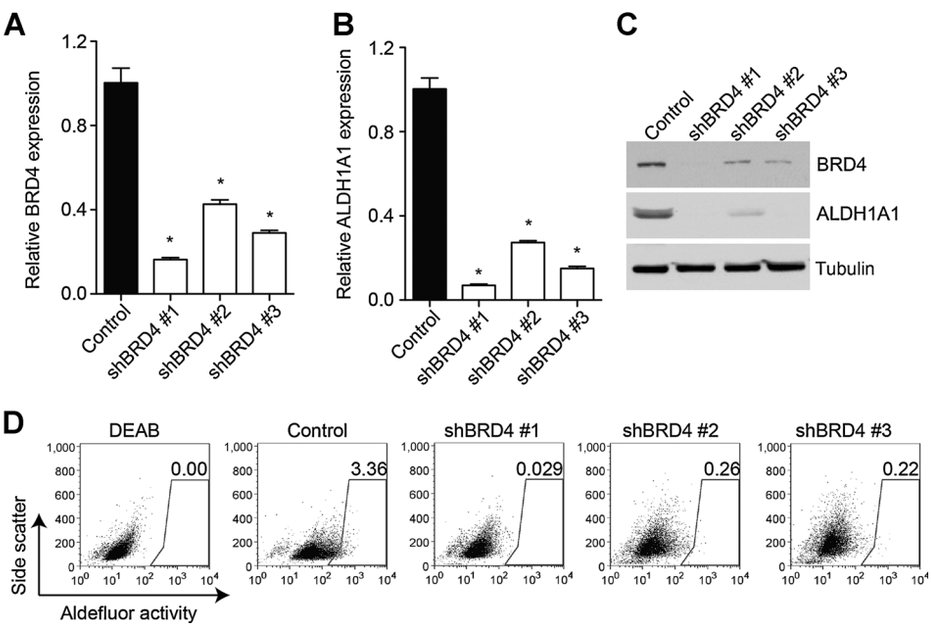

Figure 3.
BRD4 regulates ALDH1A1 expression and ALDH activity. **A–C,** OVCAR3 cells were infected with lentivirus encoding the indicated short hairpin RNA to the human *BRD4* gene (shBRD4) or control. The drug-selected cells were examined for the expression of *BRD4* (**A**) and *ALDH1A1* (**B**) mRNA by qRT-PCR or for the expression of BRD4 and ALDH1A protein expression by immunoblotting (**C**). Mean of three independent experiments with SEM. *, $P < 0.002$. **D,** same as **A**, but examined for ALDH activity by FACS. The percentage of ALDH activity–positive cells is indicated.

cisplatin in the *in vitro*–derived cisplatin-resistant EOC cell line A2780 CP70 (Fig. 2B). Furthermore, in colony formation assays, JQ1 significantly suppressed the outgrowth of EOC cells after cisplatin treatment in multiple EOC cell lines (Fig. 2C and D and Supplementary Fig. S2A and S2B). This correlated with inhibition of ALDH activity (Fig. 2E) and suppression of the upregulated

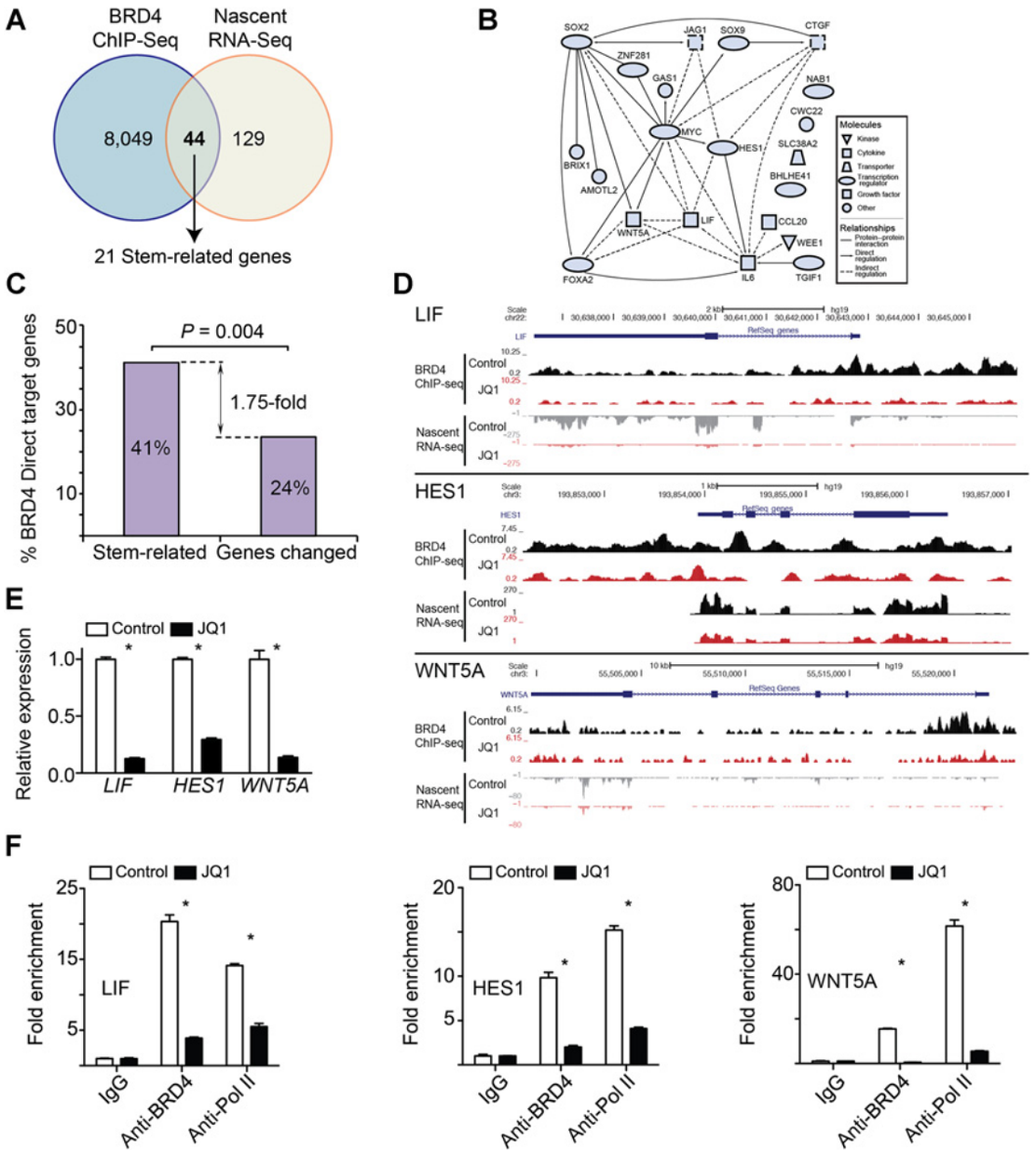

Figure 4.

JQ1 suppresses stem-related genes. **A,** diagram of the strategies used for identifying direct BRD4 target genes as an overlap between BRD4 differentially occupied genes and genes differentially expressed in response to JQ1. A total of 8,049 BRD4-binding sites showed significant reduction after JQ1 treatment (FDR < 1%). A total of 129 genes were significantly altered by JQ1 (FDR < 10%). Twenty-one of 44 direct BRD4 target genes whose expression was affected by JQ1 are stem related, which are all downregulated by JQ1. **B,** regulation and protein–protein interaction network for stem-related genes identified in **A**. **C,** enrichment analysis of direct BRD4 target genes shows a significant enrichment of stem-related genes among direct BRD4 target genes affected by JQ1 (21/51 affected stem-related genes were BRD4 direct targets compared with 282/1,196 of all genes changed, identified on the basis of the significance threshold of $P < 0.05$). **D,** BRD4 ChIP-seq and nascent RNA-seq tracks from control and JQ1-treated cells were aligned using bowtie and bowtie 2 algorithm. *LIF, HES1*, and *WNT5A* genomic locus ChIP-seq and nascent RNA-seq are displayed. **E,** validation of *LIF, HES1*, and *WNT5A* mRNA downregulation by JQ1. Relative mRNA expression level of the indicated stem-related genes was measured by qRT-PCR with or without 125 nmol/L JQ1 treatment for 24 hours. $n = 3$; *, $P < 0.001$. **F,** JQ1 reduces the association of BRD4 and Pol II with the promoters of the indicated stem-related genes. ChIP analysis of OVCAR3 cells treated with control vehicle or JQ1 (125 nmol/L) using antibodies against BRD4 or RNA Pol II for the human *LIF, HES1*, and *WNT5A* gene promoter. An isotype-matched IgG was used as a control ($n = 3$; *, $P < 0.05$). Error bars, SEM.

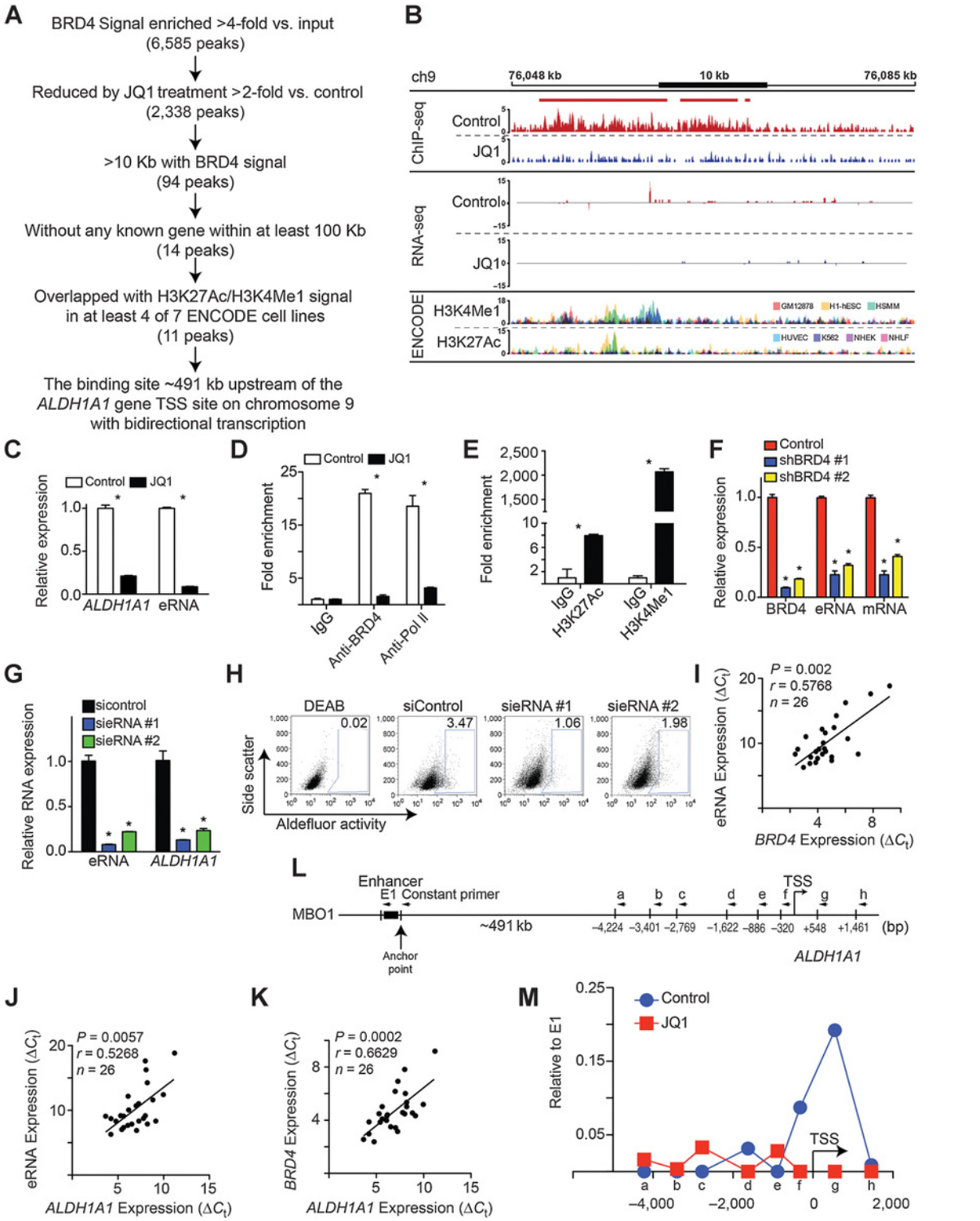

Figure 5.

BRD4 regulates *ALDH1A1* expression through a super-enhancer and its associated enhancer RNA. **A,** flow diagram of the strategies used for identifying the putative super-enhancer for *ALDH1A1* gene. **B,** BRD4 ChIP-seq and nascent RNA-seq tracks from control and JQ1-treated cells were aligned. The putative super-enhancer loci are displayed together with enhancer histone marks H3K4Me1 and H3K27Ac tracks from ENCODE database from the indicated cell lines. **C,** validation of downregulation of the eRNA and *ALDH1A1* mRNA by JQ1. OVCAR3 cells were treated with or without 125 nmol/L JQ1 for 24 hours, and the expression of *ALDH1A1* mRNA and the eRNA expression was determined by qRT-PCR. (*Continued on the following page.*)

ALDH1A1 induced by cisplatin (Fig. 2F and Supplementary Fig. S2C). We observed an increase in apoptotic markers, such as cleaved caspase-3, cleaved lamin A and cleaved PARP p85 and Annexin V in the cells treated with JQ1 and cisplatin in combination compared with either treatment alone (Fig. 2G and Supplementary Fig. S2D and S2E). Notably, JQ1 significantly decreased anchorage-independent sphere formation in ALDH-positive cells, a characteristic of putative ovarian CSCs (24), to a degree that is comparable with those observed in ALDH-negative cells (Fig. 2H–J).

The BET family is composed of BRD2, BRD3, BRD4, and the testis-specific BRDT proteins (12). BRD4 is often amplified in EOC (25). BRD4 amplification predicts a worse overall/disease-free survival in EOC patients (26). Consistent with a previous report (27), we showed that BRD4 is expressed in both EOC cell lines and primary high-grade serous EOC specimens, and BRD4 knockdown suppressed the growth of EOC cells (Supplementary Fig. S3A–S3D). Notably, cisplatin did not affect BRD4 expression (Supplementary Fig. S3E). BRD4 knockdown by multiple shRNAs and in multiple EOC cell lines suppressed ALDH1A1 expression and consequently decreased ALDH activity (Fig. 3A–D and Supplementary Fig. S3F–S3I). The oncogene *c-MYC* is a well-established target gene of BRD4 (27). JQ1-induced suppression of ALDH activity and ALDH1A1 downregulation is not a consequence of c-MYC downregulation, as *c-MYC* knockdown did not affect either ALDH1A1 expression or ALDH activity (Supplementary Fig. S3J and S3K). In contrast to BRD4 knockdown, knockdown of BRD2 or BRD3 did not suppress ALDH activity (Supplementary Fig. S3L and S3M), suggesting that BRD4 plays a major role in the observed suppression of ALDH activity by BET inhibitors, such as JQ1.

BRD4 targets the promoters of stem-related genes

BRD4 transcriptionally regulates its target gene expression (12). BRD4 is also known to regulate lineage-specific gene expression through enhancer elements (28–30), which contributes to the observed specificity and selectivity of BET inhibitors. We determined whether the observed phenotypes induced by JQ1 are due to changes in BRD4 target gene expression. Nascent transcript RNA-seq in OVCAR3 cells treated with or without JQ1 for 40 minutes was performed to identify early changes in the gene expression that are likely directly dependent on BRD4 inhibition (Fig. 4A). In addition, BRD4 ChIP followed by next-generation sequencing (ChIP-seq) analysis was performed in OVCAR3 cells treated with or without JQ1 to identify genome-wide changes in BRD4 association induced by JQ1 (Fig. 4A and Supplementary Fig. S4A and S4B). The nascent RNA-seq and ChIP-seq data are available in the Gene Expression Omnibus database (accession number GSE77568). ChIP-seq analysis indicated that BRD4 predominantly occupied promoter regions within 1 kb from transcription starting sites (Supplementary Fig. S4A and S4B). Cross-referencing of the RNA-seq and BRD4 ChIP-seq revealed that BRD4 direct target genes regulated by JQ1 treatment are significantly enriched for putative stem-related genes (Fig. 4B–C; Supplementary Fig. S4C and S4D). We validated three genes known to be implicated in CSCs, namely *LIF* (31), *HES1* (32), and *WNT5A* (33), as direct BRD4 targets that are downregulated by JQ1 (Fig. 4D–E and Supplementary Fig. S4E). This observation correlated with a decrease in the association of BRD4 and RNA polymerase II with the promoter regions of these genes after JQ1 treatment (Fig. 4F). These results support the notion that JQ1 may affect putative ovarian CSCs by regulating BRD4 binding to the promoters of the identified stem-related genes.

BRD4 regulates *ALDH1A1* expression through a super-enhancer element and its associated eRNA

JQ1 decreased *ALDH1A1* mRNA expression (Fig. 1). However, JQ1 did not affect BRD4 binding to the *ALDH1A1* promoter region (Supplementary Fig. S5A). This suggests that JQ1 regulates *ALDH1A* transcription through a distal regulatory element. As BRD4 is known to regulate super-enhancer elements (28–30), we examined the role of JQ1 in regulating super-enhancers through BRD4 (Fig. 5A). To do so, we focused on BRD4-binding regions that were enriched at least 4-fold compared with input DNA and were significantly reduced by JQ1 treatment (>2-fold, $P < 0.05$). In addition, we prioritized the list by focusing on BRD4-binding regions that spanned >10 kb and with no known genes located within at least 100 kb. We then overlapped these regions with ENCODE ChIP-seq data and considered only BRD4-binding regions that overlapped with the enhancer H3K4Me1/H3K27Ac histone marks. Our prioritization resulted in a list of 11 candidate BRD4-binding sites similar to those previously described for super-enhancers (Supplementary Table S3; ref. 28). Interestingly, one of the potential super-enhancers is 491 kb upstream of the *ALDH1A1* gene (Supplementary Table S3). On the basis of RNA-seq analysis, this region is bidirectionally transcribed into RNA albeit with low reads (Fig. 5B), which is also a known feature of super-enhancers (34, 35). We validated that JQ1 treatment decreased the expression of the RNA transcribed from the super-enhancer element (eRNA; Fig. 5C). This decrease in eRNA expression significantly correlated with the decrease in *ALDH1A1* mRNA expression (Fig. 5C). We validated that the super-enhancer region is enriched in BRD4 and Pol II binding,

(*Continued.*) **D,** same as **C**, but validated for a decrease in the association of BRD4 and Pol II with the enhancer locus by ChIP analysis. An isotype-matched IgG was used as a control. $n = 3$; *, $P < 0.0001$. **E,** validation of H3K27Ac and H3K4Me1 enhancer histone marks' association with the enhancer loci by ChIP analysis. $n = 3$; *, $P < 0.002$. **F,** BRD4 knockdown reduces the levels of eRNA expression and suppresses *ALDH1A1* expression. OVCAR3 cells were infected with lentivirus encoding the indicated shBRD4 or control. Drug-selected cells were examined for the expression of *BRD4* mRNA, eRNA, and *ALDH1A1* mRNA by qRT-PCR. $n = 3$; *, $P < 0.0001$. **G,** knockdown of the eRNA suppresses *ALDH1A1* expression. OVCAR3 cells were transfected with two independent siRNAs to the eRNA for 72 hours, and expression of the eRNA and *ALDH1A1* mRNA was determined by qRT-PCR. $n = 3$; *, $P < 0.002$. **H,** same as **G**, but examined for ALDH activity. The percentage of ALDH-positive cells is indicated. **I–K,** positive correlation between *BRD4* and eRNA (**I**), between eRNA and *ALDH1A1* (**J**), or between *BRD4* and *ALDH1A1* (**K**) in a panel of 26 cases of HGSOC. Expression of *BRD4*, eRNA, and *ALDH1A1* was determined by qRT-PCR, and correlation was determined by Spearman statistical analysis. **L,** diagrams of *ALDH1A1* genomic regions with its enhancer (black box). Arrowheads, position of primers used for detection of chromatin looping; stick bars, Mbo1 enzyme digestion sites (a–h). Constant primer at the anchor point is also indicated. TSS, *ALDH1A1* gene transcription-starting site. **M,** 3C-quantitative PCR analysis of the looping events between the enhancer and the *ALDH1A1* promoter region were detected at f and g sites, which were reduced by JQ1 (125 nmol/L) treatment for 24 hours. The relative cross-linking frequency was normalized to the closest Mbo1 digestion site E1. *x*-axis, distance from *ALDH1A1* transcription start site (TSS).

another feature of super-enhancers (Fig. 5D; ref. 35). Furthermore, we validated the enrichment of H3K27Ac and H3K4Me1 epigenetic histone modifications in the putative super-enhancer regions (Fig. 5E). Finally, knockdown of BRD4 expression was sufficient to decrease the eRNA expression, which correlated with the decrease in *ALDH1A1* mRNA (Fig. 5F). To directly determine whether the eRNA regulates *ALDH1A1* mRNA expression, we knocked down the eRNA expression using siRNAs (36, 37). Knockdown of the eRNA downregulated *ALDH1A1* mRNA expression (Fig. 5G), which correlated with a decrease in ALDH activity (Fig. 5H). Notably, there was a significant positive correlation between BRD4, eRNA, and ALDH1A1 expression in a panel of 26 cases of HGSC specimens (Fig. 5I–K). This further highlights the established regulation of eRNA by BRD4 and subsequent ALDH1A1 expression by eRNA.

An important component of enhancer function is the formation of chromatin looping, allowing enhancer and promoter interaction (36, 38, 39). We directly examined chromatin looping between the super-enhancer and *ALDH1A1* gene promoter using 3C in cells with or without JQ1 treatment. We observed a robust association between the super-enhancer and the promoter region of the *ALDH1A1* gene (Fig. 5L and M). Remarkably, JQ1 treatment abrogated the chromatin looping between the super-enhancer and the promoter of *ALDH1A1* gene (Fig. 5M). These results support the notion that JQ1 regulates transcription of *ALDH1A1* through the newly identified super-enhancer.

JQ1 inhibits expression of ALDH1A1 and its associated eRNA induced by cisplatin *in vivo* and combination of JQ1 and cisplatin improves survival

BET inhibitors have been proven safe in patients (40). ALDH-positive cells contribute to tumor progression and relapse after initial response to chemotherapy (3, 8). To determine the effects of BET inhibitor on tumor relapse after cisplatin treatment, we orthotopically transplanted luciferase-expressing OVCAR3 cells into the peritoneal cavity of immunocompromised NSG female mice. The injected cells were allowed to grow for 3 weeks to establish tumors. We randomly assigned mice into four groups and treated mice with vehicle control ($n = 12$), cisplatin (750 μg/kg every 2 weeks, $n = 12$), JQ1 (20 mg/kg daily, $n = 11$), and a combination of cisplatin and JQ1 ($n = 13$) by intraperitoneal injection for an additional 4 weeks. Doses of JQ1 and cisplatin used were determined on the basis of suppression of ALDH1A1 expression by JQ1 and regression of ovarian tumor in a pilot experiment (Supplementary Fig. S6A–S6E). Notably, the survival of the combination-treated mice was significantly extended compared with mice treated with cisplatin alone (Fig. 6A). We followed the

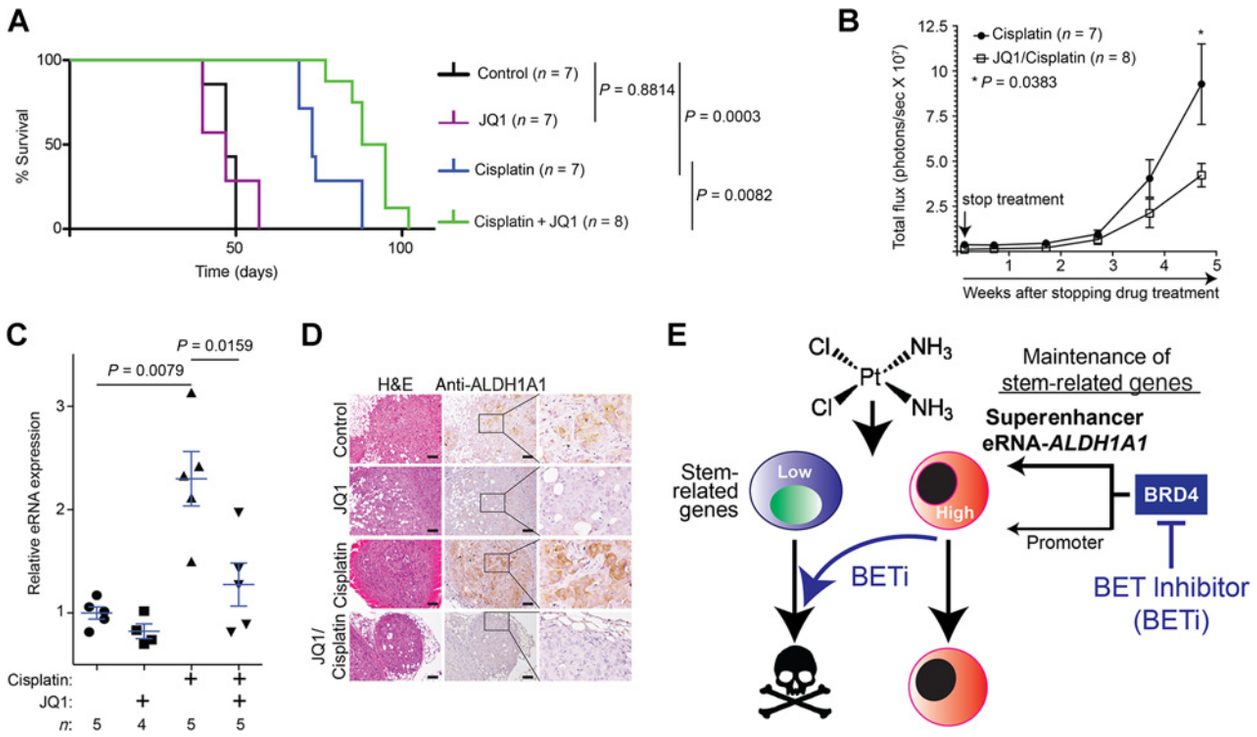

Figure 6.

The combination of JQ1 and cisplatin improves survival of tumor-bearing mice. **A,** combination of JQ1 and cisplatin improves survival of tumor-bearing mice. Kaplan–Meier survival curves of mice in the indicated groups posttreatment were plotted using Prism software. $n = 7$ for the indicated groups except in the combination group, $n = 8$. **B,** quantification of tumor growth in the indicated groups after stopping drug treatment. **C,** same as **A**. Tumors from the indicated treatment groups were examined for eRNA expression by qRT-PCR at the end of the treatment. **D,** same as **C**. Tumors were sectioned and subjected to immunohistochemical staining using antibodies against ALDH1A1. Scale bar, 100 μm. **E,** a model for the mechanism underlying the observed synergy between BET inhibitor and cisplatin.

tumor outgrowth/relapse in mice treated with cisplatin with or without JQ1 combination after stopping drug treatment. Indeed, the outgrowth of the tumors in the combination treatment group was significantly slower compared with the cisplatin only treatment group (Fig. 6B). RNA from tumors harvested from the control and the three different treatment groups was utilized for qRT-PCR analysis. We observed that eRNA expression was induced by cisplatin alone (Fig. 6C), whereas JQ1 treatment suppressed the cisplatin-induced eRNA expression (Fig. 6C). This correlated with changes in ALDH1A1 expression in these treatment groups (Fig. 6D and Supplementary Fig. S6F). *ALDH1A1* mRNA expression was also significantly downregulated in JQ1-treated tumors (Supplementary Fig. S6G). In addition, stem-related genes, such as *LIF* and *WNT5A*, were downregulated in JQ1/cisplatin-treated tumors (Supplementary Fig. S6H). However, BRD4 expression was not significantly changed in treatment groups (Supplementary Fig. S6I). Together, we conclude that a combination of JQ1 and cisplatin improves the survival of EOC-bearing mice, which correlates with the suppression of expression of ALDH1A1 and its eRNA.

Discussion

Here, we found that BET inhibitors suppress ALDH activity. This correlates with the suppression of *ALDH1A1* expression by a BRD4-regulated super-enhancer and downregulation of its encoded eRNA (Fig. 6E). BET inhibitors are now in clinical development and are safe. This suggests that BET inhibitors can be repurposed to target ALDH activity for improving platinum-based chemotherapy by inhibiting tumor relapse, a major challenge in the clinical management of EOC. Notably, BRD4 amplification/overexpression is often mutually exclusive with "BRCAness" in EOC (25). Thus, there is an even greater need for novel therapeutic strategies for this patient population given the limited therapeutic options available (2). Our experiments clearly show that BET inhibitors, an existing class of epigenetic targeting drugs, target ALDH activity, potentiate the tumor suppression induced by cisplatin, and improve survival of EOC-bearing mice *in vivo*. These findings will facilitate the rapid evaluation of this new strategy in the clinic for EOC.

BRD4 is a general transcriptional regulator that controls global gene expression patterns (12). Investigation of genes hypersensitive to BET inhibition revealed that such genes typically exhibit BRD4 occupancy at super-enhancer elements (28–30). This raises the possibility that BET inhibition is selective in gene regulation and thus confers relative specificity in a cell context–dependent manner. Our findings revealed that in response to JQ1 treatment, BRD4 assumes a key role in transcriptional control of the *ALDH1A1* gene through regulating its super-enhancer and the associated eRNA. Although BRD4 plays a key role in regulating *ALDH1A1* transcription, there are potentially other mechanisms than BRD4 expression levels that regulate ALDH1A1 expression (12). BRD4 plays a key role in CSCs by selectively regulating the *ALDH1A1* super-enhancer. In this context, BET inhibitors may selectively target CSCs by their effect on the *ALDH1A1* super-enhancer. In addition to suppressing ALDH1A1 expression and ALDH activity, JQ1 also directly suppresses the expression of stem-related genes through reducing BRD4′s association with their promoters (Fig. 4). Thus, the mode of action of BET inhibitors is multifaceted and likely involves a broad range of changes in transcription and the associated signaling pathways (Fig. 6E). Given the established role of ALDH1A1 in ovarian CSCs (4), our data support the idea that the BRD4-regulated *ALDH1A1* super-enhancer plays a key role in the observed phenotypes induced by BET inhibitors.

Our studies demonstrate that targeting BRD4 activity through the use of clinically applicably BET inhibitors represents a novel strategy for targeting ALDH activity. This correlates with suppression of *ALDH1A1* expression via a BRD4-regulated super-enhancer and its associated eRNA. Given that there is currently no clinically applicable ALDH activity inhibitor, we expect our finding to have far-reaching implications for developing future therapeutic strategies using epigenetic targeting BET inhibitors in cancers such as EOC.

Disclosure of Potential Conflicts of Interest

J.E. Bradner is the president at Novartis Institute of BioMedical Research. No potential conflicts of interest were disclosed by the other authors.

Authors' Contributions

Conception and design: Y. Yokoyama, H. Zhu, S.Y. Wu, A. Gardini, B.G. Bitler, R. Zhang

Development of methodology: Y. Yokoyama, H. Zhu, K.C. Palozola, J.E. Bradner, A.K. Sood, T. Ordog, B.G. Bitler

Acquisition of data (provided animals, acquired and managed patients, provided facilities, etc.): Y. Yokoyama, H. Zhu, J.H. Lee, S.Y. Wu, L.C. Showe, K.S. Zaret, A.K. Sood, T. Ordog, B.G. Bitler

Analysis and interpretation of data (e.g., statistical analysis, biostatistics, computational analysis): Y. Yokoyama, H. Zhu, A.V. Kossenkov, J.M. Wickramasinghe, X. Yin, A. Gardini, L.C. Showe, Q. Liu, D. Speicher, J.R. Conejo-Garcia, A.K. Sood, B.G. Bitler

Writing, review, and/or revision of the manuscript: Y. Yokoyama, H. Zhu, A.V. Kossenkov, S.Y. Wu, L.C. Showe, Q. Liu, D. Speicher, J.R. Conejo-Garcia, A.K. Sood, T. Ordog, B.G. Bitler, R. Zhang

Administrative, technical, or material support (i.e., reporting or organizing data, constructing databases): H. Zhu, K.S. Zaret, B.G. Bitler

Study supervision: Z. Zhang, B.G. Bitler, R. Zhang

Other (performed Brd4 ChIP-seq experiments and read the manuscript): Z. Zhang

Acknowledgments

We thank The Structure Genomics Consortium for providing the epigenetic inhibitors library. We also thank Drs. Gerd Blobel and Katherine Aird for critical comments.

Grant Support

This work was supported by NIH/NCI grants (R01CA163377 and R01CA202919 to R. Zhang; and CA083639 to A.K. Sood), U.S. Department of Defense (OC140632P1 and OC150446 to R. Zhang), an Ovarian Cancer Research Fund (OCRF) program project (R. Zhang), and The Jayne Koskinas & Ted Giovanis Breast Cancer Research Consortium at Wistar (R. Zhang). H. Zhu is an OCRF Ann Schreiber Mentored Investigator (372953). B.G. Bitler is supported by an NIH/NCI grant (K99CA194318). S.Y. Wu is supported by the OCRF, Foundation for Women's Cancer, and by Cancer Prevention and Research Institute of Texas training grants (RP101502 and RP101489). Support of Core Facilities was provided by Cancer Center Support Grant (CCSG) CA010815 to The Wistar Institute.

The costs of publication of this article were defrayed in part by the payment of page charges. This article must therefore be hereby marked *advertisement* in accordance with 18 U.S.C. Section 1734 solely to indicate this fact.

Received March 26, 2016; revised July 15, 2016; accepted August 11, 2016; published OnlineFirst November 1, 2016.

References

1. Martin LP, Hamilton TC, Schilder RJ. Platinum resistance: the role of DNA repair pathways. Clin Cancer Res 2008;14:1291–5.
2. Bowtell DD, Bohm S, Ahmed AA, Aspuria PJ, Bast RC Jr, Beral V, et al. Rethinking ovarian cancer II: reducing mortality from high-grade serous ovarian cancer. Nat Rev Cancer 2015;15:668–79.
3. Chen J, Li Y, Yu TS, McKay RM, Burns DK, Kernie SG, et al. A restricted cell population propagates glioblastoma growth after chemotherapy. Nature 2012;488:522–6.
4. Landen CN Jr, Goodman B, Katre AA, Steg AD, Nick AM, Stone RL, et al. Targeting aldehyde dehydrogenase cancer stem cells in ovarian cancer. Mol Cancer Ther 2010;9:3186–99.
5. Steg AD, Bevis KS, Katre AA, Ziebarth A, Dobbin ZC, Alvarez RD, et al. Stem cell pathways contribute to clinical chemoresistance in ovarian cancer. Clin Cancer Res 2012;18:869–81.
6. Choi YJ, Ingram PN, Yang K, Coffman L, Iyengar M, Bai S, et al. Identifying an ovarian cancer cell hierarchy regulated by bone morphogenetic protein 2. Proc Natl Acad Sci U S A 2015;112:E6882–8.
7. Flesken-Nikitin A, Hwang CI, Cheng CY, Michurina TV, Enikolopov G, Nikitin AY. Ovarian surface epithelium at the junction area contains a cancer-prone stem cell niche. Nature 2013;495:241–5.
8. Tomita H, Tanaka K, Tanaka T, Hara A. Aldehyde dehydrogenase 1A1 in stem cells and cancer. Oncotarget 2016;7:11018–32.
9. Garraway LA, Lander ES. Lessons from the cancer genome. Cell 2013; 153:17–37.
10. Lawrence MS, Stojanov P, Mermel CH, Robinson JT, Garraway LA, Golub TR, et al. Discovery and saturation analysis of cancer genes across 21 tumour types. Nature 2014;505:495–501.
11. Huston A, Arrowsmith CH, Knapp S, Schapira M. Probing the epigenome. Nat Chem Biol 2015;11:542–5.
12. Shi J, Vakoc CR. The mechanisms behind the therapeutic activity of BET bromodomain inhibition. Mol Cell 2014;54:728–36.
13. Filippakopoulos P, Knapp S. Targeting bromodomains: epigenetic readers of lysine acetylation. Nat Rev Drug Discov 2014;13:337–56.
14. Matei D, Fang F, Shen C, Schilder J, Arnold A, Zeng Y, et al. Epigenetic resensitization to platinum in ovarian cancer. Cancer Res 2012;72:2197–205.
15. Brown R, Curry E, Magnani L, Wilhelm-Benartzi CS, Borley J. Poised epigenetic states and acquired drug resistance in cancer. Nat Rev Cancer 2014;14:747–53.
16. Li H, Cai Q, Godwin AK, Zhang R. Enhancer of zeste homolog 2 promotes the proliferation and invasion of epithelial ovarian cancer cells. Mol Cancer Res 2010;8:1610–8.
17. Rao SS, Huntley MH, Durand NC, Stamenova EK, Bochkov ID, Robinson JT, et al. A 3D map of the human genome at kilobase resolution reveals principles of chromatin looping. Cell 2014;159:1665–80.
18. Hagege H, Klous P, Braem C, Splinter E, Dekker J, Cathala G, et al. Quantitative analysis of chromosome conformation capture assays (3C-qPCR). Nat Protoc 2007;2:1722–33.
19. Bitler BG, Aird KM, Garipov A, Li H, Amatangelo M, Kossenkov AV, et al. Synthetic lethality by targeting EZH2 methyltransferase activity in ARID1A-mutated cancers. Nat Med 2015;21:231–8.
20. Filippakopoulos P, Qi J, Picaud S, Shen Y, Smith WB, Fedorov O, et al. Selective inhibition of BET bromodomains. Nature 2010;468:1067–73.
21. Chou TC. Drug combination studies and their synergy quantification using the Chou-Talalay method. Cancer Res 2010;70:440–6.
22. Domcke S, Sinha R, Levine DA, Sander C, Schultz N. Evaluating cell lines as tumour models by comparison of genomic profiles. Nat Commun 2013; 4:2126.
23. Debeb BG, Lacerda L, Xu W, Larson R, Solley T, Atkinson R, et al. Histone deacetylase inhibitors stimulate dedifferentiation of human breast cancer cells through WNT/beta-catenin signaling. Stem Cells 2012;30:2366–77.
24. Wang Y, Cardenas H, Fang F, Condello S, Taverna P, Segar M, et al. Epigenetic targeting of ovarian cancer stem cells. Cancer Res 2014;74: 4922–36.
25. Goundiam O, Gestraud P, Popova T, De la Motte Rouge T, Fourchotte V, Gentien D, et al. Histo-genomic stratification reveals the frequent amplification/overexpression of CCNE1 and BRD4 genes in non-BRCAness high grade ovarian carcinoma. Int J Cancer 2015;137:1890–900.
26. Zhang Z, Ma P, Jing Y, Yan Y, Cai MC, Zhang M, et al. BET bromodomain inhibition as a therapeutic strategy in ovarian cancer by downregulating FoxM1. Theranostics 2016;6:219–30.
27. Baratta MG, Schinzel AC, Zwang Y, Bandopadhayay P, Bowman-Colin C, Kutt J, et al. An in-tumor genetic screen reveals that the BET bromodomain protein, BRD4, is a potential therapeutic target in ovarian carcinoma. Proc Natl Acad Sci U S A 2015;112:232–7.
28. Loven J, Hoke HA, Lin CY, Lau A, Orlando DA, Vakoc CR, et al. Selective inhibition of tumor oncogenes by disruption of super-enhancers. Cell 2013;153:320–34.
29. Whyte WA, Orlando DA, Hnisz D, Abraham BJ, Lin CY, Kagey MH, et al. Master transcription factors and mediator establish super-enhancers at key cell identity genes. Cell 2013;153:307–19.
30. Hnisz D, Abraham BJ, Lee TI, Lau A, Saint-Andre V, Sigova AA, et al. Super-enhancers in the control of cell identity and disease. Cell 2013;155: 934–47.
31. Penuelas S, Anido J, Prieto-Sanchez RM, Folch G, Barba I, Cuartas I, et al. TGF-beta increases glioma-initiating cell self-renewal through the induction of LIF in human glioblastoma. Cancer Cell 2009;15:315–27.
32. Liu ZH, Dai XM, Du B. Hes1: a key role in stemness, metastasis and multidrug resistance. Cancer Biol Ther 2015;16:353–9.
33. Povinelli BJ, Nemeth MJ. Wnt5a regulates hematopoietic stem cell proliferation and repopulation through the Ryk receptor. Stem Cells 2014;32: 105–15.
34. Kim TK, Hemberg M, Gray JM, Costa AM, Bear DM, Wu J, et al. Widespread transcription at neuronal activity-regulated enhancers. Nature 2010;465: 182–7.
35. Pott S, Lieb JD. What are super-enhancers? Nat Genet 2015;47:8–12.
36. Melo CA, Drost J, Wijchers PJ, van de Werken H, de Wit E, Oude Vrielink JA, et al. eRNAs are required for p53-dependent enhancer activity and gene transcription. Mol Cell 2013;49:524–35.
37. Schaukowitch K, Joo JY, Liu X, Watts JK, Martinez C, Kim TK. Enhancer RNA facilitates NELF release from immediate early genes. Mol Cell 2014;56: 29–42.
38. Mousavi K, Zare H, Dell'orso S, Grontved L, Gutierrez-Cruz G, Derfoul A, et al. eRNAs promote transcription by establishing chromatin accessibility at defined genomic loci. Mol Cell 2013;51:606–17.
39. Sanyal A, Lajoie BR, Jain G, Dekker J. The long-range interaction landscape of gene promoters. Nature 2012;489:109–13.
40. Herait PE, Berthon C, Thieblemont C, Raffoux E, Magarotto V, Stathis A, et al. BET-bromodomain inhibitor OTX015 shows clinically meaningful activity at nontoxic doses: interim results of an ongoing phase I trial in hematologic malignancies. In: Proceedings of the 105th Annual Meeting of the American Association for Cancer Research; 2014 Apr 5–9; San Diego, CA. Philadelphia (PA): AACR; 2014. Abstract nr CT231.

HHS Public Access

Author manuscript

Cancer Discov. Author manuscript; available in PMC 2016 May 01.

Published in final edited form as:

Cancer Discov. 2015 November ; 5(11): 1137–1154. doi:10.1158/2159-8290.CD-15-0714.

Homologous recombination deficiency: Exploiting the fundamental vulnerability of ovarian cancer

Panagiotis A. Konstantinopoulos, M.D., Ph.D.[1,3], **Raphael Ceccaldi, Ph.D.**[2,3], **Geoffrey I. Shapiro, M.D., Ph.D.**[3,4], and **Alan D. D'Andrea, M.D.**[2,3,*]

[1]Department of Medical Oncology, Medical Gynecologic Oncology Program, Dana-Farber Cancer Institute, Harvard Medical School

[2]Department of Radiation Oncology, Dana-Farber Cancer Institute, Harvard Medical School

[3]Center for DNA Damage and Repair, Dana-Farber Cancer Institute, Harvard Medical School

[4]Department of Medical Oncology, Early Drug Development Center, Dana-Farber Cancer Institute, Harvard Medical School

Abstract

Approximately 50% of epithelial ovarian cancers (EOCs) exhibit defective DNA repair via homologous recombination (HR) due to genetic and epigenetic alterations of HR pathway genes. Defective HR is an important therapeutic target in EOC as exemplified by the efficacy of platinum analogues in this disease, as well as the advent of poly-ADP ribose polymerase inhibitors which exhibit synthetic lethality when applied to HR deficient cells. Here, we describe the genotypic and phenotypic characteristics of HR deficient EOCs, discuss current and emerging approaches for targeting these tumors, and present challenges associated with these approaches focusing on development and overcoming resistance.

INTRODUCTION

Epithelial ovarian cancer (EOC) remains the most lethal gynecologic malignancy and the fifth most frequent cause of cancer-related mortality in women in United States (1). Approximately 75% of EOC patients are diagnosed with advanced disease which is curable only in a minority of the cases resulting in a modest 5-year overall survival rate of 20–30% (2, 3). The standard of care management of EOC consists of primary surgical cytoreduction followed by platinum-based chemotherapy (3, 4). Platinum analogues have been used to treat ovarian cancer since the late 1970s when clinical trials demonstrated that cisplatin was capable of achieving almost double the overall response rates and the number of complete responses compared with non-platinum agents (5, 6). Since then, platinum agents (initially cisplatin, then carboplatin which is better tolerated but equally effective (7)) have

*Address for correspondence: Alan D. D'Andrea, M.D., Dana Farber Cancer Institute, 450 Brookline Avenue, Boston, MA 02215, alan_dandrea@dfci.harvard.edu, Phone:617-632-2080 Or Panagiotis A. Konstantinopoulos, MD, Ph.D., Dana Farber Cancer Institute, 450 Brookline Avenue, Boston, MA 02215, panagiotis_konstantinopoulos@dfci.harvard.edu, Phone: 617-632-5269.

CONFLICTS OF INTEREST

Dr. Shapiro and Dr. Konstantinopoulos have served as consultants/advisory board members for Vertex. Dr. Shapiro and Dr. D'Andrea serve as consultants and receive research funding from Eli Lilly and Company.

constituted the backbone of chemotherapy used in EOC and have defined the comparison arms for the majority of the clinical trials conducted in this disease. However, despite important advancements in the efficacy of platinum chemotherapy achieved by incorporation of taxanes (8) in the 1990s and by administration of chemotherapy via the intraperitoneal (IP) route (9) in early 2000, the plateau of the survival curve has not changed appreciably (3, 8, 10–12), suggesting that alternative approaches are urgently needed.

Platinum analogs induce intrastrand and interstrand cross-links (ICLs) between purine bases of the DNA. ICLs are extremely deleterious lesions that covalently tether both duplex DNA strands and pose formidable blocks to DNA repair (13). Repair of ICLs is dependent on both Fanconi Anemia (FA) and BRCA proteins, which act in a common DNA repair pathway (also referred to as the Fanconi Anemia/BRCA pathway) that involves homologous recombination (HR) (14, 15) (Figure 1). The striking platinum sensitivity of EOC tumors is thought to be related to an underlying defect in HR-mediated DNA repair, particularly in those with high grade serous histology (approximately 70% of all EOCs). In this regard, a plethora of genetic studies, and most recently The Cancer Genome Atlas (TCGA) project, have consistently shown that high grade serous ovarian cancers (HGSOCs) are characterized by frequent genetic and epigenetic alterations of HR pathway genes, most commonly BRCA1 and BRCA2 genes (16, 17). Defective HR is an important therapeutic target in EOC, as exemplified by the central role of platinum agents in the management of this disease as well as the advent of poly-ADP ribose polymerase inhibitors (PARPis), a novel class of anticancer agents which exhibit synthetic lethal effects when applied to cells with defective HR (18–21). In this review, we discuss the molecular alterations and clinical phenotype of HR deficient EOCs, describe current and emerging approaches for targeting HR deficient ovarian cancers, and present the challenges associated with these approaches focusing on development and overcoming drug resistance.

HR PATHWAY ALTERATIONS IN EOC

Approximately 50% of HGSOCs exhibit genetic or epigenetic alterations in the FA/BRCA pathway (Figure 2) (16). Although these alterations are most commonly encountered in high grade serous histology, nonserous histologies including clear cell, endometrioid and carcinosarcomas have also been shown to harbor such alterations (22). Germline BRCA1 and BRCA2 mutations are the most common alterations, and are present in 14–15% of all EOCs (23, 24) and as high as 22.6% of HGSOCs (16, 23, 24) while somatic BRCA1 and BRCA2 mutations have been identified in 6–7% of high grade serous EOCs (16, 25). Although in the TCGA dataset there was a similar incidence of germline and somatic BRCA1 and BRCA2 mutations, BRCA1 mutations are more commonly observed (60% of all BRCA mutations) in other datasets (23, 24). Importantly, 81% of BRCA1 and 72% of BRCA2 mutations are accompanied by heterozygous loss (26) indicating that both alleles are inactivated, as predicted by Knudson’s two-hit hypothesis. The majority of germline and somatic BRCA1/2 mutations are frameshift insertions or deletions, while missense mutations are rare; mutations have been identified in all functional domains of BRCA1 (RING, coiled coil and BRCT domains) and BRCA2 (BRC, DNA binding, oligonucleotide-binding folds, and tower domains) genes (27).

Epigenetic silencing via promoter hypermethylation occurs for BRCA1, but not BRCA2, in EOC. BRCA1 promoter hypermethylation has been reported in approximately 10–20% of HGSOCs and is mutually exclusive of BRCA1/2 mutations suggesting that there is strong selective pressure to inactivate BRCA via either mutation or epigenetic silencing in this disease (26, 28, 29). Other HR pathway alterations include mutations in several FA genes (mainly PALB2, FANCA, FANCI, FANCL and FANCC), in core HR RAD genes such as RAD50, RAD51, RAD51C and RAD54L, and in DNA damage response genes involved in HR such as ATM, ATR, CHEK1 and CHEK2 (Figure 2). Interestingly, pathogenic germline RAD51C and RAD51D mutations have been identified in families with both breast and ovarian tumors but not in families with breast cancer (30, 31). RAD51C was also epigenetically silenced via promoter hypermethylation in about 2% of the cases in the TCGA dataset.

Defective HR in EOC may also occur via alterations in non-bona fide HR genes which are known to modulate the HR pathway and indirectly cause HR deficiency. PTEN deficiency has been reported to be synthetically lethal with PARP inhibition and one of the proposed mechanisms is transcriptional downregulation of RAD51(32, 33). A focal deletion region at 10q23.31 that includes only PTEN has been found in approximately 7% of high grade serous EOCs; these tumors exhibit homozygous PTEN deletion which is also associated with downregulation of PTEN at the mRNA level (26). Furthermore, several studies have reported both overexpression and amplification of EMSY as another mechanism of HR deficiency in as high as 17% of high grade sporadic EOC (34). EMSY was identified in a yeast two-hybrid screen to interact with the transactivation domain of BRCA2 leading to inhibition of its transcriptional activity (34). EMSY also colocalizes with BRCA2 at DNA damage sites and interacts with several chromatin remodeling proteins. However, EMSY is located at 11q13, a region known to be amplified in multiple cancers which contains a multiple different oncogenes including LRRC32 (GARP), and PAK112(35). Additionally, EMSY amplification has been associated with worse outcome (35); a finding that would be inconsistent if it caused HR deficiency. For these reasons, although EMSY alterations are commonly cited as a mechanism underlying deficient HR, its role remains controversial. Unlike PTEN and EMSY, the association between inactivating mutations of CDK12 and HR deficiency is clearly established (36, 37). CDK12 is one of the only 9 significantly mutated genes in ovarian cancer (3% of cases in the TCGA dataset) and is known to promote the transcription of several HR pathway genes including BRCA1. Inactivation of CDK12 leads to suppression of HR via reduced expression of BRCA1 and other HR genes, and confers PARPi sensitivity.

It is important to underscore that there may be additional mechanisms underlying defective HR in EOC. Overexpression of specific miRNAs which induce HR deficiency have been identified in breast cancer (such as mir-182 which targets BRCA1)(38) and analogous miRNAs have also been identified in ovarian cancer (such as miR-1255b, miR-148b* and miR-193b* which target BRCA1, BRCA2 and RAD51)(39). Finally, alterations in other DNA repair pathways such as nucleotide excision repair (NER) and mismatch repair (MMR) have been reported in up to 8% and 3% of high grade serous EOCs respectively (Figure 2) (40).

CLINICAL PHENOTYPE OF HR DEFICIENT EOC

Several studies have highlighted a distinct clinical phenotype associated with HR-deficient cancers, especially those with BRCA1/2 mutations. Patients with germline BRCA1/2 mutations are associated with the hereditary breast/ovarian cancer syndrome, which is characterized by familial clustering of breast and ovarian tumors (41). This syndrome has also been linked to germline mutations in other HR genes such as BARD1, BRIP1, MRE11A, NBN, RAD50, CHEK2, ATM, PALB2, RAD51C and RAD51D although the exact penetrance of these genes in terms of breast and/or ovarian cancer remains unknown (22). Large studies have also consistently demonstrated that patients with BRCA1/2-mutated ovarian cancers exhibit significantly improved overall survival compared to patients with non-BRCA mutated tumors; this effect is more pronounced for BRCA2 mutation carriers who exhibit even longer survival compared to BRCA1 carriers (26, 42, 43). Interestingly, the survival advantage of BRCA1 carriers was shown to be dependent on the location of the mutation; worse survival was observed as the mutation site moved from 5′ to 3′ end of the BRCA1 gene (42). Unlike BRCA1/2 mutations, EOCs with epigenetic silencing of BRCA1 through promoter hypermethylation appear not to respond as favorably to platinum and not to exhibit improved survival suggesting that different mechanisms of HR deficiency may confer distinct clinical phenotypes (26, 44). The survival advantage of BRCA-mutated tumors is at least partly related to their enhanced responsiveness to platinum based chemotherapy although a more indolent natural history due to intrinsic biologic differences compared to non BRCA mutated tumors may also play a role. In this regard, although available data suggest that HR deficiency may be both a predictive factor of response to first line platinum chemotherapy and a prognostic factor in EOC, it is unclear whether the prognostic significance of HR deficiency in EOC is solely due to its association with increased sensitivity to chemotherapy or due to other independent factors. For example, several lines of evidence indicate that BRCA1/2-mutated tumors may harbor more tumor-infiltrating lymphocytes and thus be more immunogenic compared to HR proficient EOCs, which may relate to a greater number of mutations observed in these tumors (45, 46). In this regard, the increased immunogenicity of HR deficient tumors may explain their prognostic significance independent of their predictive association with response to 1st line chemotherapy. Whether additional mechanisms may explain the improved survival of HR deficient tumors independently of their enhanced sensitivity to chemotherapy remains to be determined.

BRCA1/2 mutated tumors are also associated with higher grade (grade 2 or grade 3), poorly differentiated or undifferentiated tumors, higher stage (stage III or IV) at presentation, and serous histology (as opposed to endometrioid, clear cell or mucinous histologies)(23, 24, 42, 47). Finally, in terms of pattern of recurrence, BRCA1/2-mutated tumors are more likely to develop visceral metastases (parenchymal liver, lung, adrenal, spleen and brain metastases) and this effect appears more prominent for BRCA1-mutated tumors (23, 48). These clinical features may be at least partly related to the high degree of genomic instability that is characteristic of BRCA1/2-mutated tumors.

BIOMARKERS OF HR DEFICIENCY

Development of a robust biomarker which adequately captures the diverse genetic and epigenetic mechanisms of HR deficiency and is compatible with formalin fixed and paraffin embedded (FFPE) specimens remains elusive. Several approaches have been proposed, including application of gene expression profiles of BRCAness (49) or DNA repair (50), evaluating BRCA1 protein expression by immunohistochemistry (51), and assessing the wider tumor genome nucleotide sequences and mutational spectrums, or ‘sequence scars’, that may be characteristic of defective DNA repair via HR (52). Targeted mutational profiling of HR genes using next-generation sequencing has also been evaluated. BROCA is a targeted capture and massively parallel sequencing assay which accurately identifies all types of mutations of key HR genes including single-base substitutions, small insertions and deletions, and large gene rearrangements (22, 53). Identification of HR gene mutations by BROCA is highly predictive of improved primary response to platinum chemotherapy and longer overall survival in EOC (22). Alternative multigene, next generation sequencing assays are also offered in several cancer centers in the US and routinely include assessment of core HR genes (54).

HR deficient tumors exhibit large (>15Mb) sub-chromosomal deletions and harbor allelic imbalance extending to the telomeric end of the chromosomes with or without changes in overall DNA copy number. Recently, three quantitative metrics of these structural chromosomal aberrations have been developed using single nucleotide polymorphism (SNP) array data. These include: i) the whole genome tumor loss of heterozygosity (LOH) score (55), ii) the telomeric allelic imbalance (TAI) score (56) and iii) the large-scale state transitions (LST) score which quantifies chromosomal breaks between adjacent regions of at least 10 Mb (57). All three scores are highly correlated with alterations in BRCA1/2 and other HR pathway genes in ovarian cancer, and with sensitivity to platinum and PARP-inhibitors (58). These scores have been implemented either alone or in combination with targeted sequencing approaches such as the BROCA assay to achieve better sensitivity in capturing HR deficiency (58). Of note, genomic LOH was recently shown to correlate well with response to the PARPi rucaparib in a phase 2 clinical trial in EOC (ARIEL2). Specifically, among the women without the BRCA 1/2 mutations, those with high genomic LOH had an overall response rate of between 32–40%, while those without LOH had an overall response rate of just 8% (59).

A major limitation of these assays is that they are largely insensitive to reversion of HR deficiency which may occur upon development of resistance to platinum and PARP-inhibitors. When reversion of HR deficiency to HR proficiency occurs, the cumulative defects that had occurred in the cancer genome as the result of the original HR deficiency do not reverse; therefore these assays still interpret these HR proficient tumors as HR deficient. This phenomenon has been observed in BRCA1/2 mutated cell lines with BRCA1/2 reversion mutations which restore BRCA1/2 and HR function; these lines are still interpreted as HR deficient by the aforementioned assays (55). One way to overcome this problem is by development of dynamic, functional biomarkers of HR deficiency, whereby the HR pathway is mechanistically evaluated by directly assessing RAD51 foci formation via immunofluorescence or by assessing other DNA repair complexes via

immunohistochemistry (60–62). The challenge of functional biomarkers of HR deficiency is that they require the cancer specimen to be exposed to some form of DNA damage (i.e., radiation or chemotherapy) ex vivo before the RAD51 foci or other DNA repair complexes can be evaluated. This requirement precludes use of FFPE specimens, increases the technical complexity, and limits the reproducibility of these assays. Overall, there is currently no prospectively validated biomarker of HR deficiency that has been incorporated in clinical practice, and this remains an active area of investigation.

TARGETING HR DEFICIENT TUMORS

a. Conventional chemotherapy

A number of conventional chemotherapy agents that are used routinely in the management of EOC exhibit significant cytotoxicity against HR deficient tumors. Platinum analogues, which have formed the backbone of first line chemotherapy of EOC for more than 30 years, induce ICLs which are highly lethal against tumors with defective HR (Figure 1). The integral role of platinum based chemotherapy in the clinical management of EOC is further evident by the fact that management of relapsed disease is stratified based on the platinum free interval (i.e. the time between completion of platinum-based treatment and the detection of relapse; PFI>=6 months is assigned as platinum sensitive and PFI<6 months as platinum resistant disease). Clinically, patients with BRCA1/2-mutated tumors are associated with significantly higher response rates and prolonged progression-free survival after platinum based chemotherapy (26, 42, 63). These patients commonly exhibit good responses after retreatment with platinum upon development of recurrence and many of them end up receiving multiple lines of platinum chemotherapy. Of note, the enhanced sensitivity of BRCA-mutated tumors to platinum agents challenges the traditional clinical definition of platinum resistance because many of these patients respond well to platinum rechallenge even within 6 months from the end of first line platinum therapy (23).

The high correlation between HR deficiency and response to platinum chemotherapy is also highlighted by the fact that development of platinum resistance is commonly related to restoration of proficient HR via various mechanisms (discussed in more detail below). Platinum sensitivity has been used as a clinical surrogate of HR deficiency and clinical trials of PARPis have used platinum sensitivity as an eligibility criterion for selecting patients that are enriched for HR deficient tumors that would respond to PARPis (64, 65). However, it is important to underscore that platinum sensitivity may also result from defective nucleotide excision repair, and in that case it does not necessarily translate into PARPi sensitivity (40).

Non-platinum cytotoxic agents that induce double strand breaks have also been shown to be active against HR deficient tumors. Topotecan, a semisynthetic water-soluble camptothecin (CPT) analogue is FDA approved for recurrent ovarian cancer and has demonstrated response rates ranging from 13%–33% in phase II trials depending on platinum sensitivity (66, 67). In a phase III trial, topotecan demonstrated an overall objective response rate (CR +PR) of 17.0% (28.8% in platinum sensitive and 6.5% in the platinum resistant/refractory disease)(66). Topotecan inhibits the religation step of the breakage/reunion reaction of topoisomerase I (TopI) resulting in accumulation of topotecan-TopI-DNA covalent complexes which are converted to DNA double-strand breaks (DSBs) when replication forks

encounter the single-strand breaks (SSBs). Studies in yeast have demonstrated that the DSBs induced by TopI inhibitors are repaired by HR during S phase (68); the nonhomologous end joining (NHEJ) pathway is significantly less involved in repair of TopI inhibitor induced DSBs (69).

Similar to TopI inhibitors, topoisomerase II (TopII) inhibitors such as doxorubicin and etoposide are also more active in HR deficient cells and are routinely used in the management of relapsed EOC (pegylated liposomal doxorubicin (PLD) is also FDA-approved for this indication)(66, 67, 70). TopII (Top2a and b) cleave both strands of one DNA duplex simultaneously and form transient tyrosyl-DNA cleavage complex intermediates to allow another duplex to pass through the TopII-linked DSB; TopII generates DSBs in cycling cells especially during mitosis phase, in which both HR and NHEJ are available for repair (69). Etoposide and doxorubicin are TopII poisons which inhibit the religation step of the breakage/reunion reaction of TopII and trap the TopII cleavage complex intermediates. Etoposide is a non-intercalating drug which acts mainly as a TopII trap, while doxorubicin is an intercalator which not only traps TopII but also kill cells by intercalation and generation of oxygen radicals (71). Although etoposide and doxorubicin are more active in HR deficient cells, one striking difference from TopI inhibitors, is that the NHEJ pathway is significantly more involved in repair of DSBs induced by TopII than TopI inhibitors. Consistent with their enhanced activity in HR deficient cells, the activity of both etoposide and doxorubicin is much higher in the platinum sensitive compared to the platinum resistant setting (66, 70). Furthermore, treatment of BRCA-associated EOC patients with PLD has been shown to result in higher response rates, longer time to treatment failure and improved overall survival compared with non-BRCA mutated patients (72).

Finally, HR deficient cells are also sensitive to antimetabolites which induce base lesions and/or replication fork stalling such as gemcitabine. Gemcitabine is a nucleoside analog, whose metabolites (diphosphate and triphosphate nucleosides) facilitate incorporation of gemcitabine nucleotide into DNA which blocks further extension of the nascent strand and causes stalling of replication forks. Furthermore, gemcitabine irreversibly inhibits the ribonucleotide reductase enzyme leading to cell's inability to produce the deoxyribonucleotides required for DNA replication and repair, and thus inducing apoptosis. Gemcitabine is currently FDA approved in combination with carboplatin, for the treatment of EOC that has relapsed at least 6 months after completion of platinum-based therapy (i.e. in platinum sensitive disease)[73]. However, gemcitabine has also been studied and is one of the standard treatment options as a single agent in platinum resistant disease, although the response is less in that setting [74].

b. PARP-inhibition as a synthetic lethal strategy against HR-deficient cancers

i. Mechanism of action of PARPis—HR deficient cells have been shown to be extremely sensitive to poly(ADP ribose) polymerase (PARP) inhibitors (PARPis)(18, 75, 76). Different aspects of PARP1 biology have been proposed to explain the synthetic lethal interaction between PARPi and HR deficiency, but the mechanistic basis is incompletely understood (77).

Since PARP1 was originally shown to be essential for base excision repair (BER) (78, 79), preventing the repair of DNA single strand breaks by PARPis (SSBs, normally repaired by BER) would convert them into the more cytotoxic double strand breaks (DSBs) that are normally repaired by HR (80). In that scenario, an HR-proficient cell will repair these DSBs by HR, whereas these lesions will remain unrepaired and cause cytotoxicity in HR deficient cells (Figure 3(I)) (81, 82). However, some findings do not fit with this model; for instance, knockdown of XRCC1, a downstream effector of PARP1 in BER, does not affect the survival of HR-deficient cells suggesting that BER activity is not critical for HR-deficient cell survival (83).

Another proposed explanation for the PARPi-HR synthetic lethality pertains to the role of PARP1 in limiting classical-NHEJ (C-NHEJ) repair activity (83, 84). C-NHEJ is error-prone and induces genomic instability, which is believed to be particularly deleterious for HR-deficient cells (Figure 3(II)). Thus, PARPi-mediated inhibition of PARP1 would promote C-NHEJ and genome instability. Experimental evidence supporting this model are found in studies showing that the genomic instability induced by PARPi treatment in HR-deficient cells is reduced by concomitant inhibition of DNA-PK, a critical factor of C-NHEJ (18, 83). Several C-NHEJ proteins such as Ku70, Ku80, and DNA-PKcs, bind to poly(ADP ribose) polymers that are generated by PARP enzymes, and these interactions are critical for suppressing C-NHEJ (85–89); furthermore, PARP1 and Ku80 compete for DNA ends in vitro (83). Even though the role of PARP1 in limiting C-NHEJ is now well established, the link between PARPi-mediated C-NHEJ activation and the HR-deficient/PARPi synthetic lethal interaction remains to be fully elucidated.

It has also been suggested that the extreme sensitivity of HR-deficient cells to PARPi might result from the trapping of PARP1 at sites of endogenous damage (Figure 3(III))(90). When DNA damage activates PARP1(91), the PAR-dependent recruitment of additional repair proteins (92–94) simultaneously reduces PARP1 affinity for DNA (95), thereby ensuring tight control of the repair process. Since mutant PARP1 that is unable to synthesize poly(ADP ribose) polymers has been shown to be trapped on DNA and to inhibit DNA repair (95), PARPi-mediated inactivation of PARP1 may likewise induce PARP1 trapping and inhibition of DNA repair. Accordingly, recent studies have demonstrated that PARPi-mediated trapping of PARP1-DNA complexes showed higher cytotoxicity than unrepaired SSBs caused by knockdown of PARP1 (90). This mechanism may explain the cytotoxic effect of certain drug combinations such as PARPi and temozolomide or topotecan (96–98), and is believed to account for the observation that PARP1 knockdown selectively kills HR-deficient cells (18, 76, 83), as these PARP-trapping-induced DNA lesions are thought to be mostly toxic in an HR-deficient setting.

An alternative model might provide an explanation for the cytotoxicity of PARPis in certain BRCA1-deficient cells. DNA damage activates PARP1 (91), which in turn poly(ADP-ribosyl)ates or PARylates many proteins at DNA break sites to orchestrate repair (93). During the HR process, BRCA1 is recruited to damage sites by the PAR- and BRCA1-binding protein BARD1 (99). Indeed, the BARD1 PAR-binding domain is critical for BRCA1 localization to DNA damage sites, particularly when the additional mode of BRCA1 recruitment through γH2AX binding is impaired (for instance in certain BRCA1

mutated tumors). While this model (Figure 3(IV)) may explain the PARPi hypersensitivity of certain BRCA1-mutated tumors, it cannot be expanded to other HR-deficient contexts to serve as a global mechanism for PARPi sensitivity.

A clue in this regard, is the recent finding that HR-deficient cells are dependent on the alternative end joining (alt-EJ) DSB repair pathway for survival. Inhibition of proteins functioning in alt-EJ, such as PARP1 or the polymerase Polθ, is synthetically lethal with defective HR. Thus, the HR-deficiency/PARPi synthetic lethality likely stems from the simultaneous loss of HR and alt-EJ (Figure 3 (V), also discussed below)(100, 101). Finally, some PARPis likely inhibit all PARP family members and the observed synthetic lethality could arise from a compound effect, not solely that of PARP1 inhibition.

ii. PARP inhibitors in the clinical management of HR deficient ovarian cancers —PARPis, including olaparib (AZD2281), rucaparib (CO338, AG014699 and PF01367338), veliparib (ABT888), niraparib (MK4827) have been extensively studied in EOC (102). Iniparib was also initially evaluated but it is now clear that it exhibits very low PARP inhibition in vitro, and its mechanism of action in vivo remains to be elucidated. All aforementioned PARPis inhibit PARP-1 and PARP-2 in vitro at nanomolar concentrations but differ in their ability to trap PARP1 and PARP2 on the DNA SSB sites; niraparib and the newer PARPi BMN673 exhibit higher potency in trapping PARPs than olaparib and rucaparib, while ABT-888 is the least potent of all PARPis in terms of its PARP trapping ability (90). In December 2014, olaparib was granted accelerated approval by the U.S. FDA for use in EOC patients with germline BRCA1/2 mutations who have received three or more chemotherapy regimens based on the results of an international single-arm trial which demonstrated an objective response rate (ORR) of 34% and a median duration of response of 7.9 months (19, 103–105). Olaparib was previously approved in Europe (in October 2014) by the European Medicines Agency (EMA) for a different indication, i.e. for use in the maintenance treatment of patients with platinum-sensitive relapsed BRCA-mutated (germline and/or somatic) high-grade serous EOC who had a complete or partial response to platinum-based chemotherapy. This approval by the EMA was based on a randomized, double blind, phase 2 clinical trial which showed that olaparib maintenance therapy significantly prolonged progression-free survival, compared to placebo, in patients with BRCA-mutated (germline or somatic) ovarian cancer with a hazard ratio of 0.18(65, 106). Strikingly, 40% of patients with BRCA-mutated tumors that were treated with olaparib derived long term benefit, without developing progressive disease for at least 3 years after randomization. Furthermore, exposure to olaparib did not decrease subsequent sensitivity to platinum or other chemotherapies in BRCA1/2-mutated tumors; upon development of PARPi resistance, subsequent response to platinum based chemotherapy has been reported to be as high as 40% by RECIST (107). Randomized phase III trials of maintenance niraparib, rucaparib and olaparib are currently ongoing in patients with high grade serous ovarian cancer who had demonstrated a response and platinum sensitivity for both the ultimate and the penultimate platinum regimens (Table 1).

PARPis have also demonstrated activity in non-BRCA mutated EOC patients although they are not approved for these patients in any setting, either in the US or Europe. This is consistent with the fact that HR deficiency may occur in EOC via multiple mechanisms in

the absence of BRCA1/2-mutations (Figure 2). In the aforementioned phase II study of olaparib maintenance, patients whose tumors lacked a BRCA1/2 mutation also derived a benefit from olaparib with hazard ratio for PFS of 0.53(65, 106). Furthermore, in a Phase II study of high-grade serous EOC with unknown/non-mutated BRCA status, olaparib was associated with a 24% ORR and a 30% combined RECIST or CA125 response rate (105). Olaparib sensitivity was higher in platinum-sensitive compared with platinum-resistant non-BRCA-mutated tumors; 50% of non-BRCA-mutated platinum sensitive tumors responded to olaparib as compared to only 4% of non-BRCA-mutated platinum resistant tumors suggesting that platinum sensitivity may be a good surrogate of HR deficiency and PARPi response among non-BRCA-mutated EOCs. A similar correlation between olaparib and platinum sensitivity has also been found for BRCA-mutated tumors but the difference is less pronounced (105) (60% among platinum sensitive vs 33% among platinum resistant BRCA-mutated tumors) suggesting that platinum resistance cannot be used as an exclusion criterion for PARPi therapy in BRCA-mutated cancers because these tumors may be PARPi sensitive even if they are platinum resistant. PARPi studies investigating candidate biomarkers of PARPi response are currently being performed in non-BRCA-mutated EOCs.

Finally, combinations of PARPis with conventional chemotherapy such as platinum compounds and topoisomerase inhibitors have been explored in BRCA-mutated EOCs (108–110). Given that PARPis inhibit base excision repair which is partly responsible for repair of the damage caused by these chemotherapy agents, addition of PARPis may potentiate the action of these agents. However, when PARPis are combined with chemotherapy, achievement of full dose chemotherapy has been challenging because of the overlapping myelosuppression of PARP inhibitors and chemotherapy (111). In a recently reported randomized, open-label, phase 2 study, in patients with platinum-sensitive, recurrent, high-grade serous ovarian cancer who had received up to three previous courses of platinum-based chemotherapy, olaparib plus paclitaxel and carboplatin (at lower than standard doses) followed by maintenance olaparib monotherapy significantly improved progression-free survival versus paclitaxel plus carboplatin alone (given at their standard doses) with the greatest clinical benefit in BRCA-mutated tumors (PFS hazard ratio 0.22), and had an acceptable and manageable tolerability profile (109). PARPis are currently not part of the initial standard of care chemotherapy regimen for BRCA-mutated EOC (which still remains a platinum and taxane doublet), although clinical trials are exploring their incorporation into first line chemotherapy (Table 1).

c. Inhibition of the Polθ-dependent alternative end-joining (Alt-EJ) pathway as a synthetic lethal strategy against HR-deficient cancers

Recent observations indicate that PARP1 functions in a pathway required for the repair of DNA DSBs, referred to as error-prone alternative end joining (alt-EJ) or microhomology-mediated end-joining (MMEJ) (112). Furthermore, recent studies have shown that HR-deficient ovarian and breast tumors have a compensatory increase in the Polθ/PARP1-mediated alt-EJ pathway that appears to occupy a key role for their survival and proliferation (100, 101). The importance of this pathway in addition to classical NHEJ (C-NHEJ) is now increasingly appreciated (113).

Early evidence for alt-EJ came from studies in yeast and mammalian cells deficient in C-NHEJ that were still able to repair DSBs via end-joining (114, 115) and by the observation that mice deficient in C-NHEJ still exhibited chromosomal translocations and V(D)J recombination (116, 117). Molecular characterization of alt-EJ revealed that the XRCC1/DNA ligase III complex and PARP1 were involved (85, 118, 119). Initially, alt-EJ was considered merely a backup repair pathway for C-NHEJ for end-joining of chromosomal DSBs (119–121), but subsequent studies have demonstrated that alt-EJ might have a role in repairing chromosomal DSBs, depending on the biological context, such as HR deficiency (100, 101). However the use of alt-EJ for repairing DSB poses a particular threat to genomic stability because of its predilection for joining DNA breaks on different chromosomes, generating chromosomal translocations (122–124). Indeed, fill-in synthesis in alt-EJ is likely mediated by the Polθ polymerase, which is error-prone and likely produces point mutations, as well as random insertions and deletions (indels) (125)(126). Indeed, up-regulation of budding yeast Polθ appears to generate random deletions or insertions of 20–200 base pairs (127, 128). Thus, the use of alt-EJ, which could be indicative of an HR-defect, is likely to leave a mutational signature comprising indels at sites of microhomology. Characterization of such a mutational signature may ultimately define a biomarker of HR deficiency (127).

The alt-EJ genetic signature likely hinges upon Polθ, which has two distinct functions in DNA repair. First, Polθ prevents RAD51 assembly on ssDNA, and thus toxicity in HR-deficient cells. This function is mediated by the RAD51-binding domain and is distinct from the polymerase domain. Second, Polθ mediates PARP1-dependent alt-EJ replication rescue though its polymerase domain. Cells expressing a mutant Polθ polymerase exhibit reduced survival when BRCA1 is knocked down. Given the synthetic lethal interaction between HR deficiency and inhibition of Polθ (40, 101), it is important to determine which Polθ function(s) (RAD51 binding vs polymerase) should be targeted to efficiently impair the survival of HR-deficient cells (Figure 3(VI)). Although both the RAD51-binding motifs and the polymerase domain of Polθ contribute to the survival of HR-deficient cells, the exact relative contribution of each domain remains to be elucidated in order to induce selective killing of HR deficient tumors.

d. Cell cycle and DNA damage checkpoint inhibitors against HR deficient tumors

Checkpoint signaling facilitates the coordination between DNA damage response and cell cycle control to allow ample time for repair and prevent permanent DNA damage produced by replication and mitosis. Two of the PI3K-related protein kinases (PIKKs), Ataxia-telangiectasia mutated (ATM) and Ataxia-telangiectasia and Rad3-related (ATR), occupy a central role in signaling DNA damage to cell cycle checkpoints and DNA repair pathways (129). The ATM–CHK2 pathway primarily responds to double strand breaks (DSBs) to induce G1 arrest via phosphorylating and activating CHK2 and p53, while the ATR–CHK1 pathway triggers S and G2 phase arrest. ATM promotes HR by recruiting BRCA1 to DSBs but can also antagonize BRCA1 and promote NHEJ by recruiting p53 binding protein 1 (53BP1), and these antagonistic functions are cell cycle regulated. ATR is activated by DNA single-strand–double-strand junctions that arise as intermediates in nucleotide excision repair (NER), by replication stress which is defined as the slowing or stalling of replication

fork progression, and at resected DSBs. ATR triggers the intra-S phase and the G2 checkpoints via phosphorylation of CHK1 at Ser345 and Ser317 leading to its activation (130). Activated Chk1 in turns phosphorylates WEE1 (which activates this kinase) and cell division cycle 25 (CDC25A and CDC25C) phosphatases (which inhibits them) to inhibit cell cycle progression through the coordinated suppression of cyclin-dependent kinase activity (131). ATR and CHK1 also phosphorylate a number of proteins involved in HR and ICL repair, including BRCA2, RAD51, FANCD2 and FANCE. Importantly, there is significant crosstalk between the ATM/Chk2 and ATR/Chk1 pathways, and they share many substrates (131).

Abrogation of cell-cycle checkpoints leads to accumulation of DNA damage and cellular death, and this approach has shown significant promise as anticancer strategy. HR deficient EOCs are p53 mutated (which is also case for almost all high grade serous cancers) and have lost G1 checkpoint control which makes them hyper-dependent on the S and G2 checkpoints to prevent DNA damage triggering cell death (26, 132). In this regard, targeting the S and G2 checkpoints by inactivation of the ATR/CHK1/WEE1 pathway will inhibit the DNA damage-induced G2 checkpoint arrest leading to mitotic catastrophe and cell death (132). HR deficient tumors are even more sensitive to combinations of checkpoint inhibitors with DNA damaging chemotherapy drugs because they are both deficient in repairing the DNA damage caused by chemotherapy as well as susceptible to abrogation of S and G2 checkpoints.

Importantly, even in the absence of cytotoxic chemotherapy, unrepaired endogenous DNA damage in HR deficient EOC cells may sensitize them to checkpoint inhibition (132). In this regard, it has been shown that FA deficient tumor cells are hypersensitive to inhibition of CHK1, which is more pronounced when combined with platinum therapy (133). DNA repair through the FA pathway occurs primarily during S phase of the cell cycle and FA tumor cells acquire extensive DNA damage in S phase. These lesions persist throughout the remainder of the S and G2 phase, ultimately activating the G2/M checkpoint; increased accumulation of cells in the G2 phase of the cell cycle is a useful diagnostic feature of FA cells and correlates with the hyperactivation of the G2/M checkpoint (134). FA pathway deficient cancer cells have a greater requirement for CHK1 function than DNA repair proficient cells thereby supporting the presence of a therapeutic window that could be exploited in treating DNA repair deficient cancers with CHK1 inhibitors, while sparing toxicity in normal, DNA repair proficient cells (133). Although FA deficient cells are hypersensitive to cisplatin, addition of a CHK1 inhibitor further increases cytotoxicity to a significant degree. Besides abrogation of G2 and S checkpoints, it has been shown that FA deficient cells are hypersensitive to ATM inhibition suggesting that ATM and FA pathways also function in a compensatory manner to maintain genome integrity (135). As with CHK1 inhibition, the selectivity of ATM inhibition alone for FA deficient cells is modest, but the effect of combining ATM inhibition with platinum is significantly augmented in FA deficient cells (135). Importantly, a synthetic lethal interaction also exists between the ATM and ATR signaling pathways, i.e. ATR inhibitors exhibit significant antitumor activity in ATM-deficient but not ATM-proficient backgrounds (136). Taken together, between the 3 pathways, i.e. ATM, ATR and FA pathways, synthetic lethal interactions exist between all

individual pairs i.e. all FA/ATM, FA/ATR and ATR/ATM combinations are synthetically lethal.

Several approaches to inhibit the ATR/CHK1/WEE1 pathway including ATR inhibitors (such as VX-970 and AZD6738), WEE1 inhibitors (such as AZD1775) and CHK1 inhibitors (GDC-0425 and LY2606368) are currently in early clinical trial evaluation in EOC. Of note, AZD1775 has already shown clinical activity as monotherapy in BRCA-mutated tumors (137). In these trials, these agents are combined with chemotherapy, primarily drugs that cause replication stress, such as antimetabolites (particularly nucleoside analogues that cause replication arrest, such as gemcitabine), topoisomerase I poisons and DNA crosslinking agents, such as platinum agents. However, although cell cycle checkpoint inhibition offers the advantage of selective cytotoxicity by exploiting molecular alterations (p53 mutations, HR defects) that are present only in tumors cells, there is always concern for toxicity especially when they are combined with chemotherapy. In this regard, phase I trials of combinations of these agents with chemotherapeutic agents have started at lower doses of chemotherapy which are being escalated to assess for safety. Overall, abrogation of the S and G2 checkpoint via inhibitors of the ATR/CHK1/WEE1 pathway in combination with chemotherapy appears to exert a synthetic lethal interaction with HR deficient EOCs and may thus be an attractive therapeutic strategy against these tumors.

MECHANISMS OF RESISTANCE IN HR DEFICIENT EOCs

In BRCA1/2-mutated tumors, the most common acquired mechanism of resistance to cisplatin or PARPis is secondary intragenic mutations restoring the BRCA1 or BRCA2 protein functionality (Figure 4) (138, 139). Restoration of BRCA1/2 functionality occurs either by genetic events that cancel the frameshift caused by the original mutation and restore the open reading frame (ORF) leading to expression of a functional nearly-full-length protein, or by genetic reversion of the inherited mutation which also restores full-length wild-type protein. These genetic events were originally observed in BRCA2- and BRCA1-mutated cancer cells under selective pressure due to exposure to cisplatin or PARPis, and were associated with secondary genetic changes on the mutated allele that restored a functional protein and conferred platinum and PARPi resistance (Figure 4) (140–143). This mechanism of resistance is highly clinically relevant for patients with BRCA-mutated EOC who are treated with platinum-based therapy; 46% of platinum resistant BRCA-mutated EOCs exhibit tumor-specific secondary mutations that restore the ORF of either BRCA1 or BRCA2(144). Similar observations have been made in biopsies from olaparib-resistant tumors in which acquisition of secondary BRCA2 mutations restored a functional BRCA2 protein (145). Of note, multiple reversion events in BRCA1/2 genes have also been reported as a mechanism of platinum resistance in a recent study of whole-genome characterization of chemoresistant ovarian cancer (146). Strikingly, in one patient with BRCA2-mutated EOC, 12 independent BRCA2 reversion events were identified with multiple reversion events occurring even in individual tumor deposits. Furthermore, in the same study (146), reversal of BRCA1 promoter methylation has also been reported in one patient as a mechanism of platinum resistance. In that case, the primary sensitive sample showed extensive promoter methylation and low BRCA1 expression, while the sample from the relapsed disease had lost BRCA1 methylation and BRCA1 gene was expressed at

comparable levels to homologous recombination proficient tumors. Of note, a specific rather than generalized patter of altered methylation was noted at relapse in this patient. Even though BRCA mutations remain the strongest predictor for sensitivity to PARPis, not every mutation will result in the same functional defect and response to these agents. Analysis of BRCA1 missense mutations suggests that the conserved N- and C-terminal domains are most important for the response to HR-deficiency targeted therapies (147). Specifically, tumors carrying the BRCA1-C61G mutation which disrupts the N-terminal RING domain responded poorly to platinum drugs and PARPis, and rapidly developed resistance (148). Similarly, *Brca1*$^{\Delta 11/\Delta 11}$*; p53*$^{-/-}$ mouse mammary tumors, which only express the BRCA1-Δ11 isoform (generated by the exon 11 splicing) can acquire resistance to cisplatin (149, 150) showing that some hypomorphic BRCA alleles, although unable to prevent tumor development, can affect response to therapy. Interestingly, mutations in the BRCA C-terminal (BRCT) domain of BRCA1 commonly create protein products that are subject to protease-mediated degradation as they are unable to fold. HSP90 may stabilize the BRCT domain of these mutant BRCA1 proteins under PARP inhibitor selection pressure (151); the HSP90-stabilized mutant BRCA1 proteins can efficiently interact with PALB2-BRCA2-RAD51, form RAD51 foci and confer PARP inhibitor and cisplatin resistance. Treatment of resistant cells with the HSP90 inhibitor 17-dimethylaminoethylamino-17-demethoxygeldanamycin reduced mutant BRCA1 protein levels and restored their sensitivity to PARP inhibition (151).

Since PARPis function by blocking the enzymatic action of PARP enzymes, another possible mechanism of PARPi resistance may be decreased expression of PARP enzymes (Figure 4). This mechanism of resistance may be particularly relevant to the PARP-trapping mechanism of action of PARPis. A mutagenesis screen designed to identify mechanisms of resistance to PARPis revealed PARP1 loss-of-function as a potent mechanism of resistant to olaparib in mouse embryonic stem cells and in human tumors cells (152). Accordingly, PARP1 levels have also been shown to be low in human cancer cell lines that have acquired resistance to the PARPi veliparib (96). Taken together, these observations suggest the possibility that tumor-specific mutation or inhibition of PARP1 (for instance, by epigenetic silencing or increased turnover of the protein) would result in resistance and disease progression, a hypothesis that has not yet been validated in patients.

Several mechanisms of resistance involving reacquisition of DNA end resection capacities have also been described. Discovery of these mechanisms came from the observation that the requirement of BRCA1 for HR can be alleviated by concomitant loss of 53BP1. 53BP1 blocks CtIP-mediated DNA end resection via downstream effectors like Rif1 and PTIP (153–158) and thus commits DNA repair to C-NHEJ (159, 160). Loss of 53BP1 partially restores the HR defect of Brca1-deleted mouse embryonic stem cells and reverts their hypersensitivity to DNA-damaging agents (159, 160). However, a deficiency in Ligase IV, another component of the C-NHEJ pathway, does not rescue cell proliferation or HR defect in Brca1-deficient cells. Authors showed that loss of 53BP1 but not Ligase IV was able to promote ssDNA formation competent for RPA phosphorylation. These data suggest that loss of 53BP1 but not Ligase IV promotes activation of DNA end resection. This discordance might explain why combined deficiencies in Brca1/53BP1 but not Brca1/Ligase IV reverse

the HR defect in Brca1-deficient cells (159). Recently, an shRNA screen for hairpins promoting survival of BRCA1-deficient mouse mammary tumors to PARPi identified REV7 and 53BP1 as the top hits (161). REV7 was shown to promote C-NHEJ by inhibiting DNA end resection downstream of Rif1. Loss of REV7 in BRCA1-deficient cells induces CtIP-dependent end resection, leading to HR restoration and PARPi resistance (161, 162). Even though there is little evidence of such resistance mechanisms in human EOCs, a mouse model of BRCA1-associated breast cancer demonstrated low 53BP1 expression in a few olaparib-resistant BRCA1-deficient mouse tumors, suggesting that an acquired change in 53BP1 expression could occur in vivo as a resistance mechanism (163). In BRCA1-mutant cells, loss of 53BP1 confers resistance to PARPi. However, whether loss of 53BP1 confers cross-resistance to cisplatin is still elusive to date. In Brca1-deficient cell lines, shRNA-mediated loss of 53BP1 fully abolished the cisplatin sensitivity (160). However, in the olaparib-resistant BRCA1-deficient mouse tumors, the HR restoration conferred by 53BP1 loss is only partial (measured by RAD51 foci formation), and may explain the lack of cross-resistance to cisplatin (163).

Further studies are necessary to fully address whether 53BP1 loss in vivo can also confer resistance to cisplatin, to assess whether loss of REV7 also confers resistance to platinum therapy and whether these resection-dependent resistance mechanisms (described only in BRCA1-deficient cells so far) may also be relevant to other HR-deficient settings such as BRCA2 mutated cells.

Apart from the mechanisms of resistance intrinsic to the DNA damage response, pharmacological effects that alter the cellular response to PARPis may also be relevant. Several studies have shown that PARPi responses may be modified by ATP-binding cassette (ABC) transporters (164). Increased expression in tumor cells of ABC transporters, such as the P-glycoprotein (PgP) efflux pump (also known as multidrug resistance protein 1 (MDR1) or ATP-binding cassette sub-family B member 1 (ABCB1)) have been implicated in reducing the efficacy of many compounds by enhancing their extracellular translocation (Figure 4). In a genetically-engineered mouse model for BRCA1-mutated breast cancer, PARPi resistance was mediated via upregulation of the Abcb1a and Abcb1b genes encoding PgP pumps. Of note, up-regulation of ABCB1 gene through promoter fusion and translocation involving the 5′ region of the gene (most frequently with SLC25A40 gene) was found in approximately 8% of HGSOC recurrence samples in another study (146). Although not relevant to platinum analogues, this mechanism of resistance may be relevant to PARPi resistance and other drugs such as etoposide, paclitaxel and doxorubicin. Furthermore, resistance to PARPi could be reversed by coadministration of PgP inhibitors arguing that upregulation of PgP may be a clinically relevant and druggable acquired mechanism of PARPi resistance (165, 166). Of note, PgP can be inhibited in clinic (such as with tariquidar) (165); furthermore novel PARPis (such as AZD2461) have been developed that have lower affinity to PgP thereby circumventing this mechanism of PARPi resistance (163, 167).

Extensive tumor desmoplasia has also been suggested as a mechanism of resistance in a BRCA1 mutated tumor without BRCA1 reversion (146). In that case, an extensive desmoplastic stromal reaction was observed at autopsy; tumor desmoplasia has been

associated with chemoresistance and suboptimal drug uptake in pancreatic cancer and may have accounted for resistance despite persistence of HR deficiency due to the BRCA1 mutation. In another study, loss of the nucleosome remodeling factor CHD4 was found to be associated with cisplatin resistance in BRCA2 mutated tumors (168). Restoration of cisplatin resistance was independent of HR but correlated with restored cell cycle progression, reduced chromosomal aberrations, and enhanced DNA damage tolerance. Of note, BRCA2 mutant ovarian cancers with reduced CHD4 expression significantly correlated with shorter progression-free survival and shorter overall survival (168).

Interestingly, in a genetically engineered mouse model for BRCA1-deficient tumors, in which genetic reversion was made impossible by the large intragenic BRCA1 deletion, no acquired platinum drug resistance was observed (169). This raises the question whether mechanisms other than genetic BRCA1/2 reversions can result in resistance to platinum-based chemotherapy in patients (170).

Finally, besides the aforementioned resistance mechanisms, an important question relates to the nature of resistance of residual tumor cells which may respond again to platinum drugs (i.e. recurrence of disease that responds again to platinum chemotherapy). Several approaches have been attempted to target these residual cells that are not killed by first line chemotherapy. First, maintenance chemotherapy, i.e. continuing chemotherapy after achievement of complete clinical remission to first line chemotherapy has been widely studied but no chemotherapy regimen has been associated with an improved overall survival or cure rate in that setting (171). Second, increasing dose intensity approaches have also been attempted, including increasing the dose of platinum, combining platinum agents, increasing the number of cycles of chemotherapy, or using high dose chemotherapy also incorporating alternative DNA cross-linking agents such as melphalan and cyclophosphamide in combination with bone marrow transplantation or with peripheral blood stem cell support; all these approaches failed to improve outcome compared to standard chemotherapy (172). The only dose intensity approach that has been associated with improved survival was administration of chemotherapy via the intraperitoneal route which is capable of achieving high local concentrations of chemotherapy with acceptable systemic side effects (10). However, definitive data regarding comparison of IP chemotherapy versus IV dose dense chemotherapy (GOG252 study) are still pending.

In conclusion, understanding the mechanisms of resistance to PARPis in HR deficient EOCs is critical in order to identify approaches that may overcome resistance and/or minimize the emergence of secondary resistant clones.

OVERCOMING DENOVO AND ACQUIRED HR PROFICIENCY

The promise of platinum agents and PARPis in the management of ovarian cancers is tempered by the fact that HR-proficient tumors do not respond to these agents, suggesting that as many as 50% of ovarian patients (i.e. those with tumors which are de novo HR proficient) do not benefit from these drugs. Furthermore, even the 50% of EOCs, which are initially HR-deficient, eventually become HR-proficient as a result of development of resistance to platinum or PARPis. Combination of platinum or PARPis with agents that

inhibit HR may therefore represent an effective strategy to sensitize HR proficient tumors to platinum and PARPis, and thus potentially expand use of these agents into EOCs with denovo or acquired HR proficiency. Multiple strategies designed to selectively disrupt HR in cancer cells and sensitize them to PARPis or platinum have been evaluated both preclinically as well as in early clinical trials in EOC (Figure 5). Such strategies include combinations of platinum and PARPis with i) CDK1 inhibitors (inhibition of CDK1 induces HR deficiency via inhibition of phosphorylation of BRCA1 by CDK1 (173, 174)), ii) with PI3K or AKT inhibitors (inhibition of PI3K pathway leads to ERK activation/phosphorylation, increased activation of ETS1 and suppression of BRCA1/2 expression and of HR (175, 176)), iii) CDK12 inhibitors (abrogation of CDK12 leads to downregulation of HR genes as discussed above), iv) HDAC inhibitors (which induce coordinated down-regulation of HR pathway genes (177)) and v) HSP90 inhibitors (which induce HR deficiency because multiple HR proteins including BRCA1 are HSP90 clients (178) and they may also overcome HSP90-mediated stabilization of BRCA1 mutant proteins as a mechanism of PARPi resistance (151)). Preclinical evaluation has demonstrated that CDK1-, CDK12-, PI3K-, AKT-, HDAC- and HSP90-inhibitors are able to inhibit HR and sensitize HR proficient cells to PARPis and/or platinum. Of note, phase I clinical evaluation of olaparib with PI3K inhibitors (BYL719 or BKM120) or the AKT inhibitor (AZD5363) in ovarian and breast cancers provided evidence of response in patients who were expected to have HR proficient tumors thereby providing proof of principle for this approach.

Interestingly, in a randomized, open-label, phase 2 study, the combination of olaparib plus cediranib (which is a VEGFR1, VEGFR2 and VEGFR3 inhibitor) significantly improved PFS in recurrent platinum sensitive EOC compared to olaparib alone, and the greatest benefit was observed among patients without BRCA1/2 mutations (64). Although a number of mechanisms may explain this result, this finding may also indicate that there is greater synergism between these two drugs in the setting of HR proficient tumors. In this regard, VEGFR3 inhibition has been shown to downregulate BRCA gene expression, reverse chemotherapy resistance and restore chemosensitivity in resistant cell lines in which a BRCA2 mutation had reverted to wild type (179). It is therefore possible that cediranib may be enhancing the response to olaparib in HR proficient tumors via inhibition of HR (due to VEGFR3 inhibition).

An important challenge for the clinical development of these combinations of HR inhibitors with PARPis is the potentially low therapeutic window between normal and cancer cells and thus the risk of enhanced toxicity. Therefore, careful Phase I evaluation of these combinations will be required, with increased focus on proof of mechanism pharmacodynamic studies. Nonetheless, thus far, the clinical trials of olaparib combinations with PI3K pathway inhibitors have not shown any alarming signals besides the expected non-overlapping toxicities of these agents.

CONCLUSIONS

Approximately 50% of EOCs exhibit defective DNA repair via HR and represent a distinct EOC subtype with unique clinical characteristics that have important implications for management. Germline and somatic BRCA1/2 mutations are the most common mechanisms

of HR deficiency but multiple alternative mechanisms also contribute to this phenomenon in EOC. HR deficiency explains the enhanced sensitivity of EOC to platinum based chemotherapy and is an important therapeutic strategy in this disease. The striking activity of PARPis in HR deficient EOCs highlights the potential of synthetic lethality as anticancer strategy and is first molecular targeted therapy approved in this disease. Additional, potentially non-cross resistant, synthetic lethal approaches such as inhibition of Alt-EJ pathway and cell cycle checkpoint inhibition are exciting novel approaches against HR deficient cancers.

Although PARPis are now FDA approved in patients with BRCA1/2-mutated EOCs, patients with HR deficient/non-BRCA-mutated tumors do not have access to these agents outside a clinical trial. This highlights the importance of development of a robust and prospectively validated biomarker of HR deficiency that is capable to identify non-BRCA-mutated patients who may benefit from these agents. Another challenge is denovo and acquired resistance which are often encountered in clinic and have tempered the enthusiasm for the potential of PARPis in HR deficient EOCs. Understanding the mechanisms of PARPi resistance and their relation to platinum resistance may aid the development of novel non-cross resistant therapies and may help optimize the sequence of how these agents are incorporated in the clinical management of HR deficient EOC. Finally, combinations of PARPis with agents that inhibit HR are exciting strategies to sensitize HR proficient tumors to platinum and PARPis, and thus potentially expand use of these agents into EOCs with denovo or acquired HR proficiency. Initial reports from the clinical evaluation of these combinations provide clinical proof of principle for this approach without prohibitive toxicities.

Acknowledgments

This research was supported by a Stand Up To Cancer – Ovarian Cancer Research Fund-Ovarian Cancer National Alliance-National Ovarian Cancer Coalition Dream Team Translational Research Grant (Grant Number: SU2C-AACR-DT16-15). Stand Up To Cancer is a program of the Entertainment Industry Foundation. Research grants are administered by the American Association for Cancer Research, the scientific partner of SU2C. This work was also supported by grants from the U.S. National Institutes of Health (P50CA168504), and the Breast Cancer Research Foundation (to A.D.D.). As well as support from the Susan Smith Center for Women's Cancers, and the Department of Defense Ovarian Cancer Academy Award (W81XWH-10-1-0585) (to P.A.K.).

References

1. Siegel RL, Miller KD, Jemal A. Cancer statistics, 2015. CA: a cancer journal for clinicians. 2015; 65:5–29. [PubMed: 25559415]
2. Herzog TJ. The current treatment of recurrent ovarian cancer. Curr Oncol Rep. 2006; 8:448–54. [PubMed: 17040623]
3. Konstantinopoulos PA, Awtrey CS. Management of ovarian cancer: a 75-year-old woman who has completed treatment. JAMA. 2012; 307:1420–9. [PubMed: 22396438]
4. Cannistra SA. Cancer of the ovary. N Engl J Med. 2004; 351:2519–29. [PubMed: 15590954]
5. Rossof AH, Talley RW, Stephens R, Thigpen T, Samson MK, Groppe C Jr, et al. Phase II evaluation of cis-dichlorodiammineplatinum(II) in advanced malignancies of the genitourinary and gynecologic organs: a Southwest Oncology Group Study. Cancer Treat Rep. 1979; 63:1557–64. [PubMed: 498155]

6. Thigpen T, Shingleton H, Homesley H, LaGasse L, Blessing J. cis-Dichlorodiammineplatinum(II) in the treatment of gynecologic malignancies: phase II trials by the Gynecologic Oncology Group. Cancer Treat Rep. 1979; 63:1549–55. [PubMed: 498154]
7. Ozols RF, Bundy BN, Greer BE, Fowler JM, Clarke-Pearson D, Burger RA, et al. Phase III trial of carboplatin and paclitaxel compared with cisplatin and paclitaxel in patients with optimally resected stage III ovarian cancer: a Gynecologic Oncology Group study. Journal of clinical oncology : official journal of the American Society of Clinical Oncology. 2003; 21:3194–200. [PubMed: 12860964]
8. McGuire WP, Hoskins WJ, Brady MF, Kucera PR, Partridge EE, Look KY, et al. Cyclophosphamide and cisplatin compared with paclitaxel and cisplatin in patients with stage III and stage IV ovarian cancer. N Engl J Med. 1996; 334:1–6. [PubMed: 7494563]
9. Cannistra SA. Intraperitoneal chemotherapy comes of age. N Engl J Med. 2006; 354:77–9. [PubMed: 16394306]
10. Armstrong DK, Bundy B, Wenzel L, Huang HQ, Baergen R, Lele S, et al. Intraperitoneal cisplatin and paclitaxel in ovarian cancer. N Engl J Med. 2006; 354:34–43. [PubMed: 16394300]
11. Siegel R, Naishadham D, Jemal A. Cancer statistics, 2013. CA: a cancer journal for clinicians. 2013; 63:11–30. [PubMed: 23335087]
12. Winter WE 3rd, Maxwell GL, Tian C, Carlson JW, Ozols RF, Rose PG, et al. Prognostic factors for stage III epithelial ovarian cancer: a Gynecologic Oncology Group Study. Journal of clinical oncology : official journal of the American Society of Clinical Oncology. 2007; 25:3621–7. [PubMed: 17704411]
13. Kelland L. The resurgence of platinum-based cancer chemotherapy. Nat Rev Cancer. 2007; 7:573–84. [PubMed: 17625587]
14. D'Andrea AD. Susceptibility pathways in Fanconi's anemia and breast cancer. N Engl J Med. 2010; 362:1909–19. [PubMed: 20484397]
15. Kennedy RD, D'Andrea AD. DNA repair pathways in clinical practice: lessons from pediatric cancer susceptibility syndromes. Journal of clinical oncology : official journal of the American Society of Clinical Oncology. 2006; 24:3799–808. [PubMed: 16896009]
16. Integrated genomic analyses of ovarian carcinoma. Nature. 2012; 474:609–15.
17. Bast RC Jr, Hennessy B, Mills GB. The biology of ovarian cancer: new opportunities for translation. Nat Rev Cancer. 2009; 9:415–28. [PubMed: 19461667]
18. Farmer H, McCabe N, Lord CJ, Tutt AN, Johnson DA, Richardson TB, et al. Targeting the DNA repair defect in BRCA mutant cells as a therapeutic strategy. Nature. 2005; 434:917–21. [PubMed: 15829967]
19. Fong PC, Boss DS, Yap TA, Tutt A, Wu P, Mergui-Roelvink M, et al. Inhibition of poly(ADP-ribose) polymerase in tumors from BRCA mutation carriers. N Engl J Med. 2009; 361:123–34. [PubMed: 19553641]
20. Jagtap P, Szabo C. Poly(ADP-ribose) polymerase and the therapeutic effects of its inhibitors. Nat Rev Drug Discov. 2005; 4:421–40. [PubMed: 15864271]
21. Ratnam K, Low JA. Current development of clinical inhibitors of poly(ADP-ribose) polymerase in oncology. Clinical cancer research : an official journal of the American Association for Cancer Research. 2007; 13:1383–8. [PubMed: 17332279]
22. Pennington KP, Walsh T, Harrell MI, Lee MK, Pennil CC, Rendi MH, et al. Germline and somatic mutations in homologous recombination genes predict platinum response and survival in ovarian, fallopian tube, and peritoneal carcinomas. Clinical cancer research : an official journal of the American Association for Cancer Research. 2014; 20:764–75. [PubMed: 24240112]
23. Alsop K, Fereday S, Meldrum C, deFazio A, Emmanuel C, George J, et al. BRCA mutation frequency and patterns of treatment response in BRCA mutation-positive women with ovarian cancer: a report from the Australian Ovarian Cancer Study Group. Journal of clinical oncology : official journal of the American Society of Clinical Oncology. 2012; 30:2654–63. [PubMed: 22711857]
24. Pal T, Permuth-Wey J, Betts JA, Krischer JP, Fiorica J, Arango H, et al. BRCA1 and BRCA2 mutations account for a large proportion of ovarian carcinoma cases. Cancer. 2005; 104:2807–16. [PubMed: 16284991]

25. Hennessy BT, Timms KM, Carey MS, Gutin A, Meyer LA, Flake DD 2nd, et al. Somatic mutations in BRCA1 and BRCA2 could expand the number of patients that benefit from poly (ADP ribose) polymerase inhibitors in ovarian cancer. Journal of clinical oncology : official journal of the American Society of Clinical Oncology. 2010; 28:3570–6. [PubMed: 20606085]
26. TCGA. Integrated genomic analyses of ovarian carcinoma. Nature. 2011; 474:609–15. [PubMed: 21720365]
27. Rebbeck TR, Mitra N, Wan F, Sinilnikova OM, Healey S, McGuffog L, et al. Association of type and location of BRCA1 and BRCA2 mutations with risk of breast and ovarian cancer. JAMA. 2015; 313:1347–61. [PubMed: 25849179]
28. Baldwin RL, Nemeth E, Tran H, Shvartsman H, Cass I, Narod S, et al. BRCA1 promoter region hypermethylation in ovarian carcinoma: a population-based study. Cancer research. 2000; 60:5329–33. [PubMed: 11034065]
29. Esteller M, Silva JM, Dominguez G, Bonilla F, Matias-Guiu X, Lerma E, et al. Promoter hypermethylation and BRCA1 inactivation in sporadic breast and ovarian tumors. J Natl Cancer Inst. 2000; 92:564–9. [PubMed: 10749912]
30. Loveday C, Turnbull C, Ramsay E, Hughes D, Ruark E, Frankum JR, et al. Germline mutations in RAD51D confer susceptibility to ovarian cancer. Nat Genet. 2011; 43:879–82. [PubMed: 21822267]
31. Meindl A, Hellebrand H, Wiek C, Erven V, Wappenschmidt B, Niederacher D, et al. Germline mutations in breast and ovarian cancer pedigrees establish RAD51C as a human cancer susceptibility gene. Nat Genet. 2010; 42:410–4. [PubMed: 20400964]
32. Mendes-Pereira AM, Martin SA, Brough R, McCarthy A, Taylor JR, Kim JS, et al. Synthetic lethal targeting of PTEN mutant cells with PARP inhibitors. EMBO Mol Med. 2009; 1:315–22. [PubMed: 20049735]
33. Shen WH, Balajee AS, Wang J, Wu H, Eng C, Pandolfi PP, et al. Essential role for nuclear PTEN in maintaining chromosomal integrity. Cell. 2007; 128:157–70. [PubMed: 17218262]
34. Hughes-Davies L, Huntsman D, Ruas M, Fuks F, Bye J, Chin SF, et al. EMSY links the BRCA2 pathway to sporadic breast and ovarian cancer. Cell. 2003; 115:523–35. [PubMed: 14651845]
35. Brown LA, Kalloger SE, Miller MA, Shih Ie M, McKinney SE, Santos JL, et al. Amplification of 11q13 in ovarian carcinoma. Genes Chromosomes Cancer. 2008; 47:481–9. [PubMed: 18314909]
36. Bajrami I, Frankum JR, Konde A, Miller RE, Rehman FL, Brough R, et al. Genome-wide profiling of genetic synthetic lethality identifies CDK12 as a novel determinant of PARP1/2 inhibitor sensitivity. Cancer research. 2013; 74:287–97. [PubMed: 24240700]
37. Joshi PM, Sutor SL, Huntoon CJ, Karnitz LM. Ovarian cancer-associated mutations disable catalytic activity of CDK12, a kinase that promotes homologous recombination repair and resistance to cisplatin and poly(ADP-ribose) polymerase inhibitors. The Journal of biological chemistry. 2014; 289:9247–53. [PubMed: 24554720]
38. Moskwa P, Buffa FM, Pan Y, Panchakshari R, Gottipati P, Muschel RJ, et al. miR-182-mediated downregulation of BRCA1 impacts DNA repair and sensitivity to PARP inhibitors. Molecular cell. 2011; 41:210–20. [PubMed: 21195000]
39. Choi YE, Pan Y, Park E, Konstantinopoulos P, De S, D'Andrea A, et al. MicroRNAs down-regulate homologous recombination in the G1 phase of cycling cells to maintain genomic stability. Elife (Cambridge). 2014; 3:e02445.
40. Ceccaldi R, O'Connor KW, Mouw KW, Li AY, Matulonis UA, D'Andrea AD, et al. A Unique Subset of Epithelial Ovarian Cancers with Platinum Sensitivity and PARP Inhibitor Resistance. Cancer research. 2015; 75:628–34. [PubMed: 25634215]
41. King MC, Marks JH, Mandell JB. Breast and ovarian cancer risks due to inherited mutations in BRCA1 and BRCA2. Science. 2003; 302:643–6. [PubMed: 14576434]
42. Bolton KL, Chenevix-Trench G, Goh C, Sadetzki S, Ramus SJ, Karlan BY, et al. Association between BRCA1 and BRCA2 mutations and survival in women with invasive epithelial ovarian cancer. JAMA. 2012; 307:382–90. [PubMed: 22274685]
43. Boyd J, Sonoda Y, Federici MG, Bogomolniy F, Rhei E, Maresco DL, et al. Clinicopathologic features of BRCA-linked and sporadic ovarian cancer. JAMA. 2000; 283:2260–5. [PubMed: 10807385]

44. Ruscito I, Dimitrova D, Vasconcelos I, Gellhaus K, Schwachula T, Bellati F, et al. BRCA1 gene promoter methylation status in high-grade serous ovarian cancer patients--a study of the tumour Bank ovarian cancer (TOC) and ovarian cancer diagnosis consortium (OVCAD). Eur J Cancer. 2014; 50:2090–8. [PubMed: 24889916]
45. Soslow RA, Han G, Park KJ, Garg K, Olvera N, Spriggs DR, et al. Morphologic patterns associated with BRCA1 and BRCA2 genotype in ovarian carcinoma. Mod Pathol. 2011; 25:625–36. [PubMed: 22193042]
46. Strickland K, Howitt BE, Rodig SJ, Ritterhouse L, D'Andrea AD, Matulonis UA, et al. Tumor infiltrating and peritumoral T cells and expression of PD-L1 in BRCA1/2-mutated high grade serous ovarian cancers. J Clin Oncol. 2015; 33(suppl):abstr 5512.
47. Soegaard M, Kjaer SK, Cox M, Wozniak E, Hogdall E, Hogdall C, et al. BRCA1 and BRCA2 mutation prevalence and clinical characteristics of a population-based series of ovarian cancer cases from Denmark. Clinical cancer research : an official journal of the American Association for Cancer Research. 2008; 14:3761–7. [PubMed: 18559594]
48. Gourley C, Michie CO, Roxburgh P, Yap TA, Harden S, Paul J, et al. Increased incidence of visceral metastases in scottish patients with BRCA1/2-defective ovarian cancer: an extension of the ovarian BRCAness phenotype. Journal of clinical oncology : official journal of the American Society of Clinical Oncology. 2010; 28:2505–11. [PubMed: 20406939]
49. Konstantinopoulos PA, Spentzos D, Karlan BY, Taniguchi T, Fountzilas E, Francoeur N, et al. Gene expression profile of BRCAness that correlates with responsiveness to chemotherapy and with outcome in patients with epithelial ovarian cancer. Journal of clinical oncology : official journal of the American Society of Clinical Oncology. 2010; 28:3555–61. [PubMed: 20547991]
50. Kang J, D'Andrea AD, Kozono D. A DNA repair pathway-focused score for prediction of outcomes in ovarian cancer treated with platinum-based chemotherapy. J Natl Cancer Inst. 2012; 104:670–81. [PubMed: 22505474]
51. Weberpals JI, Tu D, Squire JA, Amin MS, Islam S, Pelletier LB, et al. Breast cancer 1 (BRCA1) protein expression as a prognostic marker in sporadic epithelial ovarian carcinoma: an NCIC CTG OV.16 correlative study. Ann Oncol. 2011; 22:2403–10. [PubMed: 21368065]
52. Stratton MR. Exploring the genomes of cancer cells: progress and promise. Science. 2011; 331:1553–8. [PubMed: 21436442]
53. Walsh T, Casadei S, Lee MK, Pennil CC, Nord AS, Thornton AM, et al. Mutations in 12 genes for inherited ovarian, fallopian tube, and peritoneal carcinoma identified by massively parallel sequencing. Proc Natl Acad Sci U S A. 2011; 108:18032–7. [PubMed: 22006311]
54. Wagle N, Berger MF, Davis MJ, Blumenstiel B, Defelice M, Pochanard P, et al. High-throughput detection of actionable genomic alterations in clinical tumor samples by targeted, massively parallel sequencing. Cancer discovery. 2012; 2:82–93. [PubMed: 22585170]
55. Abkevich V, Timms KM, Hennessy BT, Potter J, Carey MS, Meyer LA, et al. Patterns of genomic loss of heterozygosity predict homologous recombination repair defects in epithelial ovarian cancer. Br J Cancer. 2012; 107:1776–82. [PubMed: 23047548]
56. Birkbak NJ, Wang ZC, Kim JY, Eklund AC, Li Q, Tian R, et al. Telomeric allelic imbalance indicates defective DNA repair and sensitivity to DNA-damaging agents. Cancer discovery. 2012; 2:366–75. [PubMed: 22576213]
57. Popova T, Manie E, Rieunier G, Caux-Moncoutier V, Tirapo C, Dubois T, et al. Ploidy and large-scale genomic instability consistently identify basal-like breast carcinomas with BRCA1/2 inactivation. Cancer research. 2012; 72:5454–62. [PubMed: 22933060]
58. Timms KM, Abkevich V, Hughes E, Neff C, Reid J, Morris B, et al. Association of BRCA1/2 defects with genomic scores predictive of DNA damage repair deficiency among breast cancer subtypes. Breast Cancer Res. 2014; 16:475. [PubMed: 25475740]
59. Swisher E, Brenton J, Kaufmann S, Oza A, Coleman RL, O'Malley D, et al. 215 Updated clinical and preliminary correlative results of ARIEL2, a Phase 2 study to identify ovarian cancer patients likely to respond to rucaparib. European Journal of Cancer. 50:73.
60. Graeser M, McCarthy A, Lord CJ, Savage K, Hills M, Salter J, et al. A marker of homologous recombination predicts pathologic complete response to neoadjuvant chemotherapy in primary

breast cancer. Clinical cancer research : an official journal of the American Association for Cancer Research. 2010; 16:6159–68. [PubMed: 20802015]

61. Mukhopadhyay A, Elattar A, Cerbinskaite A, Wilkinson SJ, Drew Y, Kyle S, et al. Development of a functional assay for homologous recombination status in primary cultures of epithelial ovarian tumor and correlation with sensitivity to poly(ADP-ribose) polymerase inhibitors. Clinical cancer research : an official journal of the American Association for Cancer Research. 2010; 16:2344–51. [PubMed: 20371688]
62. Polo SE, Jackson SP. Dynamics of DNA damage response proteins at DNA breaks: a focus on protein modifications. Genes Dev. 2011; 25:409–33. [PubMed: 21363960]
63. Yang D, Khan S, Sun Y, Hess K, Shmulevich I, Sood AK, et al. Association of BRCA1 and BRCA2 mutations with survival, chemotherapy sensitivity, and gene mutator phenotype in patients with ovarian cancer. JAMA. 2011; 306:1557–65. [PubMed: 21990299]
64. Liu JF, Barry WT, Birrer M, Lee JM, Buckanovich RJ, Fleming GF, et al. Combination cediranib and olaparib versus olaparib alone for women with recurrent platinum-sensitive ovarian cancer: a randomised phase 2 study. Lancet Oncol. 2014; 15:1207–14. [PubMed: 25218906]
65. Ledermann J, Harter P, Gourley C, Friedlander M, Vergote I, Rustin G, et al. Olaparib maintenance therapy in platinum-sensitive relapsed ovarian cancer. N Engl J Med. 2012; 366:1382–92. [PubMed: 22452356]
66. Gordon AN, Fleagle JT, Guthrie D, Parkin DE, Gore ME, Lacave AJ. Recurrent epithelial ovarian carcinoma: a randomized phase III study of pegylated liposomal doxorubicin versus topotecan. Journal of clinical oncology : official journal of the American Society of Clinical Oncology. 2001; 19:3312–22. [PubMed: 11454878]
67. Naumann RW, Coleman RL. Management strategies for recurrent platinum-resistant ovarian cancer. Drugs. 2011; 71:1397–412. [PubMed: 21812505]
68. Nitiss J, Wang JC. DNA topoisomerase-targeting antitumor drugs can be studied in yeast. Proc Natl Acad Sci U S A. 1988; 85:7501–5. [PubMed: 2845409]
69. Maede Y, Shimizu H, Fukushima T, Kogame T, Nakamura T, Miki T, et al. Differential and common DNA repair pathways for topoisomerase I- and II-targeted drugs in a genetic DT40 repair cell screen panel. Mol Cancer Ther. 2014; 13:214–20. [PubMed: 24130054]
70. Ozols RF. Oral etoposide for the treatment of recurrent ovarian cancer. Drugs. 1999; 58(Suppl 3): 43–9. [PubMed: 10711841]
71. Doroshow JH. Role of hydrogen peroxide and hydroxyl radical formation in the killing of Ehrlich tumor cells by anticancer quinones. Proc Natl Acad Sci U S A. 1986; 83:4514–8. [PubMed: 3086887]
72. Safra T, Borgato L, Nicoletto MO, Rolnitzky L, Pelles-Avraham S, Geva R, et al. BRCA Mutation Status and Determinant of Outcome in Women with Recurrent Epithelial Ovarian Cancer Treated with Pegylated Liposomal Doxorubicin. Mol Cancer Ther. 2011; 10:2000–7. [PubMed: 21835933]
73. Pfisterer J, Plante M, Vergote I, du Bois A, Hirte H, Lacave AJ, et al. Gemcitabine plus carboplatin compared with carboplatin in patients with platinum-sensitive recurrent ovarian cancer: an intergroup trial of the AGO-OVAR, the NCIC CTG, and the EORTC GCG. Journal of clinical oncology : official journal of the American Society of Clinical Oncology. 2006; 24:4699–707. [PubMed: 16966687]
74. Lorusso D, Di Stefano A, Fanfani F, Scambia G. Role of gemcitabine in ovarian cancer treatment. Ann Oncol. 2006; 17(Suppl 5):v188–94. [PubMed: 16807454]
75. Brody LC. Treating cancer by targeting a weakness. The New England journal of medicine. 2005; 353:949–50. [PubMed: 16135843]
76. Bryant HE, Schultz N, Thomas HD, Parker KM, Flower D, Lopez E, et al. Specific killing of BRCA2-deficient tumours with inhibitors of poly(ADP-ribose) polymerase. Nature. 2005; 434:913–7. [PubMed: 15829966]
77. Scott CL, Swisher EM, Kaufmann SH. Poly (adp-ribose) polymerase inhibitors: recent advances and future development. Journal of clinical oncology : official journal of the American Society of Clinical Oncology. 2015; 33:1397–406. [PubMed: 25779564]

78. De Vos M, Schreiber V, Dantzer F. The diverse roles and clinical relevance of PARPs in DNA damage repair: current state of the art. Biochemical pharmacology. 2012; 84:137–46. [PubMed: 22469522]

79. Dantzer F, Schreiber V, Niedergang C, Trucco C, Flatter E, De La Rubia G, et al. Involvement of poly(ADP-ribose) polymerase in base excision repair. Biochimie. 1999; 81:69–75. [PubMed: 10214912]

80. McCabe N, Turner NC, Lord CJ, Kluzek K, Bialkowska A, Swift S, et al. Deficiency in the repair of DNA damage by homologous recombination and sensitivity to poly(ADP-ribose) polymerase inhibition. Cancer research. 2006; 66:8109–15. [PubMed: 16912188]

81. Iglehart JD, Silver DP. Synthetic lethality--a new direction in cancer-drug development. The New England journal of medicine. 2009; 361:189–91. [PubMed: 19553640]

82. Yap TA, Sandhu SK, Carden CP, de Bono JS. Poly(ADP-ribose) polymerase (PARP) inhibitors: Exploiting a synthetic lethal strategy in the clinic. CA: a cancer journal for clinicians. 2011; 61:31–49. [PubMed: 21205831]

83. Patel AG, Sarkaria JN, Kaufmann SH. Nonhomologous end joining drives poly(ADP-ribose) polymerase (PARP) inhibitor lethality in homologous recombination-deficient cells. Proceedings of the National Academy of Sciences of the United States of America. 2011; 108:3406–11. [PubMed: 21300883]

84. De Lorenzo SB, Patel AG, Hurley RM, Kaufmann SH. The Elephant and the Blind Men: Making Sense of PARP Inhibitors in Homologous Recombination Deficient Tumor Cells. Frontiers in oncology. 2013; 3:228. [PubMed: 24062981]

85. Wang M, Wu W, Wu W, Rosidi B, Zhang L, Wang H, et al. PARP-1 and Ku compete for repair of DNA double strand breaks by distinct NHEJ pathways. Nucleic acids research. 2006; 34:6170–82. [PubMed: 17088286]

86. Gagne JP, Isabelle M, Lo KS, Bourassa S, Hendzel MJ, Dawson VL, et al. Proteome-wide identification of poly(ADP-ribose) binding proteins and poly(ADP-ribose)-associated protein complexes. Nucleic acids research. 2008; 36:6959–76. [PubMed: 18981049]

87. Fattah F, Lee EH, Weisensel N, Wang Y, Lichter N, Hendrickson EA. Ku regulates the non-homologous end joining pathway choice of DNA double-strand break repair in human somatic cells. PLoS genetics. 2010; 6:e1000855. [PubMed: 20195511]

88. Hochegger H, Dejsuphong D, Fukushima T, Morrison C, Sonoda E, Schreiber V, et al. Parp-1 protects homologous recombination from interference by Ku and Ligase IV in vertebrate cells. The EMBO journal. 2006; 25:1305–14. [PubMed: 16498404]

89. Paddock MN, Bauman AT, Higdon R, Kolker E, Takeda S, Scharenberg AM. Competition between PARP-1 and Ku70 control the decision between high-fidelity and mutagenic DNA repair. DNA repair. 2011; 10:338–43. [PubMed: 21256093]

90. Murai J, Huang SY, Das BB, Renaud A, Zhang Y, Doroshow JH, et al. Trapping of PARP1 and PARP2 by Clinical PARP Inhibitors. Cancer research. 2012; 72:5588–99. [PubMed: 23118055]

91. Langelier MF, Pascal JM. PARP-1 mechanism for coupling DNA damage detection to poly(ADP-ribose) synthesis. Current opinion in structural biology. 2013; 23:134–43. [PubMed: 23333033]

92. Ahel I, Ahel D, Matsusaka T, Clark AJ, Pines J, Boulton SJ, et al. Poly(ADP-ribose)-binding zinc finger motifs in DNA repair/checkpoint proteins. Nature. 2008; 451:81–5. [PubMed: 18172500]

93. Gagne JP, Pic E, Isabelle M, Krietsch J, Ethier C, Paquet E, et al. Quantitative proteomics profiling of the poly(ADP-ribose)-related response to genotoxic stress. Nucleic acids research. 2012; 40:7788–805. [PubMed: 22669911]

94. Masson M, Niedergang C, Schreiber V, Muller S, Menissier-de Murcia J, de Murcia G. XRCC1 is specifically associated with poly(ADP-ribose) polymerase and negatively regulates its activity following DNA damage. Molecular and cellular biology. 1998; 18:3563–71. [PubMed: 9584196]

95. Satoh MS, Lindahl T. Role of poly(ADP-ribose) formation in DNA repair. Nature. 1992; 356:356–8. [PubMed: 1549180]

96. Liu X, Han EK, Anderson M, Shi Y, Semizarov D, Wang G, et al. Acquired resistance to combination treatment with temozolomide and ABT-888 is mediated by both base excision repair and homologous recombination DNA repair pathways. Molecular cancer research : MCR. 2009; 7:1686–92. [PubMed: 19825992]

97. Murai J, Zhang Y, Morris J, Ji J, Takeda S, Doroshow JH, et al. Rationale for poly(ADP-ribose) polymerase (PARP) inhibitors in combination therapy with camptothecins or temozolomide based on PARP trapping versus catalytic inhibition. The Journal of pharmacology and experimental therapeutics. 2014; 349:408–16. [PubMed: 24650937]

98. Patel AG, Flatten KS, Schneider PA, Dai NT, McDonald JS, Poirier GG, et al. Enhanced killing of cancer cells by poly(ADP-ribose) polymerase inhibitors and topoisomerase I inhibitors reflects poisoning of both enzymes. The Journal of biological chemistry. 2012; 287:4198–210. [PubMed: 22158865]

99. Li M, Yu X. Function of BRCA1 in the DNA damage response is mediated by ADP-ribosylation. Cancer cell. 2013; 23:693–704. [PubMed: 23680151]

100. Ceccaldi R, Liu JC, Amunugama R, Hajdu I, Primack B, Petalcorin MI, et al. Homologous-recombination-deficient tumours are dependent on Poltheta-mediated repair. Nature. 2015; 518:258–62. [PubMed: 25642963]

101. Mateos-Gomez PA, Gong F, Nair N, Miller KM, Lazzerini-Denchi E, Sfeir A. Mammalian polymerase theta promotes alternative NHEJ and suppresses recombination. Nature. 2015; 518:254–7. [PubMed: 25642960]

102. Liu JF, Konstantinopoulos PA, Matulonis UA. PARP inhibitors in ovarian cancer: Current status and future promise. Gynecol Oncol. 2014; 133:362–9. [PubMed: 24607283]

103. Audeh MW, Carmichael J, Penson RT, Friedlander M, Powell B, Bell-McGuinn KM, et al. Oral poly(ADP-ribose) polymerase inhibitor olaparib in patients with BRCA1 or BRCA2 mutations and recurrent ovarian cancer: a proof-of-concept trial. Lancet. 2010; 376:245–51. [PubMed: 20609468]

104. Fong PC, Yap TA, Boss DS, Carden CP, Mergui-Roelvink M, Gourley C, et al. Poly(ADP)-ribose polymerase inhibition: frequent durable responses in BRCA carrier ovarian cancer correlating with platinum-free interval. Journal of clinical oncology : official journal of the American Society of Clinical Oncology. 2010; 28:2512–9. [PubMed: 20406929]

105. Gelmon KA, Tischkowitz M, Mackay H, Swenerton K, Robidoux A, Tonkin K, et al. Olaparib in patients with recurrent high-grade serous or poorly differentiated ovarian carcinoma or triple-negative breast cancer: a phase 2, multicentre, open-label, non-randomised study. Lancet Oncol. 2011; 12:852–61. [PubMed: 21862407]

106. Ledermann J, Harter P, Gourley C, Friedlander M, Vergote I, Rustin G, et al. Olaparib maintenance therapy in patients with platinum-sensitive relapsed serous ovarian cancer: a preplanned retrospective analysis of outcomes by BRCA status in a randomised phase 2 trial. Lancet Oncol. 2014; 15:852–61. [PubMed: 24882434]

107. Ang JE, Gourley C, Powell CB, High H, Shapira-Frommer R, Castonguay V, et al. Efficacy of chemotherapy in BRCA1/2 mutation carrier ovarian cancer in the setting of PARP inhibitor resistance: a multi-institutional study. Clinical cancer research : an official journal of the American Association for Cancer Research. 2013; 19:5485–93. [PubMed: 23922302]

108. Kummar S, Chen A, Ji J, Zhang Y, Reid JM, Ames M, et al. Phase I study of PARP inhibitor ABT-888 in combination with topotecan in adults with refractory solid tumors and lymphomas. Cancer research. 2011; 71:5626–34. [PubMed: 21795476]

109. Oza AM, Cibula D, Benzaquen AO, Poole C, Mathijssen RH, Sonke GS, et al. Olaparib combined with chemotherapy for recurrent platinum-sensitive ovarian cancer: a randomised phase 2 trial. Lancet Oncol. 2014; 16:87–97. [PubMed: 25481791]

110. Lee JM, Hays JL, Annunziata CM, Noonan AM, Minasian L, Zujewski JA, et al. Phase I/Ib study of olaparib and carboplatin in BRCA1 or BRCA2 mutation-associated breast or ovarian cancer with biomarker analyses. J Natl Cancer Inst. 2014; 106:dju089. [PubMed: 24842883]

111. Rajan A, Carter CA, Kelly RJ, Gutierrez M, Kummar S, Szabo E, et al. A phase I combination study of olaparib with cisplatin and gemcitabine in adults with solid tumors. Clinical cancer research : an official journal of the American Association for Cancer Research. 2012; 18:2344–51. [PubMed: 22371451]

112. Boboila C, Alt FW, Schwer B. Classical and alternative end-joining pathways for repair of lymphocyte-specific and general DNA double-strand breaks. Advances in immunology. 2012; 116:1–49. [PubMed: 23063072]

113. Deriano L, Roth DB. Modernizing the nonhomologous end-joining repertoire: alternative and classical NHEJ share the stage. Annual review of genetics. 2013; 47:433–55.
114. Boulton SJ, Jackson SP. Saccharomyces cerevisiae Ku70 potentiates illegitimate DNA double-strand break repair and serves as a barrier to error-prone DNA repair pathways. The EMBO journal. 1996; 15:5093–103. [PubMed: 8890183]
115. Kabotyanski EB, Gomelsky L, Han JO, Stamato TD, Roth DB. Double-strand break repair in Ku86- and XRCC4-deficient cells. Nucleic acids research. 1998; 26:5333–42. [PubMed: 9826756]
116. Zhu C, Mills KD, Ferguson DO, Lee C, Manis J, Fleming J, et al. Unrepaired DNA breaks in p53-deficient cells lead to oncogenic gene amplification subsequent to translocations. Cell. 2002; 109:811–21. [PubMed: 12110179]
117. Corneo B, Wendland RL, Deriano L, Cui X, Klein IA, Wong SY, et al. Rag mutations reveal robust alternative end joining. Nature. 2007; 449:483–6. [PubMed: 17898768]
118. Audebert M, Salles B, Calsou P. Involvement of poly(ADP-ribose) polymerase-1 and XRCC1/DNA ligase III in an alternative route for DNA double-strand breaks rejoining. The Journal of biological chemistry. 2004; 279:55117–26. [PubMed: 15498778]
119. Wang H, Rosidi B, Perrault R, Wang M, Zhang L, Windhofer F, et al. DNA ligase III as a candidate component of backup pathways of nonhomologous end joining. Cancer research. 2005; 65:4020–30. [PubMed: 15899791]
120. Verkaik NS, Esveldt-van Lange RE, van Heemst D, Bruggenwirth HT, Hoeijmakers JH, Zdzienicka MZ, et al. Different types of V(D)J recombination and end-joining defects in DNA double-strand break repair mutant mammalian cells. European journal of immunology. 2002; 32:701–9. [PubMed: 11870614]
121. Wang H, Perrault AR, Takeda Y, Qin W, Wang H, Iliakis G. Biochemical evidence for Ku-independent backup pathways of NHEJ. Nucleic acids research. 2003; 31:5377–88. [PubMed: 12954774]
122. Simsek D, Jasin M. Alternative end-joining is suppressed by the canonical NHEJ component Xrcc4-ligase IV during chromosomal translocation formation. Nature structural & molecular biology. 2010; 17:410–6.
123. Zhang Y, Jasin M. An essential role for CtIP in chromosomal translocation formation through an alternative end-joining pathway. Nature structural & molecular biology. 2011; 18:80–4.
124. Zhang Y, Gostissa M, Hildebrand DG, Becker MS, Boboila C, Chiarle R, et al. The role of mechanistic factors in promoting chromosomal translocations found in lymphoid and other cancers. Advances in immunology. 2010; 106:93–133. [PubMed: 20728025]
125. Yousefzadeh MJ, Wood RD. DNA polymerase POLQ and cellular defense against DNA damage. DNA repair. 2013; 12:1–9. [PubMed: 23219161]
126. Kent T, Chandramouly G, McDevitt SM, Ozdemir AY, Pomerantz RT. Mechanism of microhomology-mediated end-joining promoted by human DNA polymerase theta. Nature structural & molecular biology. 2015; 22:230–7.
127. Alexandrov LB, Nik-Zainal S, Wedge DC, Aparicio SA, Behjati S, Biankin AV, et al. Signatures of mutational processes in human cancer. Nature. 2013; 500:415–21. [PubMed: 23945592]
128. McVey M, Lee SE. MMEJ repair of double-strand breaks (director's cut): deleted sequences and alternative endings. Trends Genet. 2008; 24:529–38. [PubMed: 18809224]
129. Curtin NJ. DNA repair dysregulation from cancer driver to therapeutic target. Nat Rev Cancer. 2012; 12:801–17. [PubMed: 23175119]
130. Flynn RL, Zou L. ATR: a master conductor of cellular responses to DNA replication stress. Trends Biochem Sci. 2011; 36:133–40. [PubMed: 20947357]
131. Chen T, Stephens PA, Middleton FK, Curtin NJ. Targeting the S and G2 checkpoint to treat cancer. Drug Discov Today. 2012; 17:194–202. [PubMed: 22192883]
132. Evers B, Helleday T, Jonkers J. Targeting homologous recombination repair defects in cancer. Trends Pharmacol Sci. 2010; 31:372–80. [PubMed: 20598756]
133. Chen CC, Kennedy RD, Sidi S, Look AT, D'Andrea A. CHK1 inhibition as a strategy for targeting Fanconi Anemia (FA) DNA repair pathway deficient tumors. Mol Cancer. 2009; 8:24. [PubMed: 19371427]

134. Pulsipher M, Kupfer GM, Naf D, Suliman A, Lee JS, Jakobs P, et al. Subtyping analysis of Fanconi anemia by immunoblotting and retroviral gene transfer. Mol Med. 1998; 4:468–79. [PubMed: 9713825]
135. Kennedy RD, Chen CC, Stuckert P, Archila EM, De la Vega MA, Moreau LA, et al. Fanconi anemia pathway-deficient tumor cells are hypersensitive to inhibition of ataxia telangiectasia mutated. J Clin Invest. 2007; 117:1440–9. [PubMed: 17431503]
136. Weber AM, Ryan AJ. ATM and ATR as therapeutic targets in cancer. Pharmacol Ther. 2015; 149:124–38. [PubMed: 25512053]
137. Do KT, Wilsker D, Balasubramanian P, Zlott J, Jeong W, Lawrence SM, et al. Phase I trial of AZD1775 (MK1775), a wee1 kinase inhibitor, in patients with refractory solid tumors. J Clin Oncol. 2014; 60:4009.
138. Lord CJ, Ashworth A. Mechanisms of resistance to therapies targeting BRCA-mutant cancers. Nature medicine. 2013; 19:1381–8.
139. Bouwman P, Jonkers J. Molecular pathways: how can BRCA-mutated tumors become resistant to PARP inhibitors? Clinical cancer research : an official journal of the American Association for Cancer Research. 2014; 20:540–7. [PubMed: 24270682]
140. Sakai W, Swisher EM, Karlan BY, Agarwal MK, Higgins J, Friedman C, et al. Secondary mutations as a mechanism of cisplatin resistance in BRCA2-mutated cancers. Nature. 2008; 451:1116–20. [PubMed: 18264087]
141. Edwards SL, Brough R, Lord CJ, Natrajan R, Vatcheva R, Levine DA, et al. Resistance to therapy caused by intragenic deletion in BRCA2. Nature. 2008; 451:1111–5. [PubMed: 18264088]
142. Swisher EM, Sakai W, Karlan BY, Wurz K, Urban N, Taniguchi T. Secondary BRCA1 mutations in BRCA1-mutated ovarian carcinomas with platinum resistance. Cancer research. 2008; 68:2581–6. [PubMed: 18413725]
143. Sakai W, Swisher EM, Jacquemont C, Chandramohan KV, Couch FJ, Langdon SP, et al. Functional restoration of BRCA2 protein by secondary BRCA2 mutations in BRCA2-mutated ovarian carcinoma. Cancer research. 2009; 69:6381–6. [PubMed: 19654294]
144. Norquist B, Wurz KA, Pennil CC, Garcia R, Gross J, Sakai W, et al. Secondary somatic mutations restoring BRCA1/2 predict chemotherapy resistance in hereditary ovarian carcinomas. Journal of clinical oncology : official journal of the American Society of Clinical Oncology. 2011; 29:3008–15. [PubMed: 21709188]
145. Barber LJ, Sandhu S, Chen L, Campbell J, Kozarewa I, Fenwick K, et al. Secondary mutations in BRCA2 associated with clinical resistance to a PARP inhibitor. The Journal of pathology. 2013; 229:422–9. [PubMed: 23165508]
146. Patch AM, Christie EL, Etemadmoghadam D, Garsed DW, George J, Fereday S, et al. Whole-genome characterization of chemoresistant ovarian cancer. Nature. 2015; 521:489–94. [PubMed: 26017449]
147. Bouwman P, van der Gulden H, van der Heijden I, Drost R, Klijn CN, Prasetyanti P, et al. A high-throughput functional complementation assay for classification of BRCA1 missense variants. Cancer discovery. 2013; 3:1142–55. [PubMed: 23867111]
148. Drost R, Bouwman P, Rottenberg S, Boon U, Schut E, Klarenbeek S, et al. BRCA1 RING function is essential for tumor suppression but dispensable for therapy resistance. Cancer cell. 2011; 20:797–809. [PubMed: 22172724]
149. Shafee N, Smith CR, Wei S, Kim Y, Mills GB, Hortobagyi GN, et al. Cancer stem cells contribute to cisplatin resistance in Brca1/p53-mediated mouse mammary tumors. Cancer research. 2008; 68:3243–50. [PubMed: 18451150]
150. Tammaro C, Raponi M, Wilson DI, Baralle D. BRCA1 exon 11 alternative splicing, multiple functions and the association with cancer. Biochemical Society transactions. 2012; 40:768–72. [PubMed: 22817731]
151. Johnson N, Johnson SF, Yao W, Li YC, Choi YE, Bernhardy AJ, et al. Stabilization of mutant BRCA1 protein confers PARP inhibitor and platinum resistance. Proc Natl Acad Sci U S A. 2013; 110:17041–6. [PubMed: 24085845]

152. Pettitt SJ, Rehman FL, Bajrami I, Brough R, Wallberg F, Kozarewa I, et al. A genetic screen using the PiggyBac transposon in haploid cells identifies Parp1 as a mediator of olaparib toxicity. PloS one. 2013; 8:e61520. [PubMed: 23634208]
153. Chapman JR, Barral P, Vannier JB, Borel V, Steger M, Tomas-Loba A, et al. RIF1 is essential for 53BP1-dependent nonhomologous end joining and suppression of DNA double-strand break resection. Molecular cell. 2013; 49:858–71. [PubMed: 23333305]
154. Di Virgilio M, Callen E, Yamane A, Zhang W, Jankovic M, Gitlin AD, et al. Rif1 prevents resection of DNA breaks and promotes immunoglobulin class switching. Science. 2013; 339:711–5. [PubMed: 23306439]
155. Feng L, Fong KW, Wang J, Wang W, Chen J. RIF1 counteracts BRCA1-mediated end resection during DNA repair. The Journal of biological chemistry. 2013; 288:11135–43. [PubMed: 23486525]
156. Escribano-Diaz C, Orthwein A, Fradet-Turcotte A, Xing M, Young JT, Tkac J, et al. A cell cycle-dependent regulatory circuit composed of 53BP1-RIF1 and BRCA1-CtIP controls DNA repair pathway choice. Molecular cell. 2013; 49:872–83. [PubMed: 23333306]
157. Zimmermann M, Lottersberger F, Buonomo SB, Sfeir A, de Lange T. 53BP1 regulates DSB repair using Rif1 to control 5′ end resection. Science. 2013; 339:700–4. [PubMed: 23306437]
158. Callen E, Di Virgilio M, Kruhlak MJ, Nieto-Soler M, Wong N, Chen HT, et al. 53BP1 mediates productive and mutagenic DNA repair through distinct phosphoprotein interactions. Cell. 2013; 153:1266–80. [PubMed: 23727112]
159. Bunting SF, Callen E, Wong N, Chen HT, Polato F, Gunn A, et al. 53BP1 inhibits homologous recombination in Brca1-deficient cells by blocking resection of DNA breaks. Cell. 2010; 141:243–54. [PubMed: 20362325]
160. Bouwman P, Aly A, Escandell JM, Pieterse M, Bartkova J, van der Gulden H, et al. 53BP1 loss rescues BRCA1 deficiency and is associated with triple-negative and BRCA-mutated breast cancers. Nature structural & molecular biology. 2010; 17:688–95.
161. Xu G, Chapman JR, Brandsma I, Yuan J, Mistrik M, Bouwman P, et al. REV7 counteracts DNA double-strand break resection and affects PARP inhibition. Nature. 2015; 521:541–4. [PubMed: 25799992]
162. Boersma V, Moatti N, Segura-Bayona S, Peuscher MH, van der Torre J, Wevers BA, et al. MAD2L2 controls DNA repair at telomeres and DNA breaks by inhibiting 5′ end resection. Nature. 2015; 521:537–40. [PubMed: 25799990]
163. Jaspers JE, Kersbergen A, Boon U, Sol W, van Deemter L, Zander SA, et al. Loss of 53BP1 causes PARP inhibitor resistance in Brca1-mutated mouse mammary tumors. Cancer discovery. 2013; 3:68–81. [PubMed: 23103855]
164. Choi YH, Yu AM. ABC transporters in multidrug resistance and pharmacokinetics, and strategies for drug development. Current pharmaceutical design. 2014; 20:793–807. [PubMed: 23688078]
165. Rottenberg S, Jaspers JE, Kersbergen A, van der Burg E, Nygren AO, Zander SA, et al. High sensitivity of BRCA1-deficient mammary tumors to the PARP inhibitor AZD2281 alone and in combination with platinum drugs. Proceedings of the National Academy of Sciences of the United States of America. 2008; 105:17079–84. [PubMed: 18971340]
166. Oplustilova L, Wolanin K, Mistrik M, Korinkova G, Simkova D, Bouchal J, et al. Evaluation of candidate biomarkers to predict cancer cell sensitivity or resistance to PARP-1 inhibitor treatment. Cell cycle. 2012; 11:3837–50. [PubMed: 22983061]
167. Li X, Delzer J, Voorman R, de Morais SM, Lao Y. Disposition and drug-drug interaction potential of veliparib (ABT-888), a novel and potent inhibitor of poly(ADP-ribose) polymerase. Drug metabolism and disposition: the biological fate of chemicals. 2011; 39:1161–9. [PubMed: 21436403]
168. Guillemette S, Serra RW, Peng M, Hayes JA, Konstantinopoulos PA, Green MR, et al. Resistance to therapy in BRCA2 mutant cells due to loss of the nucleosome remodeling factor CHD4. Genes Dev. 2015; 29:489–94. [PubMed: 25737278]
169. Rottenberg S, Nygren AO, Pajic M, van Leeuwen FW, van der Heijden I, van de Wetering K, et al. Selective induction of chemotherapy resistance of mammary tumors in a conditional mouse

model for hereditary breast cancer. Proc Natl Acad Sci U S A. 2007; 104:12117–22. [PubMed: 17626183]

170. Borst P, Rottenberg S, Jonkers J. How do real tumors become resistant to cisplatin? Cell cycle. 2008; 7:1353–9. [PubMed: 18418074]
171. Markman M, Liu PY, Wilczynski S, Monk B, Copeland LJ, Alvarez RD, et al. Phase III randomized trial of 12 versus 3 months of maintenance paclitaxel in patients with advanced ovarian cancer after complete response to platinum and paclitaxel-based chemotherapy: a Southwest Oncology Group and Gynecologic Oncology Group trial. Journal of clinical oncology : official journal of the American Society of Clinical Oncology. 2003; 21:2460–5. [PubMed: 12829663]
172. Ozols RF. Ovarian cancer: is dose intensity dead? J Clin Oncol. 2007; 25:4157–8. [PubMed: 17698802]
173. Johnson N, Li YC, Walton ZE, Cheng KA, Li D, Rodig SJ, et al. Compromised CDK1 activity sensitizes BRCA-proficient cancers to PARP inhibition. Nature medicine. 2011; 17:875–82.
174. Johnson SF, Johnson N, Chi D, Primack B, D'Andrea AD, Lim E, et al. Abstract 1788: The CDK inhibitor dinaciclib sensitizes triple-negative breast cancer cells to PARP inhibition. Cancer Res. 2013; 73:1788.
175. Ibrahim YH, Garcia-Garcia C, Serra V, He L, Torres-Lockhart K, Prat A, et al. PI3K inhibition impairs BRCA1/2 expression and sensitizes BRCA-proficient triple-negative breast cancer to PARP inhibition. Cancer discovery. 2012; 2:1036–47. [PubMed: 22915752]
176. Juvekar A, Burga LN, Hu H, Lunsford EP, Ibrahim YH, Balmana J, et al. Combining a PI3K inhibitor with a PARP inhibitor provides an effective therapy for BRCA1-related breast cancer. Cancer discovery. 2012; 2:1048–63. [PubMed: 22915751]
177. Konstantinopoulos PA, Wilson AJ, Saskowski J, Wass E, Khabele D. Suberoylanilide hydroxamic acid (SAHA) enhances olaparib activity by targeting homologous recombination DNA repair in ovarian cancer. Gynecol Oncol. 2014; 133:599–606. [PubMed: 24631446]
178. Choi YE, Battelli C, Watson J, Liu J, Curtis J, Morse AN, et al. Sublethal concentrations of 17-AAG suppress homologous recombination DNA repair and enhance sensitivity to carboplatin and olaparib in HR proficient ovarian cancer cells. Oncotarget. 2014; 5:2678–87. [PubMed: 24798692]
179. Lim JJ, Yang K, Taylor-Harding B, Wiedemeyer WR, Buckanovich RJ. VEGFR3 inhibition chemosensitizes ovarian cancer stemlike cells through down-regulation of BRCA1 and BRCA2. Neoplasia. 2014; 16:343–53. e1–2. [PubMed: 24862760]

STATEMENT OF SIGNIFICANCE

Defective DNA repair via homologous recombination is a pivotal vulnerability of epithelial ovarian cancer, particularly of the high grade serous histologic subtype. Targeting defective HR offers the unique opportunity of exploiting molecular differences between tumor and normal cells, thereby inducing cancer-specific synthetic lethality; the promise and challenges of these approaches in ovarian cancer are discussed in this review.

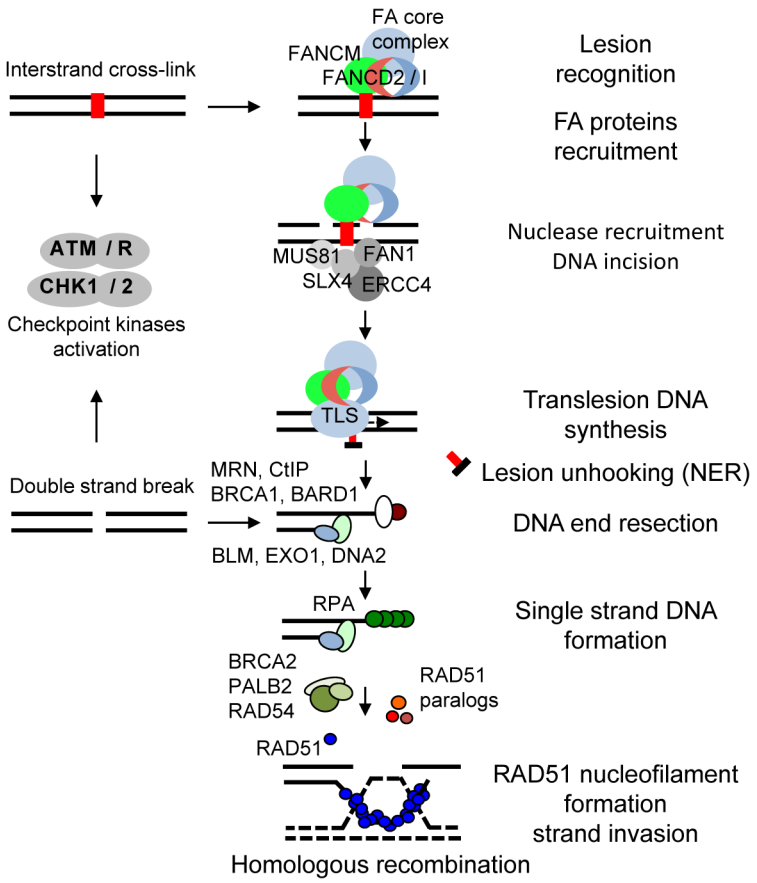

Figure 1. Cooperation of the Fanconi Anemia (FA) and BRCA1/2 proteins in a common ICL repair pathway

Stalling of replication forks on DNA ICLs induces lesion recognition by the FANCM–FAAP24–MHF1/2 complex and subsequent recruitment of the FA core complex, which in turn recruits the mono-ubiquitinated FANCD2-FANCI to the ICL region. FANCM also initiates checkpoint response, which phosphorylates multiple FA proteins. Ubiquitinated FANCD2 acts as a landing pad for recruiting several nucleases to coordinate nucleolytic incisions. Unhooking the DNA leaves the cross-linked nucleotides tethered to the complementary strand, which are bypassed by TLS polymerases. DNA incisions create a DSB, which is then repaired by HR. Downstream FA proteins such as BRCA1, BRCA2, and PALB2 promote RAD51-dependent strand invasion and resolution of recombinant intermediates.

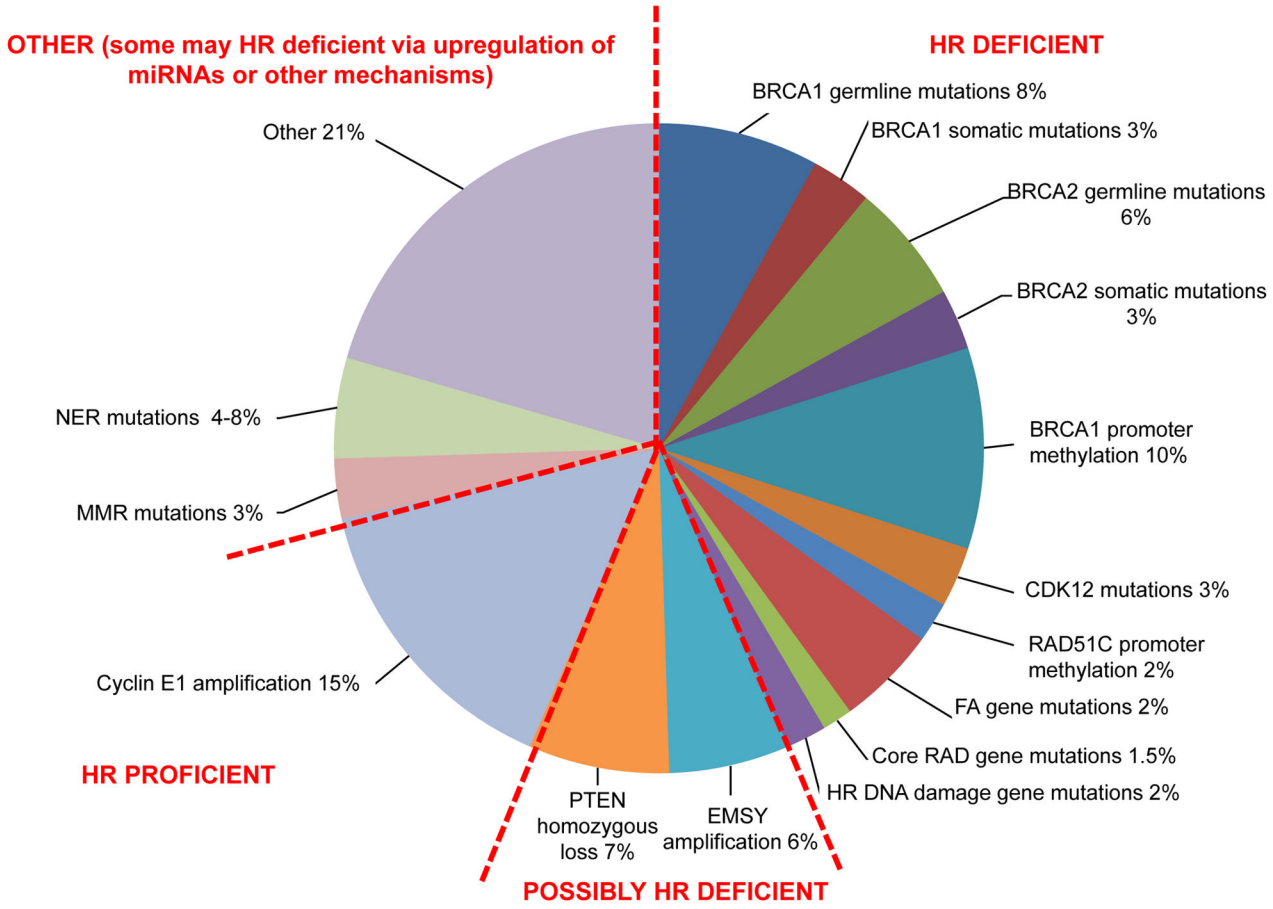

Figure 2. Approximately 50% of high grade serous EOC have alterations in HR repair genes

Frequency of genetic and epigenetic changes involving HR pathway genes or non-HR pathway genes that modulate HR pathway. FA/BRCA pathway alterations have been experimentally found to be associated with HR deficiency (***HR deficient tumors on the right***). PTEN deletion and EMSY amplification have been reported to confer HR deficiency but data are evolving (***Possibly HR deficient tumors on the bottom***). Tumors with cyclin E1 (CCNE1) amplification are enriched for HR proficiency (***HR proficient tumors on the left***) and are associated with inferior outcome and response to platinum based chemotherapy. Among the remaining tumors, some may be HR deficient via miRNA upregulation or other unknown mechanisms.

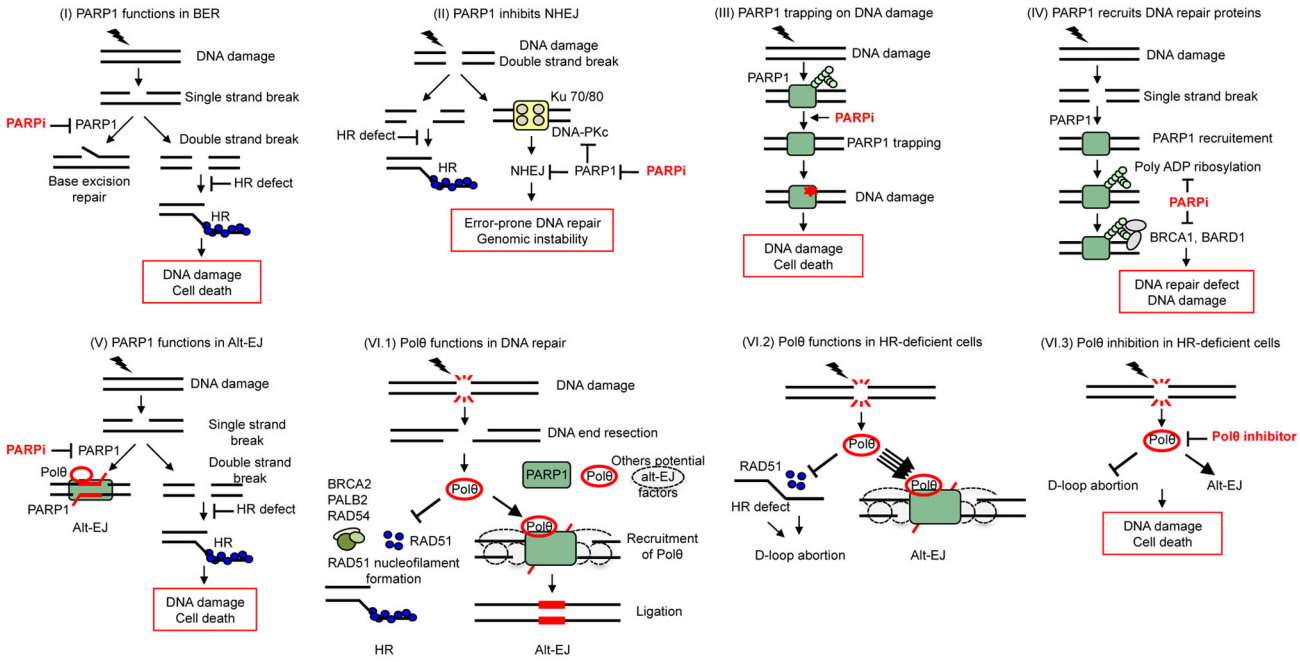

Figure 3. Mechanisms of synthetic lethality between PARP1 or POLQ inhibition and HR deficiency

Inhibition of PARP1 activity in BER (I) and C-NHEJ (II) is toxic in HR-deficient cells and explains the observed PARPi-HR synthetic lethality. (III) PARPi's induce PARP1 trapping on DNA lesions which is highly toxic in HR-deficient cells. (IV) PAR-mediated recruitment of the BARD1-BRCA1 complex is impaired by PARPi, resulting in the persistence of DNA lesions that are toxic to HR-deficient cells. (V) Inhibition of PARP1/Polθ-mediated Alt-EJ is toxic in HR-deficient cells. (VI.1) Under physiological conditions, Polθ expression is low and its impact on the repair of DNA double-strand breaks (DSB) is limited. Polθ limits RAD51-ssDNA filament assembly and subsequent HR activity; at the same time, it promotes alt-EJ through its polymerase domain.. (VI.2) Upon an HR defect, Polθ expression increases substantially and channels DSB repair into alt-EJ. (VI.3) In the case of an HR defect, inhibition of Polθ causes cell death through the persistence of toxic RAD51 intermediates and inhibition of alt-EJ.

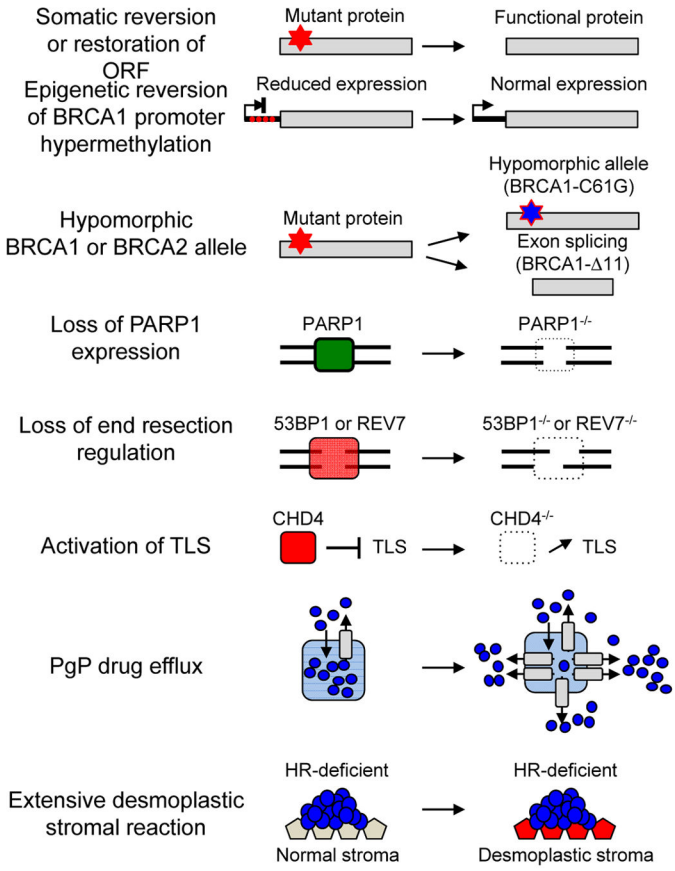

Mechanisms of resistance	PARPi	Cisplatin
Genetic reversion	resistant	resistant
Epigenetic reversion	resistant	resistant
Hypomorphic alllele	resistant	resistant
Loss of PARP1 expression	resistant	sensitive
Loss of end resection regulation	resistant	sensitive (53BP1); ? (REV7)
TLS Activation	resistant	resistant
PGP drug efflux	resistant	sensitive
Extensive stromal reaction	resistant*	resistant

Figure 4. Mechanisms of PARPi resistance in HR deficient cells

Known mechanisms conferring PARPi resistance in tumors cells and cross-resistance to cisplatin are indicated. An acquired genetic reversion of the original truncating mutations restores functional protein expression inducing PARPi resistance. Alternatively, acquired epigenetic reversion of BRCA1 promoter hypermethylation can restore normal BRCA1 protein expression levels conferring PARPi resistance. Hypomorphic alleles, such as BRCA1-C61G or BRCA1-Δ11, are unable to prevent tumor development but confer resistance to PARPi. Tumor cells may also become PARPi resistant through loss of PARP1 expression. Rescue of DNA end-resection in BRCA1-deficient tumors through loss of 53BP1 or REV7, increases HR capacity and confers resistance to PARPi. Loss of CHD4, a negative regulator of translesion synthesis (TLS), enhances DNA damage tolerance and induces PARPi resistance. Increased in P-glycoprotein (PGP)–mediated efflux, notably through ABCB1 upregulation (via fusion with SLC25A40) reduces intracellular PARPi concentrations inducing resistance. Desmoplastic stromal reaction is associated with reduced drug uptake conferring chemoresistance. (*: Although this mechanism has been described for cisplatin it might also apply for PARPi).

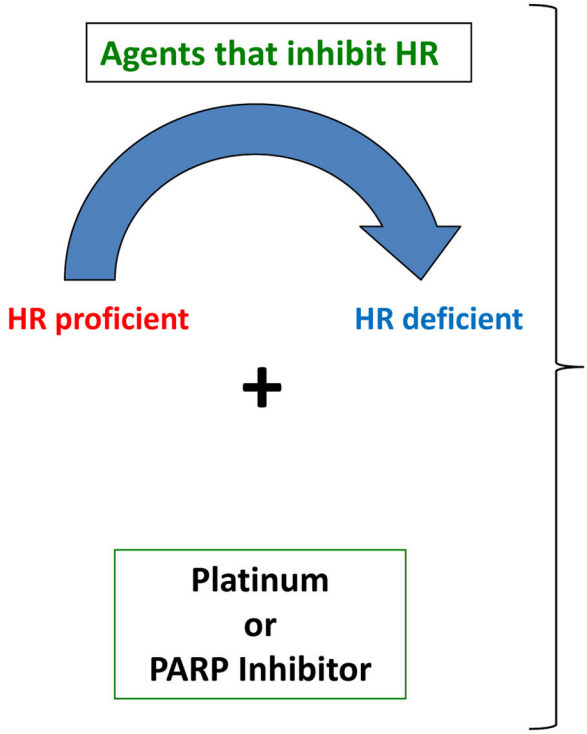

Combinations	Possible Mechanism of HR suppression	Status
PARPi/CDK1 inhibitors	Inhibition of phosphorylation of BRCA1	Phase I clinical trial (Veliparib+dinaciclib)
PARPi/PI3K pathway inhibitors	Increased activation of ETS1 and suppression of BRCA1/2 expression	Phase I clinical trials (Olaparib + BKM120) (Olaparib + AZD5363)
PARPi/VEGFR3 inhibitors	Downregulation of BRCA1/2 gene expression	Randomized Phase II trial (Olaparib+Cediranib)
PARPi/HSP90 inhibitors	BRCA1 and other HR pathway genes are HSP90 client proteins	Preclinical
PARPi/HDAC inhibitors	Downregulation of HR pathway genes	Preclinical
PARPi/CDK12 inhibitors	Downregulation of HR pathway genes	Phase I clinical trial (Veliparib+dinaciclib)

Figure 5. PARPi combinations against HR proficient tumors

Rationale behind use of specific PARPi combinations as a strategy against HR proficient tumors. Specifically, use of agents that inhibit HR such as CDK1- or HSP90 inhibitors may render HR proficient tumors into HR deficient and thus sensitize them to platinum or PARPis. The proposed mechanism of HR suppression and the clinical status of these PARPi combinations are presented in the right panel.

Table 1

Important previous and ongoing Phase II/III studies of PARPis in EOC

Setting	Study Identifier	Agents	Design	Patients/Accrual	Primary Endpoint	Results/Status
First Line/Maintenance	NCT01844986	Olaparib Vs Placebo	Phase III, Randomized, Double Blind, Placebo Controlled	BRCA mutated high grade serous or high grade endometrioid ovarian cancer N = 344	PFS	Ongoing
Recurrent/Maintenance	NCT00753545	Olaparib Vs Placebo	Phase II, Randomized, Double Blind, Placebo Controlled	Recurrent platinum sensitive high grade serous N=265	PFS	BRCAm PFS: 11.2 vs 4.3 months, HR=0.18 NonBRCAm PFS: 7.4 vs 5.5 months, HR=0.54
Recurrent/Maintenance	NCT01847274	Niraparib Vs Placebo	Phase III, Randomized, Double Blind, Placebo Controlled	Platinum sensitive recurrent high grade serous endometrioid/ BRCA stratified N=360	PFS	Ongoing
Recurrent/Maintenance	NCT01874353	Olaparib Vs Placebo	Phase III, Randomized, Double Blind, Placebo Controlled	Recurrent platinum sensitive BRCAm high grade serous or endometrioid EOC N=264	PFS	Ongoing
Recurrent/Maintenance	NCT01968213	Rucaparib Vs Placebo	Phase III, Randomized, Double Blind, Placebo Controlled	Platinum sensitive recurrent high grade serous endometrioid/ BRCA stratified N=540	PFS	Ongoing
Recurrent/Maintenance	NCT01081951	Olaparib/Carbo/Taxol Vs Carbo/Taxol	Randomized Phase II, Open Label	Platinum sensitive recurrent HGSC (both BRCAm and nonBRCAm) N=90	PFS	ALL: 12.2 vs 9·6 months, HR=0·51 BRCAm: HR=0.21
Recurrent	NCT01116648	Olaparib/Cediraniib Vs Olaparib	Randomized Phase II, Open Label	Platinum sensitive recurrent HGSC (both BRCAm and nonBRCAm) N=90	PFS	ALL: 17·7 vs 9·0 months, HR=0·42 BRCAm: 19.4 vs 16.5 months, HR=0.55 nonBRCAm: 16.5 vs 5.7 months, HR=0.32

Association and prognostic significance of BRCA1/2-mutation status with neoantigen load, number of tumor-infiltrating lymphocytes and expression of PD-1/PD-L1 in high grade serous ovarian cancer

Kyle C. Strickland[1], Brooke E. Howitt[1], Sachet A. Shukla[2,4], Scott Rodig[1], Lauren L. Ritterhouse[1], Joyce F. Liu[3], Judy E. Garber[4], Dipanjan Chowdhury[5], Catherine J. Wu[2,4], Alan D. D'Andrea[5], Ursula A. Matulonis[3], Panagiotis A. Konstantinopoulos[3]

[1]Department of Pathology, Brigham and Women's Hospital, Harvard Medical School, Boston, MA, USA

[2]The Broad Institute of Harvard and MIT, Cambridge, MA, USA

[3]Medical Gynecologic Oncology Program, Dana Farber Cancer Institute, Harvard Medical School, Boston, MA, USA

[4]Department of Medical Oncology, Dana Farber Cancer Institute, Harvard Medical School, Boston, MA, USA

[5]Division of Genomic Stability and DNA Repair, Dana Farber Cancer Institute, Harvard Medical School, Boston, MA, USA

Correspondence to: Panagiotis A. Konstantinopoulos, **e-mail:** panagiotis_konstantinopoulos@dfci.harvard.edu

Keywords: *high grade serous ovarian cancer, BRCA1 and BRCA2 mutations, homologous recombination DNA repair, immunogenicity, PD-1 and PD-L1*

Received: *October 12, 2015* ***Accepted:*** *January 24, 2016* ***Published:*** *February 09, 2016*

ABSTRACT

Immune checkpoint inhibitors (e.g., anti-PD-1 and anti-PD-L1 antibodies) have demonstrated remarkable efficacy against hypermutated cancers such as melanomas and lung carcinomas. One explanation for this effect is that hypermutated lesions harbor more tumor-specific neoantigens that stimulate recruitment of an increased number of tumor-infiltrating lymphocytes (TILs), which is counterbalanced by overexpression of immune checkpoints such as PD-1 or PD-L1. Given that BRCA1/2-mutated high grade serous ovarian cancers (HGSOCs) exhibit a higher mutational load and a unique mutational signature with an elevated number of larger indels up to 50 bp, we hypothesized that they may also harbor more tumor-specific neoantigens, and, therefore, exhibit increased TILs and PD-1/PD-L1 expression. Here, we report significantly higher predicted neoantigens in BRCA1/2-mutated tumors compared to tumors without alterations in homologous recombination (HR) genes (HR-proficient tumors). Tumors with higher neoantigen load were associated with improved overall survival and higher expression of immune genes associated with tumor cytotoxicity such as genes of the TCR, the IFN-gamma and the TNFR pathways. Furthermore, immunohistochemistry studies demonstrated that BRCA1/2-mutated tumors exhibited significantly increased CD3+ and CD8+ TILs, as well as elevated expression of PD-1 and PD-L1 in tumor-associated immune cells compared to HR-proficient tumors. Survival analysis showed that both BRCA1/2-mutation status and number of TILs were independently associated with outcome. Of note, two distinct groups of HGSOCs, one with very poor prognosis (HR proficient with low number of TILs) and one with very good prognosis (BRCA1/2-mutated tumors with high number of TILs) were defined. These findings support a link between BRCA1/2-mutation status, immunogenicity and survival, and suggesting that BRCA1/2-mutated HGSOCs may be more sensitive to PD-1/PD-L1 inhibitors compared to HR-proficient HGSOCs.

INTRODUCTION

Immune checkpoint inhibitors (e.g., anti–PD-1 and anti–PD-L1 antibodies) have demonstrated remarkable efficacy against hypermutated cancers such as melanomas, lung carcinomas and those with underlying mismatch repair-deficiency [1–3]. One explanation for this effect is that tumors with higher mutational loads harbor more tumor-specific neoantigens that stimulate recruitment of an increased number of tumor-infiltrating lymphocytes (TILs) which is counterbalanced by overexpression of immune checkpoint modulators, such as PD-1 or PD-L1 [4–7]. In support of this, recent analyses of TCGA data have implicated neoantigen load in driving T cell responses [8], and some have identified novel associations between specific genomic alterations such as polymerase e (POLE) mutations or microsatellite instability (MSI) and increased immune infiltrates and expression of immune checkpoints in hypermutated tumors [9, 10].

Approximately 50% of high grade serous ovarian cancers (HGSOCs) harbor genetic and epigenetic alterations in gene members of the homologous recombination (HR) DNA repair pathway, most commonly in BRCA1 and BRCA2 genes [11, 12]. BRCA1/2-mutation status is a favorable prognostic factor in this disease [11, 13, 14], which may be traditionally thought to be primarily due to the enhanced responsiveness of BRCA1/2-mutated tumors to platinum-based chemotherapy. However, it is possible that alternative intrinsic biologic properties of BRCA1/2-mutated HGSOCs (e.g., increased immunogenicity) contribute to the improved outcomes observed in these patients. In this regard, it has been shown that HR deficient HGSOCs (including those with BRCA1/2-mutations) depend on alternative, low fidelity mechanisms for double-strand break (DSB) repair, such as the Polθ/PARP1-mediated alternative end-joining (alt-EJ) pathway [15, 16]. DSB repair via alt-EJ utilizes microhomology at rearrangement junctions to rejoin DSBs and is mediated by the error-prone Polθ polymerase, which produces point mutations as well as random insertions and deletions (indels) at sites of microhomology [17]. Not surprisingly, BRCA1/2-mutated HGSOCs have been shown to possess a higher number of mutations compared to non-BRCA1/2-mutated tumors [18], with an elevated number of larger indels (up to 50 bp) with overlapping microhomology at breakpoint junctions [19]. Given their higher mutational load and unique mutational signature, we hypothesized that BRCA1/2-mutated tumors may harbor more tumor-specific neoantigens, and, therefore, increased tumor-infiltrating lymphocytes (TILs) [7] as well as demonstrate increased expression of the immune checkpoint modulators, PD-1 and PD-L1.

In this study, we formally evaluated the association of BRCA1/2-mutation status with neoantigen load, number of TILs and expression of PD-1 and PD-L1 in HGSOC. Furthermore, given that both BRCA1/2-mutation status and number of TILs are known favorable prognostic factors in this disease, we assessed whether BRCA1/2-mutated HGSOCs are independently associated with survival after adjusting for neoantigen load or number of TILs.

RESULTS

HR deficient HGSOCs exhibit higher neoantigen load compared to HR proficient tumors

Initially, we compared the neoantigen load between BRCA1/2-mutated HGSOCs versus all remaining tumors in the TCGA dataset. Prediction of neoantigen load was performed using sequencing data from the ovarian TCGA dataset which included whole-exome sequencing data from 316 HGSOCs [11]. 71 of 316 samples were excluded from our analysis because they were comprised of only single-end reads using the SOLiD platform and thus not amenable to accurate HLA typing. Inference of HLA type was successfully performed for the remaining 245 of HGSOCs, and prediction of neoantigen load was performed using a pipeline based on the NetMHCpan [20, 21] tool that predicts MHC class I binding peptides. We predicted neoepitopes individual to each tumor arising from tumor-specific somatic mutations that could generate peptides predicted to bind to personal HLA alleles.

There was no statistically significant difference in the neoantigen load between BRCA1/2-mutated (germline and somatic) HGSOCs ($n = 54$) versus all remaining non-BRCA1/2-mutated tumors ($n = 191$) ($p = 0.15$, Figure 1A). However, it is now well established that some non-BRCA1/2-mutated tumors may still be HR deficient due to alterations in other HR genes. Therefore, we divided non-BRCA1/2-mutated tumors into two cohorts: 1) non-BRCA1/2 mutated HGSOCs with HR pathway alterations (HR-deficient/non-BRCA1/2-mutations cohort, $n = 69$) and 2) non-BRCA1/2-mutated HGSOCs without known alterations in the HR pathway (non-BRCA1/2-mutated and HR proficient cohort, $n = 122$). The HR-deficient/non-BRCA1/2-mutated cohort included HGSOCs with mutations in Fanconi Anemia (FA) genes, mutations in core HR RAD genes (including RAD50, RAD51 and RAD54L), mutations in DNA damage response genes involved in HR such as ATM and ATR, homozygous deletion of PTEN, amplification or mutation of EMSY, and promoter hypermethylation of BRCA1 or RAD51C.

We observed a higher neoantigen load in the BRCA1/2-mutated subset (median: 51, range: 11–199) compared to the HR-proficient subset (median: 37.5, range: 2–196) (two-sided *t*-test, $p = 0.008$, Figure 1B). Furthermore, the HR-deficient/non-BRCA1/2-mutated subset (median: 51, range: 7–279) harbored a higher neoantigen load compared to the HR-proficient subset (two-sided *t*-test, $p = 0.003$, Figure 1B).Collectively, the neoantigen load of the combined group of HR defective tumors (BRCA1/2 mutated plus HR defective

/wt BRCA) (n = 123) was significantly higher than that of HR proficient tumors (n = 122), median 51 vs 37.5 respectively, p = 0.001 (Figure 1C). Conversely, there was no statistically significant difference in neoantigen load between BRCA1/2-mutated and HR-deficient/non-BRCA1/2-mutated subsets (two-sided t-test, p = 0.76) or between BRCA1-mutated versus BRCA2-mutated tumors (two-sided t-test, p = 0.32, Figure 1D). To summarize, HR deficient tumors, either BRCA1/2-mutated or non-BRCA1/2-mutated, demonstrated significantly higher neoantigen loads than HR proficient tumors (i.e. those without BRCA1/2-mutations and without any other HR pathway gene alterations).

Lower neoantigen load is associated with inferior overall survival in the TCGA dataset

We evaluated the prognostic significance of neoantigen load in the TCGA dataset. Strikingly, tumors with the lowest quartile (Figure 1E) or lowest quintile (Figure 1F) of neoantigen load in the TCGA dataset were associated with significantly lower overall survival (OS) compared to the remaining tumors. There was no association of neoantigen load with disease free survival (DFS) using any cut-offs. As was previously reported [11], BRCA1/2-mutated tumors were associated with improved OS in the TCGA dataset. Importantly, in a multivariate analysis including BRCA1/2-mutation status and neoantigen load, BRCA1/2-mutation status retained its prognostic significance independently of neoantigen load (Supplementary Table 1). However, neoantigen load did not retain its prognostic significance after adjusting for BRCA1/2-mutation status in the TCGA dataset regardless of the cut-off (i.e. both using low quartile and low quintile), Supplementary Table 1.

Furthermore, we interrogated the TCGA dataset to determine whether tumors with high neoantigen load also exhibited greater expression of immune genes associated with tumor cytotoxicity. Specifically, we evaluated the expression of genes in the TCR signaling pathway (CD3G, CD3D, CD3E, LCK, LCP2, CD247, HLA-DPB1, HLA-DOB, ITK, PTPRC), the IFN-gamma pathway (STAT6,

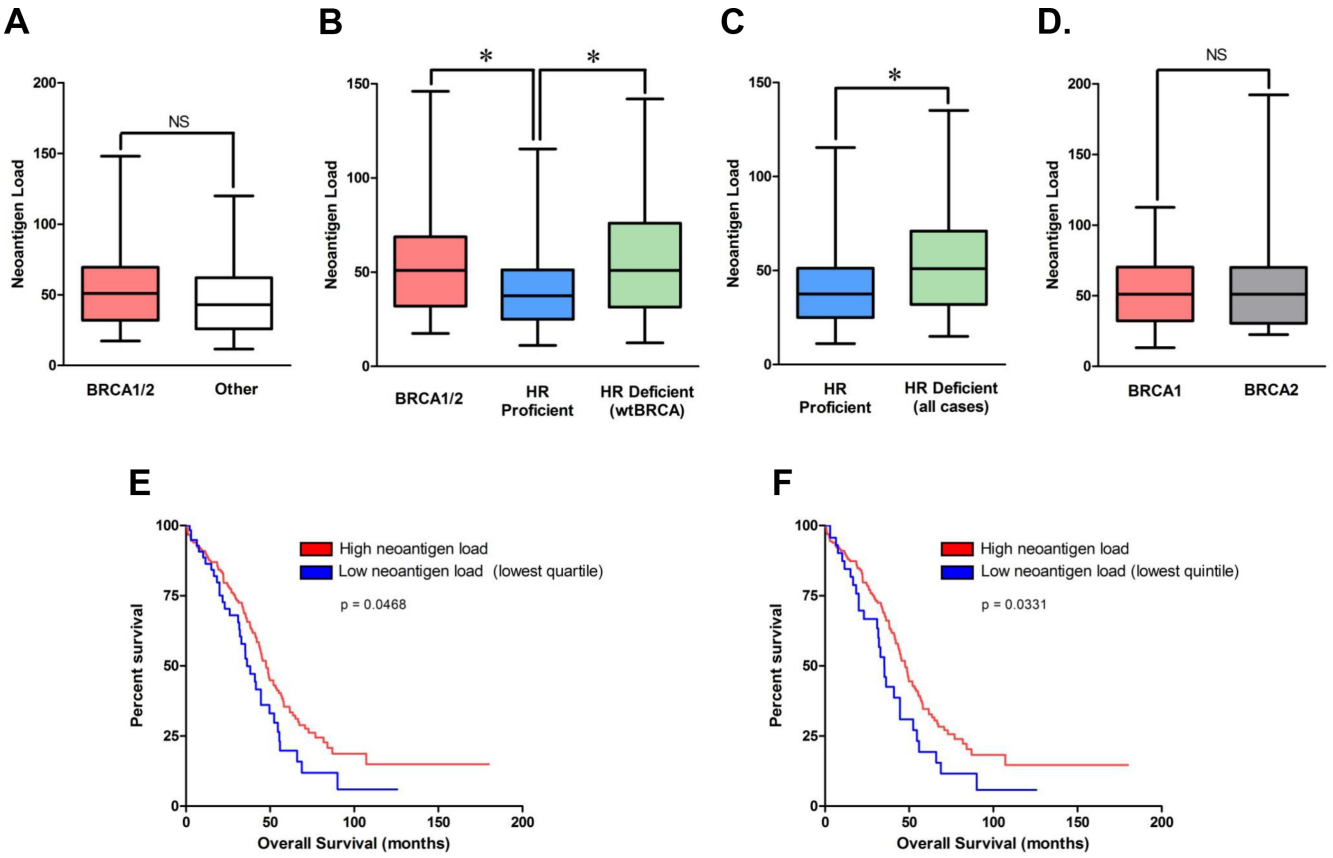

Figure 1: Neoantigen load in BRCA1/2-mutated, non-BRCA1/2-mutated/HR-deficient and HR proficient cohorts, and association with outcome in the TCGA dataset. (**A**) Predicted neoantigen load in BRCA1/2-mutated (n = 54) vs all remaining non-BRCA1/2-mutated tumors (n = 191). (**B**) Predicted neoantigen load in BRCA1/2-mutated (n = 54), HR deficient/non-BRCA1/2-mutated (n = 69) and HR proficient tumors (n = 122). (**C**) Predicted neoantigen load of HR-deficient (n = 123) vs HR-proficient (n = 122). (**D**) Predicted neoantigen load of BRCA1- versus BRCA2-mutated tumors. (**E**) Tumors in the lowest quartile of neoantigen load were associated with significantly lower overall survival compared to the remaining tumors. Of the 60 tumors in the lower quartile, 20 were HR deficient and 40 were HR proficient. (**F**) Tumors in the lowest quintile of neoantigen load were associated with significantly lower overall survival compared to the remaining tumors. Of the 47 tumors in the lower quintile, 19 were HR deficient and 28 were HR proficient.

TFF3, PRKCA, TGFBR2, PIM1, PRKCH, PRKCQ, IRF4) and the TNFR pathway (TRAF1, PRF1, MAPKAPK3, TNFRSF1B, CCM2, GZMB, BIRC3, MAP3K14), and we assessed whether they were differentially expressed between tumors with high neoantigen load versus those with low antigen load (lowest quartile). Indeed, we found that several genes were statistically significantly differentially expressed between tumors with high neoantigen load versus those with low antigen load (HLA-DOB $p = 0.05$, GZMB $p = 0.011$, CD3G $p < 0.001$, CD3E $p = 0.027$, CD3D $p < 0.001$, CD247 $p = 0.003$, PRF1 $p = 0.018$, LCP2 $p = 0.007$, LCK $p = 0.023$, ITK $p = 0.012$, IRF4 $p = 0.001$, PTPRC $p = 0.026$). Strikingly, each of these genes were upregulated in the tumors with high neoantigen load compared to those with low neoantigen load. Furthermore, PD-L1 was upregulated in the tumors with high neoantigen load compared to those with low neoantigen load ($p = 0.03$).

BRCA1/2-mutated HGSOCs harbor increased CD3+ and CD8+ TILs compared to HR proficient HGSOCs

Based on our findings from the neoantigen prediction analysis in the TCGA dataset (Figure 2A), we assessed whether there was any difference in TILs between BRCA1/2-mutated and HR proficient HGSOCs in a separate cohort of patients referred to our institution. This cohort included two groups of patients, a BRCA1/2-mutated group and an HR proficient group. The BRCA1/2-mutated group was comprised of 37 HGSOCs (29 with BRCA1 and 8 with BRCA2 mutations) with BRCA1/2 germline mutations identified by genetic testing (Figure 2B). The HR-proficient group (i.e., tumors without HR alterations) comprised 16 ovarian cancers which were identified in a two-step process (Figure 2B). First, Next Generation Sequencing (NGS) was performed to exclude tumors with mutations in HR genes, and this analysis identified 17 such tumors. These 17 tumors were subsequently evaluated for BRCA1 expression to exclude the possibility of BRCA1 promoter hypermethylation by immunohistochemistry, a method which has been previously reported to have a sensitivity of 86% and specificity of 97% for detecting loss of BRCA1 protein expression [22]. As a result of this testing, 1 tumor was found to have staining in less than 5% of tumor cells with the presence of a strong internal control (Figure 3), which was excluded from the HR-proficient (HR intact) group. Interestingly, review of the NGS data for this case demonstrated that this tumor had a single copy deletion of the BRCA1 gene, suggesting that BRCA1 loss was likely due to single copy deletion of BRCA1 and epigenetic silencing of the complementary allele. Ultimately, the HR proficient group consisted of 16 tumors without mutations in HR pathway genes and without BRCA1 loss by IHC.

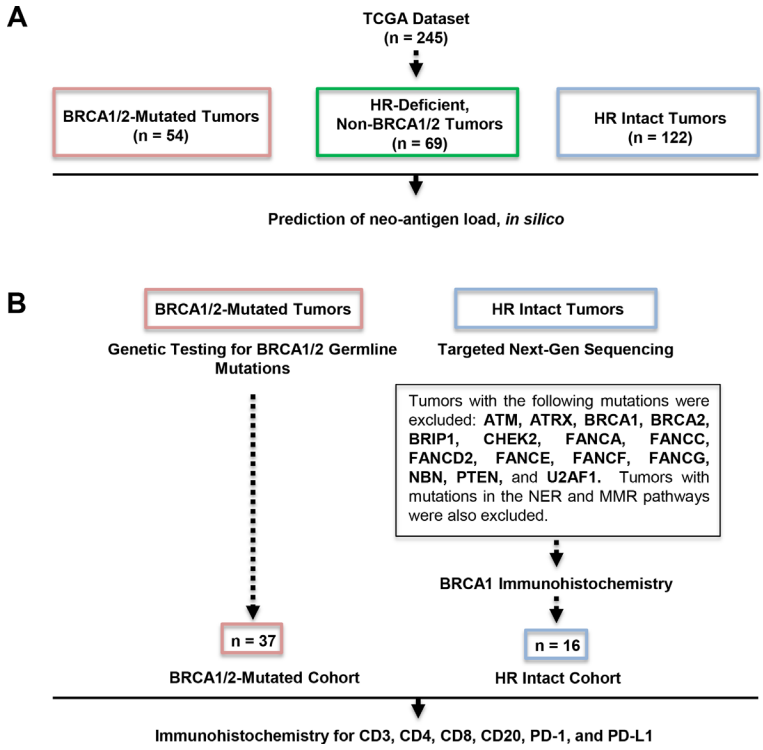

Figure 2: Outline of our study cohorts. (**A**) Prediction of neoantigen load in the TCGA dataset. (**B**) Determination of BRCA1/2-mutated and HR proficient subsets in our institutional cohort. The BRCA1/2-mutated group was comprised of 37 HGSOCs with BRCA1/2 germline mutations (29 with BRCA1 and 8 with BRCA2 mutations) identified by genetic testing (left). The HR-proficient (HR intact) group (i.e. group without HR alterations) comprised 16 ovarian cancers which were identified in a two-step process (right). First, NGS excluded tumors with mutations in HR genes and this analysis identified 17 such tumors. Tumor was excluded based on absent BRCA1 expression by immunohistochemistry.

Immunohistochemistry (IHC) in the two patient groups demonstrated that BRCA1/2-mutated tumors exhibited a significantly higher number of CD3+ TILs (mean 42.9 vs 20.7, p = 0.001, Figure 4A and 4B) and CD8+ TILs (34.5 vs 15.2, p = 0.002, Figure 4A and 4D) compared to HR-proficient tumors. Figure 4A shows the IHC staining of a representative BRCA1/2-mutated tumor with CD3+ and CD8+ TILs, as well as a representative HR-proficient case with reduced CD3+ or CD8+ TILs. There was no statistically significant difference in CD4+ or CD20+ TILs between BRCA1/2-mutated and HR-proficient tumors (Figure 4C and 4E), but we observed a substantially higher CD8/CD4 ratio in BRCA1/2-mutated versus HR-proficient tumors (3.3 vs 1.2, p = 0.003). There was no statistically significant difference in CD3+ and CD8+ TILs between BRCA1 and BRCA2 mutated tumors (p = 0.13 and p = 0.63 respectively).

BRCA1/2-mutated HGSOCs harbor increased PD-1 and PD-L1 expression compared to HR proficient HGSOCs

We then evaluated PD-1 and PD-L1 expression both in the intraepithelial and peritumoral immune cells of BRCA1/2-mutated versus HR-proficient tumors by immunohistochemistry (Figure 5A). Expression of PD-1 in intraepithelial and peritumoral lymphocytes was significantly more frequent in BRCA1/2-mutated compared to HR-proficient HGSOCs (p = 0.003 and p = 0.005 respectively, Figure 5B). Furthermore, PD-L1 expression in intraepithelial and peritumoral immune cells was also more frequently observed in BRCA1/2-mutated tumors compared to the HR-proficient tumors (p = 0.016 and p = 0.019 respectively, Figure 5B). However, within tumor cells, PD-L1 expression was not found to be different between the two cohorts (Figure 5B). Of note,

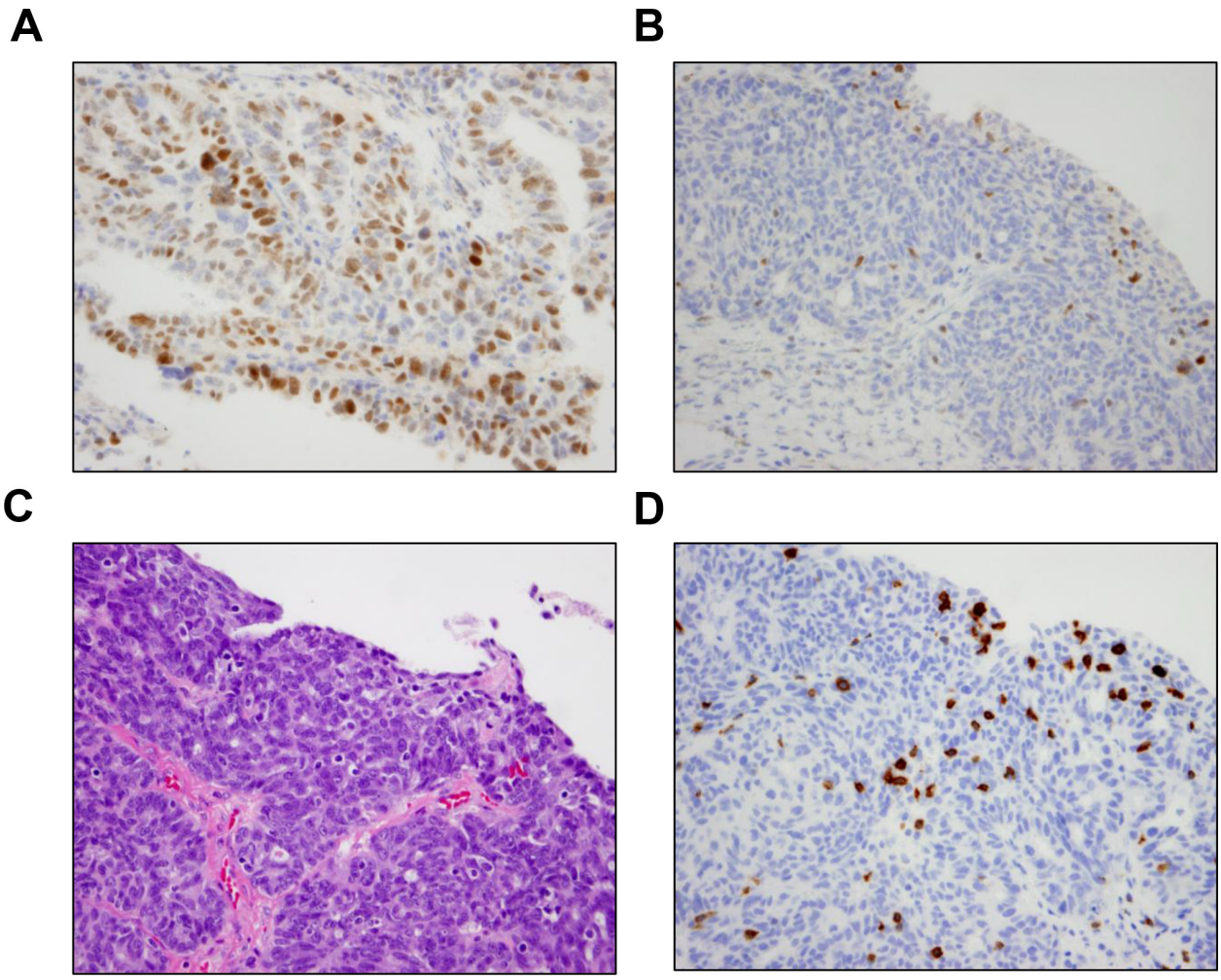

Figure 3: Results of BRCA1 immunohistochemistry. (**A**) Positive BRCA1 IHC in a representative case. BRCA1 expression was positive by IHC in 16 of the 17 tumors without HR alterations identified by NGS. (**B**) BRCA1 IHC was negative in one tumor that did not harbor HR alterations by NGS. Focal BRCA1 positivity was present in lymphocytes. Interestingly, review of the NGS data for this case demonstrated that the tumor had a single copy deletion of the BRCA1 gene, suggesting that BRCA1 loss in this tumor was likely due to single copy deletion of BRCA1 and epigenetic silencing of the complementary allele. (**C**) Corresponding area of tumor on H & E stain demonstrates the presence of intratumoral lymphocytes. (**D**) The presence of intraepithelial lymphocytes was confirmed by a CD3 IHC.

there was a significant correlation between CD3+ and both CD8+ and PD-1 positive TILs in tumors from both cohorts (Supplementary Figure 1, both $p < 0.001$).

Prognostic significance of BRCA1/2-mutation status and number of CD3+ TILs

As expected from previous studies [11, 13, 14], BRCA1/2-mutated tumors exhibited improved OS compared to HR-proficient HGSOCs ($p = 0.012$) in our institutional cohort (Figure 6A). Furthermore, as has been previously reported, the number of CD3+ TILs was associated with survival [23]. Specifically, HGSOCs with equal or above the median number of CD3+ TILs (i.e. ≥ 35 CD3+ TILs/HPF) exhibited improved OS compared to tumors with below the median number of CD3+ TILs (i.e. < 35 CD+3 TILs/HPF) (Figure 6B, $p = 0.046$). The best discrimination for OS in our cohort was achieved using a cut-off of 13 CD3+ TILs/HPF, whereby tumors with ≥ 13 TILs/HPF exhibited significantly higher OS compared to tumors with < 13 TILs/HPF (Figure 6C, $p < 0.001$). A similar association was observed between CD3+ TILs and DFS in our cohort (Supplementary Figure 2). Importantly, in multivariate analysis consisting of BRCA1/2-mutation status and CD3+ TILs, both BRCA1/2-mutation status (HR = 0.315, 90% C.I. 0.103–0.964, $p = 0.043$) and CD3 + TILs (HR = 0.147, 90% C.I. 0.05–0.436, $p = 0.001$) remained independently associated with OS. Based on the number of TILs and BRCA1/2-mutation status, we defined a very good prognostic group (BRCA-mutated tumors and high CD3+ count, median OS 229.2 months) and a very poor prognostic group (HR-proficient tumors and low CD3+ count, median OS 20.6 months); the remaining tumors (either BRCA-mutated with low CD3+ count or with HR proficient with high CD3+ count) exhibited intermediate OS (median OS 56.3 months) (Figure 6D).

DISCUSSION

BRCA1/2-mutated HGSOCs are HR deficient and depend on the error-prone Polθ/PARP1-mediated alt-EJ pathway for double-strand break repair [15, 16]. As a result, BRCA1/2-mutated HGSOCs possess a higher number of mutations [18, 24] with larger indels (up to 50 bp) and overlapping microhomology at breakpoint junctions [19]. Given their elevated mutational load and unique mutational signature, we hypothesized that BRCA1/2-mutated tumors may harbor more tumor-specific neoantigens, and therefore demonstrate, increased tumor-infiltrating lymphocytes (TILs) [7], as well as increased expression of immune checkpoint modulators PD-1 and PD-L1. Indeed, according to our neoantigen prediction analysis in the TCGA dataset, BRCA1/2-mutated HGSOCs exhibit significantly higher

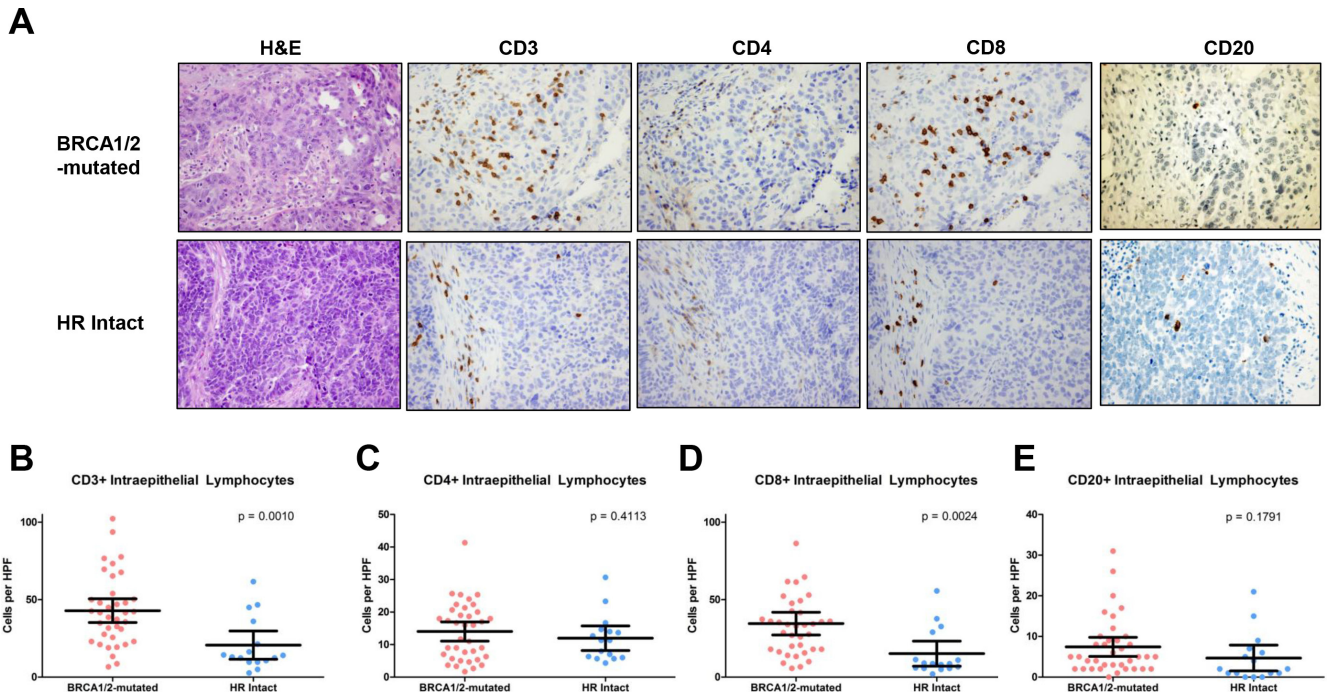

Figure 4: CD3+, CD4+ CD8+ and CD20+ intraepithelial lymphocytes in BRCA1/2-mutated vs HR proficient tumors. (**A**) Photomicrographs of representative BRCA1/2-mutated and HR-intact tumors depicting H & E staining and immunohistochemistry for CD3, CD4, CD8 and CD20. (**B**) Quantification and comparison of CD3+ TILs from BRCA1/2-mutated and HR intact tumors. (**C**) Quantification and comparison of CD4+ TILs from BRCA1/2-mutated and HR intact tumors. (**D**) Quantification and comparison of CD8+ TILs from BRCA1/2-mutated and HR intact tumors. (**E**) Quantification and comparison of CD20+ TILs from BRCA1/2-mutated and HR intact tumors.

neoantigen load compared to HR proficient HGSOCs (i.e. tumors without any HR pathway alterations). Of note, HR deficient HGSOCs that were not BRCA1/2-mutated (i.e. the HR deficient/non-BRCA1/2-mutated cohort) also harbored significantly higher neoantigen load compared to HR proficient tumors. The comparatively higher neoantigen load of HR deficient HGSOCs (regardless of whether they were BRCA1/2-mutated or not) is likely related to the unique mutational signature of HR deficient tumors, which is present regardless of whether HR deficiency is due to BRCA1/2-mutations or other HR alterations [19]. In this regard, within HR deficient tumors, we observed similar neoantigen load between BRCA1/2-mutated tumors and those with alternative HR alterations (HR-deficient/non-BRCA1/2-mutated cohort), as well as a similar neoantigen load between BRCA1- and BRCA2-mutated tumors.

In addition to a low neoantigen load, HR-proficient tumors exhibited significantly lower numbers of CD3+ and CD8+ TILs, as well as lower expression of the inhibitory immune checkpoint modulators, PD-1 and PD-L1, compared to BRCA1/2-mutated tumors. This observation is consistent with the hypothesis that an elevated neoantigen load leads to an increased number of TILs that are counterbalanced by overexpression of immune checkpoint modulators [4–6]. Although PD-L1 expression in tumor-infiltrating immune cells was different between HR-proficient and BRCA1/2-mutated tumors, PD-L1 expression in cancer cells was not different. It is important to underscore that PD-L1 expression in tumor-infiltrating immune cells does not always correlate with PD-L1 expression in cancer cells. As such, response to anti-PD-L1 antibody MPDL3280A has been previously shown to correlate with tumor-infiltrating immune cell PD-L1 expression but not expression of PD-L1 in tumor cells [25]. Collectively, our findings suggest that BRCA1/2-mutated HGSOCs may be more sensitive to PD-1/PD-L1 inhibitors compared to HR-proficient HGSOCs.

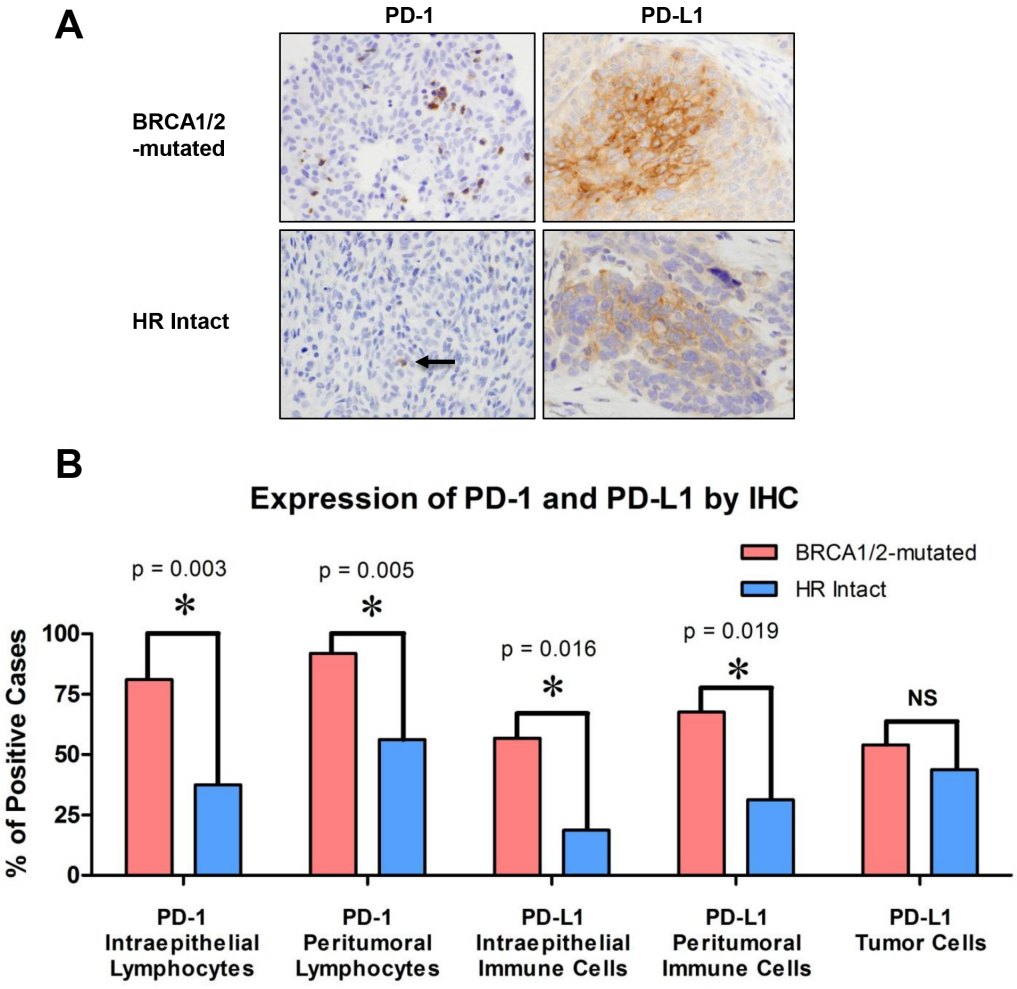

Figure 5: PD-1 and PD-L1 expression in the intraepithelial and peritumoral immune cells of BRCA1/2-mutated versus HR-proficient tumors. (**A**) Photomicrographs of representative BRCA1/2-mutated and HR-intact tumors depicting H & E staining and immunohistochemistry for PD-1 and PD-L1. Photomicrographs depict cases from each study group that were scored as positive. (**B**) Bar graphs illustrating the number of tumors with increased PD-1 and PD-L1 positive intraepithelial and peritumoral immune cells, as well as the number of tumors positive for PD-L1 in tumor cells of BRCA1/2-mutated and HR intact cases.

Additionally, we noted that the number of CD3+ TILs significantly correlated with the number of PD-1-positive lymphocytes (Supplementary Figure 1), suggesting that, in this setting, the number of CD3+ cells could be used as a surrogate marker of PD-1 positivity. However, further investigation is required to determine if the number of TILs can predict responsiveness to anti-PD-1 or anti-PD-L1 immunotherapies. Similar to the neoantigen load prediction in the TCGA dataset, we observed no difference in the number of TILs between BRCA1- and BRCA2-mutated tumors in our patient cohort. Although previous studies have demonstrated that BRCA1 HGSOCs exhibit increased number of TILs [24, 26–28], our findings suggest that the same also applies for BRCA2-mutated HGSOCs. Most importantly, our study is the first to indicate that HGSOCs without HR alterations (HR proficient HGSOCs) represent a unique subset of tumors with lower neoantigen load, lower number of TILs and lower PD-1 and PD-L1 expression.

Finally, given that elevated TILs is a well-documented favorable prognostic factor in HGSOC [23, 29], our findings suggest that enhanced immunogenicity may also explain the improved OS of BRCA1/2-mutated tumors. Importantly, BRCA1/2-mutation status was independently associated with OS after adjusting either for neoantigen load in the TCGA dataset or for number of TILs in our patient cohort, a finding that suggests that alternative factors that are intrinsic to BRCA1/2-mutated tumors (such as enhanced response to platinum chemotherapy among other possibilities) may also contribute to the improved OS of these tumors, independently of their association with elevated number of TILs. Strikingly, BRCA1/2-mutated tumors with elevated TILs were associated with the best prognosis in our patient cohort while tumors that were both HR-proficient-tumors and had low number of TILs exhibited the worst prognosis (Figure 6D).

In contrast to the number of TILs, neoantigen load was significantly associated with OS but not PFS. It is possible that an association between neoantigen load and PFS may exist but was not observed in the TCGA dataset. Of note, only patients with neoantigen load in the

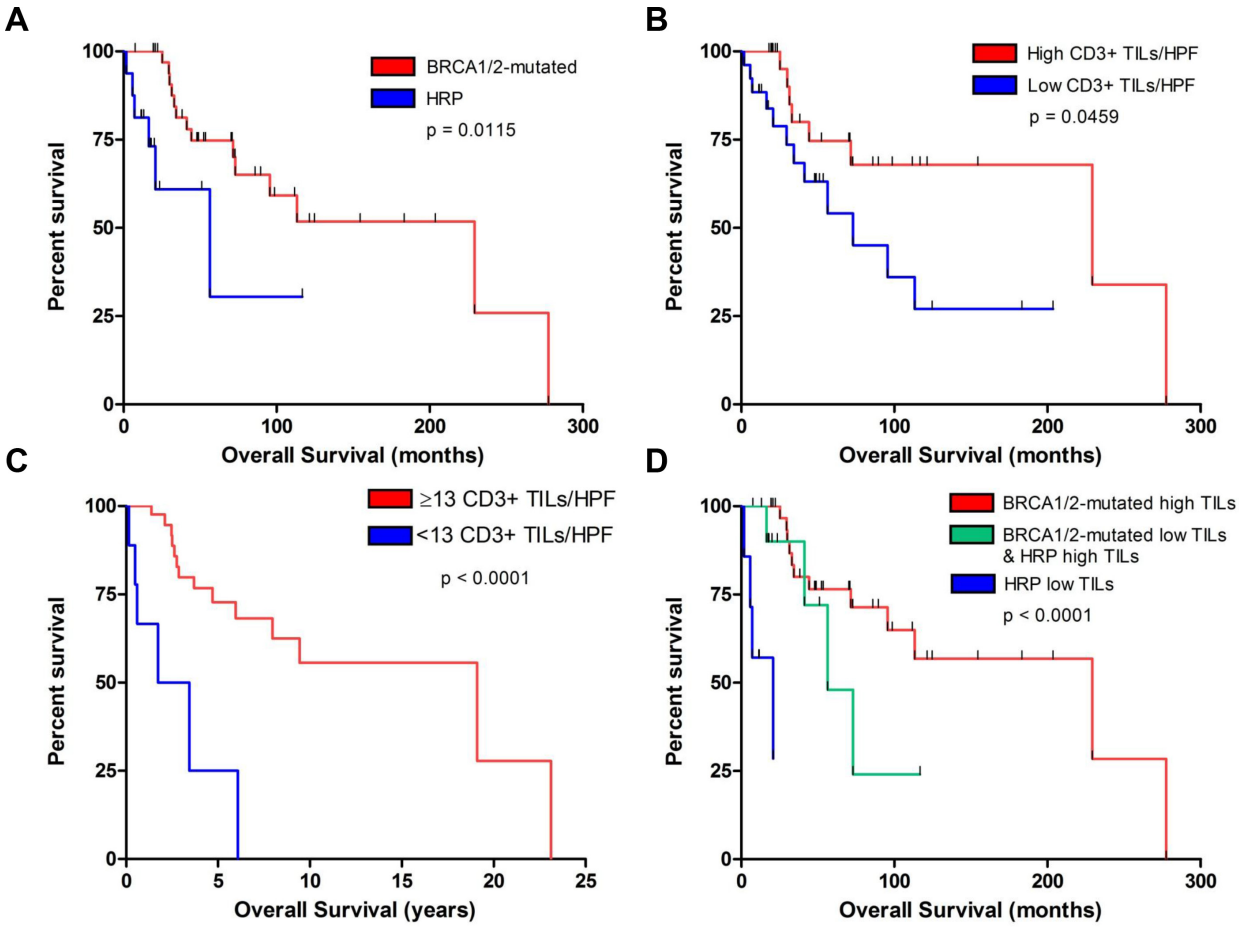

Figure 6: Association of CD3+ TILs and BRCA1/2-mutation status with survival in our institutional cohort. (**A**) Overall survival of patients with BRCA1/2-mutated (red) versus HR intact (HRP, blue) tumors. (**B**) Overall survival of patients with tumors containing above median number of CD3+ TILs/HPF (red) versus the remaining tumors (blue). (**C**) Overall survival of patients with tumors containing ≥ 13 CD3+ TILs/HPF (red) versus those containing < 13 CD3+ TILs/HPF (blue). (**D**) Overall survival of patients with BRCA1/2-mutated tumors with a high number of TILs (≥ 13 TILs/HPF) (red), HR proficient tumors (HRP) with a low number of TILs (< 13 TILs/HPF) (blue), and BRCA1/2-mutated tumors with low TILs or HRP tumors with high TILs (green).

lower quartile or quintile had lower OS, suggesting that additional factors are likely responsible. Furthermore, it is important to underscore that PFS is a marker of outcome that reflects more the responsiveness to first line chemotherapy and less the biological aggressiveness of the disease is (which is more globally reflected by OS). Therefore, lower neoantigen load may reflect more aggressive disease and thus inferior OS but not necessarily worse response to first line chemotherapy.

In conclusion, our findings support a link between BRCA1/2-mutation status, immunogenicity and improved survival in HGSOC, and support inclusion of BRCA1/2-mutations and other HR alterations as exploratory biomarkers in immunotherapy trials in this disease. Furthermore, our study suggests that BRCA1/2-mutated HGSOCs may be more sensitive to PD-1/PD-L1 inhibitors compared to HR-proficient HGSOCs.

MATERIALS AND METHODS

Prediction of HLA type and neoantigen load

Inference of HLA type was performed by applying the POLYSOLVER (POLYmorphic loci reSOLVER) tool [30] to whole-exome sequencing (WES) data generated from The Cancer Genome Atlas (TCGA) consortium as previously described [31]. Polysolver has previously been validated on a set of 253 HapMap samples with experimentally determined HLA genotypes, where it was found to have ~97% mean overall accuracy at the protein-coding level [31]. In brief, this algorithm selects and aligns putative HLA reads to an imputed library of full-length genomic HLA allele sequences. The alignments then serve as a basis for the inference step that incorporates the number and base qualities of aligned reads, the empirical library insert size distribution and population-based allele frequencies. For prediction of neoantigen load, we used previously curated lists of somatic mutations (somatic single nucleotide variants and somatic insertions and deletions) for each of these samples (Sage Bionetworks' Synapse resource: http://www.synapse.org/#!synapse:syn1729383 and Lawrence et al. [32]) from which individual-specific HLA-binding peptides were identified by a neoantigen prediction pipeline [30] that uses detected somatic mutations in the individual. Binding affinities of all possible 9 and 10-mer mutant peptides to the corresponding POLYSOLVER-inferred HLA alleles were predicted using NetMHCpan (v2.4) [21]. All predicted binders with an affinity < 500 nM were used to evaluate the neoantigen load.

Next generation sequencing

In order to identify tumors without HR alterations, HGSOC samples were subjected to targeted Next-Generation sequencing (NGS) assay (OncoPanel), performed at the Center for Advanced Molecular Diagnostics (Department of Pathology, Brigham and Women's Hospital) [33]. This assay has been extensively validated and is used as a CLIA-approved clinical molecular test in our institution without any additional sequencing assays to validate the findings. FFPE samples were digested in proteinase K overnight and DNA was isolated according to the manufacturer's protocol (QIAamp DNA Mini Kit, QIAGEN, Gaithersburg, MD, USA). All cases with at least 50 ng of DNA (up to 200 ng) were subjected to next-generation sequencing (NGS) of the complete exons of 275 oncogenes and tumor suppressor genes. Ninety-one intronic regions across 30 genes were also included for the evaluation of structural rearrangements. Targeted sequences were captured using a solution-phase Agilent SureSelect hybrid capture kit (Agilent Technologies, Inc, Santa Clara, CA, USA), and massively parallel sequencing was performed on an Illumina HiSeq 2500 sequencer (Illumina, Inc, San Diego, CA, USA). Mutation calls were made using Mutect and GATK software (Broad Institute, Cambridge, MA, USA) and gene-level copy number alterations at the level of individual genes were assessed using VisCap Cancer (Dana Farber Cancer Institute, Boston, MA, USA). Tumors were assessed for mutations in the following HR-pathway genes: ATM, ATRX, BRCA1, BRCA2, BRIP1, CHEK2, FANCA, FANCC, FANCD2, FANCE, FANCF, FANCG, NBN, PTEN, and U2AF1. Additionally, tumors with mutations in the nucleotide excision repair (NER) and mismatch repair (MMR) pathways were excluded from the HR-proficient cohort. We thus identified 17 tumors without mutations in one or more of these HR pathway genes.

BRCA1 immunohistochemistry

The 17 tumors identified via NGS were subsequently evaluated for BRCA1 by immunohistochemistry to assess for BRCA1 loss due to epigenetic silencing. Immunohistochemistry for BRCA1 was performed in a manner previously described [22]. The sensitivity and specificity for BRCA1 immunohistochemistry has previously been established and found to detect BRCA1 mutations and promoter hypermethylation with 86% sensitivity and 97% specificity [22].

Immunohistochemistry and evaluation of tumor associated lymphocytes

Paraffin-embedded, formalin-fixed tissue blocks of chemotherapy-naive biopsy and resection specimens were retrieved from the Brigham and Women's Hospital Department of Pathology archives. For all cases, IHC was performed for CD3, CD4, CD8, CD20, PD-1, and PD-L1 slides using standard protocols (Supplementary Table 2). TILs were defined as intraepithelial lymphocytes (i.e. cells

that were clearly located within tumor epithelium rather than peritumoral stroma). Photomicrographs were taken of three areas enriched for intraepithelial CD3+ lymphocytes (40X objective) with blinding to mutational status. For the analysis of all markers, areas of acute inflammation and necrosis were avoided. Photomicrographs of the corresponding tumor location were obtained for CD4 and CD8 stains. Counts of intraepithelial lymphocytes were performed manually with blinding to mutation status, and the average was determined from counts of three high power fields (HPFs), as previously described [9]. A separate photomicrograph was obtained in an area enriched for CD20+ intraepithelial lymphocytes. The number of intraepithelial PD-1 positive lymphocytes was determined as the average count from three HPFs. For statistical analyses, an average of 1 or greater PD-1-positive cells per HPF was considered positive. Peritumoral T-cells were scored using a semi-quantitative system (minimal (0), mild (1+), moderate (2+), and marked (3+)), with a score of mild or greater used as a cutoff for elevated peritumoral lymphocytic response. PD-L1 in intraepithelial and peritumoral immune cells was also evaluated using a semi-quantitative scoring system (negative (0), mild (1+), moderate (2+)). Tumor cell expression of PD-L1 was evaluated in a semi-quantitatively as above, similar to methods previously described. [34] Positive tumor expression of PD-L1 was defined as greater than or equal to 5% of tumor cells with PD-L1 positivity.

Statistical analyses

Statistical comparisons of lymphocyte counts between BRCA1/2-mutated and HR-intact tumors were performed using unpaired, two-tailed Student's *t*-test, Fisher's exact test, and Spearman correlations in GraphPad Prism (v5). Kaplan-Meier survival curves and multivariate Cox regression analyses were performed using SPSS software.

ACKNOWLEDGMENTS

CJW acknowledges support from the Blavatnik Family Foundation and NIH/NCI (1R01CA155010-04), and is a Scholar of the Leukemia and Lymphoma Society. PAK acknowledges support from the DOD Ovarian Cancer Academy Award W81XWH-10-1-0585 and the Susan Smith Center for Women's Cancers. ADA and PAK acknowledge support from Stand Up To Cancer—Ovarian Cancer Research Fund-Ovarian Cancer National Alliance-National Ovarian Cancer Coalition Dream Team Translational Research Grant (grant number: SU2C-AACR-DT16-15).

SR has received research funding from Bristol-Myers Squibb and Roche-Ventana. All other authors have no conflicts of interests or financial disclosures to declare.

CONFLICTS OF INTEREST

The authors declare that they have no conflicts of interest to report.

REFERENCES

1. Brahmer JR, Tykodi SS, Chow LQ, Hwu WJ, Topalian SL, Hwu P, Drake CG, Camacho LH, Kauh J, Odunsi K, Pitot HC, Hamid O, Bhatia S, et al. Safety and activity of anti-PD-L1 antibody in patients with advanced cancer. N Engl J Med. 2012; 366:2455–2465.
2. Topalian SL, Hodi FS, Brahmer JR, Gettinger SN, Smith DC, McDermott DF, Powderly JD, Carvajal RD, Sosman JA, Atkins MB, Leming PD, Spigel DR, Antonia SJ, et al. Safety, activity, and immune correlates of anti-PD-1 antibody in cancer. N Engl J Med. 2012; 366:2443–2454.
3. Le DT, Uram JN, Wang H, Bartlett BR, Kemberling H, Eyring AD, Skora AD, Luber BS, Azad NS, Laheru D, Biedrzycki B, Donehower RC, Zaheer A, et al. PD-1 Blockade in Tumors with Mismatch-Repair Deficiency. N Engl J Med. 2015; 372:2509–2520.
4. Xiao Y, Freeman GJ. The microsatellite instable subset of colorectal cancer is a particularly good candidate for checkpoint blockade immunotherapy. Cancer Discov. 2015; 5:16–18.
5. Llosa NJ, Cruise M, Tam A, Wicks EC, Hechenbleikner EM, Taube JM, Blosser RL, Fan H, Wang H, Luber BS, Zhang M, Papadopoulos N, Kinzler KW, et al. The vigorous immune microenvironment of microsatellite instable colon cancer is balanced by multiple counter-inhibitory checkpoints. Cancer Discov. 2014; 5:43–51.
6. Hussein YR, Weigelt B, Levine DA, Schoolmeester JK, Dao LN, Balzer BL, Liles G, Karlan B, Kobel M, Lee CH, Soslow RA. Clinicopathological analysis of endometrial carcinomas harboring somatic POLE exonuclease domain mutations. Mod Pathol. 2015; 28:505–514.
7. Rooney MS, Shukla SA, Wu CJ, Getz G, Hacohen N. Molecular and genetic properties of tumors associated with local immune cytolytic activity. Cell. 2015; 160:48–61.
8. Brown SD, Warren RL, Gibb EA, Martin SD, Spinelli JJ, Nelson BH, Holt RA. Neo-antigens predicted by tumor genome meta-analysis correlate with increased patient survival. Genome Res. 2014; 24:743–750.
9. Howitt BE, Shukla SA, Sholl LM, Ritterhouse LL, Watkins JC, Rodig S, Stover E, Strickland KC, D'Andrea AD, Wu CJ, Matulonis UA, Konstantinopoulos PA. Association of Polymerase e-Mutated and Microsatellite-Instable Endometrial Cancers With Neoantigen Load, Number of Tumor-Infiltrating Lymphocytes, and Expression of PD-1 and PD-L1. JAMA Oncol. 2015; 1:1319–23.
10. Llosa NJ, Cruise M, Tam A, Wicks EC, Hechenbleikner EM, Taube JM, Blosser RL, Fan H, Wang H, Luber BS, Zhang M, Papadopoulos N, Kinzler KW, et al. The vigorous immune microenvironment of microsatellite instable

colon cancer is balanced by multiple counter-inhibitory checkpoints. Cancer Discov. 2015; 5:43–51.

11. TCGA. Integrated genomic analyses of ovarian carcinoma. Nature. 2011; 474:609–615.
12. Konstantinopoulos PA, Ceccaldi R, Shapiro GI, D'Andrea AD. Homologous Recombination Deficiency: Exploiting the Fundamental Vulnerability of Ovarian Cancer. Cancer Discov. 2015; 5:1137–54.
13. Bolton KL, Chenevix-Trench G, Goh C, Sadetzki S, Ramus SJ, Karlan BY, Lambrechts D, Despierre E, Barrowdale D, McGuffog L, Healey S, Easton DF, Sinilnikova O, et al. Association between BRCA1 and BRCA2 mutations and survival in women with invasive epithelial ovarian cancer. JAMA. 2012; 307:382–390.
14. Boyd J, Sonoda Y, Federici MG, Bogomolniy F, Rhei E, Maresco DL, Saigo PE, Almadrones LA, Barakat RR, Brown CL, Chi DS, Curtin JP, Poynor EA, et al. Clinicopathologic features of BRCA-linked and sporadic ovarian cancer. JAMA. 2000; 283:2260–2265.
15. Ceccaldi R, Liu JC, Amunugama R, Hajdu I, Primack B, Petalcorin MI, O'Connor KW, Konstantinopoulos PA, Elledge SJ, Boulton SJ, Yusufzai T, D'Andrea AD. Homologous-recombination-deficient tumours are dependent on Poltheta-mediated repair. Nature. 2015; 518:258–262.
16. Mateos-Gomez PA, Gong F, Nair N, Miller KM, Lazzerini-Denchi E, Sfeir A. Mammalian polymerase theta promotes alternative NHEJ and suppresses recombination. Nature. 2015; 518:254–257.
17. Yousefzadeh MJ, Wood RD. DNA polymerase POLQ and cellular defense against DNA damage. DNA repair. 2013; 12:1–9.
18. Birkbak NJ, Kochupurakkal B, Izarzugaza JM, Eklund AC, Li Y, Liu J, Szallasi Z, Matulonis UA, Richardson AL, Iglehart JD, Wang ZC. Tumor mutation burden forecasts outcome in ovarian cancer with BRCA1 or BRCA2 mutations. PLoS One. 2013; 8:e80023.
19. Alexandrov LB, Nik-Zainal S, Wedge DC, Aparicio SA, Behjati S, Biankin AV, Bignell GR, Bolli N, Borg A, Borresen-Dale AL, Boyault S, Burkhardt B, Butler AP, et al. Signatures of mutational processes in human cancer. Nature. 2013; 500:415–421.
20. Shukla SA, Rajasagi M, Tiao G, Dixon PM, Lawrence MS, Stevens J, Lane WJ, Dellagatta JL, Steelman S, Sougnez C, Cibulskis K, Kiezun A, Brusic V, et al. Comprehensive analysis of cancer-associated somatic mutations in class I HLA genes. Nat Biotechnol. 2015; 33:1152–8.
21. Nielsen M, Lundegaard C, Blicher T, Lamberth K, Harndahl M, Justesen S, Roder G, Peters B, Sette A, Lund O, Buus S. NetMHCpan, a method for quantitative predictions of peptide binding to any HLA-A and -B locus protein of known sequence. PLoS One. 2007; 2:e796.
22. Garg K, Levine DA, Olvera N, Dao F, Bisogna M, Secord AA, Berchuck A, Cerami E, Schultz N, Soslow RA. BRCA1 immunohistochemistry in a molecularly characterized cohort of ovarian high-grade serous carcinomas. Am J Surg Pathol. 2013; 37:138–146.
23. Zhang L, Conejo-Garcia JR, Katsaros D, Gimotty PA, Massobrio M, Regnani G, Makrigiannakis A, Gray H, Schlienger K, Liebman MN, Rubin SC, Coukos G. Intratumoral T cells, recurrence, and survival in epithelial ovarian cancer. N Engl J Med. 2003; 348:203–213.
24. Patch AM, Christie EL, Etemadmoghadam D, Garsed DW, George J, Fereday S, Nones K, Cowin P, Alsop K, Bailey PJ, Kassahn KS, Newell F, Quinn MC, et al. Whole-genome characterization of chemoresistant ovarian cancer. Nature. 2015; 521:489–494.
25. Herbst RS, Soria JC, Kowanetz M, Fine GD, Hamid O, Gordon MS, Sosman JA, McDermott DF, Powderly JD, Gettinger SN, Kohrt HE, Horn L, Lawrence DP, et al. Predictive correlates of response to the anti-PD-L1 antibody MPDL3280A in cancer patients. Nature. 2014; 515:563–567.
26. Soslow RA, Han G, Park KJ, Garg K, Olvera N, Spriggs DR, Kauff ND, Levine DA. Morphologic patterns associated with BRCA1 and BRCA2 genotype in ovarian carcinoma. Mod Pathol. 2011; 25:625–636.
27. Clarke B, Tinker AV, Lee CH, Subramanian S, van de Rijn M, Turbin D, Kalloger S, Han G, Ceballos K, Cadungog MG, Huntsman DG, Coukos G, Gilks CB. Intraepithelial T cells and prognosis in ovarian carcinoma: novel associations with stage, tumor type, and BRCA1 loss. Mod Pathol. 2009; 22:393–402.
28. George J, Alsop K, Etemadmoghadam D, Hondow H, Mikeska T, Dobrovic A, deFazio A, Smyth GK, Levine DA, Mitchell G, Bowtell DD. Nonequivalent gene expression and copy number alterations in high-grade serous ovarian cancers with BRCA1 and BRCA2 mutations. Clin Cancer Res. 2013; 19:3474–3484.
29. Sato E, Olson SH, Ahn J, Bundy B, Nishikawa H, Qian F, Jungbluth AA, Frosina D, Gnjatic S, Ambrosone C, Kepner J, Odunsi T, Ritter G, et al. Intraepithelial CD8+ tumor-infiltrating lymphocytes and a high CD8+/regulatory T cell ratio are associated with favorable prognosis in ovarian cancer. Proc Natl Acad Sci U S A. 2005; 102:18538–18543.
30. Rajasagi M, Shukla SA, Fritsch EF, Keskin DB, DeLuca D, Carmona E, Zhang W, Sougnez C, Cibulskis K, Sidney J, Stevenson K, Ritz J, Neuberg D, et al. Systematic identification of personal tumor-specific neoantigens in chronic lymphocytic leukemia. Blood. 2014; 124:453–62.
31. Shukla SA, Rooney MS, Rajasagi M, Tiao G, Dixon PM, Lawrence MS, Stevens J, Lane WJ, Dellagatta JL, Steelman S, Sougnez C, Cibulskis K, Kiezun A, et al. Comprehensive analysis of cancer-associated somatic mutations in class I HLA genes. Nat Biotechnol. 2015; 33:1152–1158.
32. Lawrence MS, Stojanov P, Mermel CH, Robinson JT, Garraway LA, Golub TR, Meyerson M, Gabriel SB, Lander ES, Getz G. Discovery and saturation analysis of cancer genes across 21 tumour types. Nature. 2014; 505:495–501.
33. Wagle N, Berger MF, Davis MJ, Blumenstiel B, Defelice M, Pochanard P, Ducar M, Van Hummelen P, Macconaill LE,

Hahn WC, Meyerson M, Gabriel SB, Garraway LA. High-throughput detection of actionable genomic alterations in clinical tumor samples by targeted, massively parallel sequencing. Cancer Discov. 2012; 2:82–93.

34. Hamanishi J, Mandai M, Iwasaki M, Okazaki T, Tanaka Y, Yamaguchi K, Higuchi T, Yagi H, Takakura K, Minato N, Honjo T, Fujii S. Programmed cell death 1 ligand 1 and tumor-infiltrating CD8+ T lymphocytes are prognostic factors of human ovarian cancer. Proc Natl Acad Sci U S A. 2007; 104:3360–3365.

HHS Public Access

Author manuscript

Cell Rep. Author manuscript; available in PMC 2016 January 28.

Published in final edited form as:

Cell Rep. 2016 January 26; 14(3): 429–439. doi:10.1016/j.celrep.2015.12.046.

Platinum and PARP inhibitor resistance due to over-expression of microRNA-622 in BRCA1-mutant ovarian cancer

Young Eun Choi[1], **Khyati Meghani**[1], **Marie-Eve Brault**[1], **Lucas Leclerc**[1], **Yizhou J He**[1], **Tovah A Day**[2], **Kevin M Elias**[3], **Ronny Drapkin**[4], **David M Weinstock**[2], **Fanny Dao**[5], **Karin K. Shih**[5], **Ursula Matulonis**[2], **Douglas A. Levine**[5], **Panagiotis A. Konstantinopoulos**[2,†], and **Dipanjan Chowdhury**[1,†]

[1]Department of Radiation Oncology, Division of Genomic Stability and DNA Repair, Dana-Farber Cancer Institute, Harvard Medical School, Boston, MA 02215, USA

[2]Department of Medical Oncology, Dana-Farber Cancer Institute, Harvard Medical School, Boston, MA 02215, USA

[3]Division of Gynecologic Oncology, Department of Obstetrics and Gynecology and Reproductive Biology, Brigham and Women's Hospital, Boston, MA02215, USA

[4]Ovarian Cancer Research Center, Department of Obstetrics and Gynecology, University of Pennsylvania, Perelman School of Medicine, Philadelphia, PA 19104, USA

[5]Department of Surgery, Memorial Sloan Kettering Cancer Center, New York, NY, USA; Weill Cornell Medical College, New York, NY10065, USA

Abstract

High-grade serous ovarian carcinomas (HGSOCs) with BRCA1/2 mutations exhibit improved outcome and sensitivity to double-strand DNA break (DSB)-inducing agents [i.e. platinum and Poly(ADP-ribose) polymerase inhibitors (PARPis)] due to an underlying defect in homologous recombination (HR). However, resistance to platinum and PARPis represents a significant barrier to the long-term survival of these patients. Although, BRCA1/2-reversion mutations are a clinically validated resistance mechanism, they account for less than half of platinum resistant BRCA1/2-mutated HGSOCs. We uncover a resistance mechanism by which a microRNA, miR-622 induces resistance to PARPis and platinum in BRCA1-mutant HGSOCs by targeting the Ku complex and restoring HR-mediated DSB repair., Physiologically, miR-622 inversely correlates with Ku expression during the cell cycle, suppressing non-homologous end joining and facilitating HR-mediated DSB repair in S-phase. Importantly, high expression of miR-622 in BRCA1-deficient HGSOCs is associated with worse outcome after platinum chemotherapy, indicating microRNA-mediated resistance through HR rescue.

[†]Corresponding authors: dipanjan_chowdhury@dfci.harvard.edu and panagiotis_konstantinopoulos@dfci.harvard.edu, 450 Brookline Ave, JF517, Boston, MA 02215, Tel: 1617 582 8639, Fax: 1617 582 8213.

The authors have no financial conflicts

INTRODUCTION

Approximately 15-20% of patients with epithelial ovarian cancer (EOC) harbor germline (10-15%) or somatic (6-7%) *BRCA1* or *BRCA2* mutations(TCGA, 2011). Furthermore, epigenetic silencing *of BRCA1* via promoter hypermethylation occurs in approximately 10-20% of EOCs. Due to the underlying defect in DNA repair via homologous recombination (HR), patients with *BRCA1/2*-inactivated EOCs exhibit enhanced sensitivity to platinum analogues and other cytotoxic drugs that induce double strand DNA breaks (DSBs) such as the poly-ADP ribose polymerase inhibitors (PARPis)(Fong et al., 2009). Of these drugs, olaparib was granted accelerated approval by the U.S. FDA for use in EOC patients with germline *BRCA1/2* mutations (Fong et al., 2009). However, a substantial fraction of these patients do not respond or eventually develop resistance to these agents suggesting that *de novo* and acquired platinum and PARPi resistance is a significant clinical problem in HR-defective EOCs. The most common mechanism of resistance to these agents in *BRCA1/2*-mutated tumors is secondary intragenic mutations restoring BRCA1 or BRCA2 protein functionality; 46% of platinum resistant BRCA-mutated EOCs exhibit tumor-specific secondary mutations that restore the ORF of either BRCA1 or BRCA2(Norquist et al., 2011).

The interplay of the two major mechanistically distinct DSB repair pathways, HR and non-homologous end joining (NHEJ) (Chapman et al., 2012b; Ciccia and Elledge, 2010) is also critical for resistance to platinum and PARPis. Surprisingly, the sensitivity of BRCA1-mutant tumors to PARP inhibitors is almost completely abolished by loss of the NHEJ factor 53BP1 (Bouwman et al., 2010; Bunting et al., 2010; Chapman et al., 2012a), which also correlates with the restoration of competent HR. Furthermore a recent small hairpin (sh) RNA screen for hairpins promoting survival of BRCA1-deficient mouse mammary tumors to PARPi identified 53BP1 and REV7, a factor implicated in NHEJ, as the top hits (Boersma et al., 2015; Xu et al., 2015). However, unlike BRCA1/2 reversion mutations, these resistance mechanisms have not been shown to be clinically relevant for patients with BRCA1/2-inactivated EOCs. However, it is feasible that the NHEJ pathway may be relevant for PARPi resistance in EOCs, and other NHEJ factors may contribute to the resistant phenotype.

Here, we uncover mechanism of resistance to PARPi and platinum in BRCA1-mutated EOCs that involves miRNA-mediated regulation of NHEJ. Specifically, we have identified a miRNA, miR-622 that regulates the expression of the Ku-complex and specifically suppresses NHEJ during S-phase. Consistent with this effect, overexpression of miR-622 rescues the HR-deficiency of BRCA1-mutant ovarian tumor lines and induces resistance to PARPi and platinum-based drugs. Furthermore, expression of miR-622 in two cohorts of patients with *BRCA1*-inactivated EOCs correlates with reduced disease-free survival after platinum-based therapy, suggesting direct clinical relevance in patients with EOC

RESULTS

miR-622 'desensitizes' BRCA1 mutant cells to PARP inhibitors/platinum-based therapy

Recently, we used PARPi sensitivity as a marker for HR-deficiency to conduct a functional screen for identifying miRNAs that down-regulate HR in a breast cancer line, MDA-MB231(Choi et al., 2014). We characterized the miRNAs (miR-1255b, miR-193b* and miR-148b*) that suppress HR by down-regulating the expression of BRCA1, BRCA2 and RAD51. Strikingly, in that screen, six miRNAs (miR-644, miR-492, miR-613, miR-577, miR-622 and miR-126*)(Choi et al., 2014) demonstrated a surprising trend of inducing PARPi resistance. Our original screen was conducted in a BRCA-proficient breast tumor line MDA-MB231 and we assessed the impact of these miRNAs on PARPi sensitivity in MDA-MB231. Considering the BRCA mutant cells are responsiveness to PARPi, and therefore we also examined the impact of these miRNAs in a BRCA1-mutant breast line, MDA-MB436. There was no significant impact of miR-644, miR-492, miR-613, miR-577 and miR-126* on PARPi sensitivity in MDA-MB231 and MDA-MB436 cells (Supp Fig. 1A), however miR-622 significantly induced resistance to the clinical grade PARP inhibitors, olaparib and veliparib, specifically in the MDA-MB436 cells (Supp Fig. 1B). Furthermore, we tested the impact of miR-622 on PARPi sensitivity on the BRCA1-mutant EOC line, UWB1.289 and found that overexpression of miR-622 caused resistance to both PARPis, olaparib and veliparib (ABT-888) (Fig. 1A). Interestingly, miR-622 expression also caused resistance to the platinum-based chemotherapeutic agents, carboplatin and cisplatin in the BRCA1-mutated UWB1.289 cells (Fig. 1A). Importantly, restoring BRCA1 expression in UWB1.289 cells completely negates the impact of miR-622 on PARPi sensitivity and also sensitivity to platinum drugs (Supp Fig. 1C). In order to exclude the possibility that the Brca1-mutant lines MDA-MB436 and UWB1.289 have acquired other unaccounted mutations which may contribute to the phenotype induced by miR-622, we expressed miR-622 in BRCA1-null mouse embryonic fibroblasts (MEF) and assessed sensitivity to olaparib and cisplatin. Consistent with our previous results, miR-622 significantly 'desensitized'BRCA1−/−MEFs to both drugs (Fig. 1B) but did not impact the sensitivity of their wild type counterparts (Supp Fig. 1D). Together, these data suggest that the impact of miR-622 on PARPi and platinum-based therapy is specific to the loss of BRCA1.

Expression of miR-622 correlates with response to platinum chemotherapy in BRCA1-inactivated EOCs

To evaluate the association between miR-622 expression and platinum response in EOCs with BRCA1 inactivation, we assessed data from the ovarian TCGA dataset(TCGA, 2011). In that dataset, 89 EOCs (all HGSOCs) exhibited BRCA1-inactivation; 38 EOCs harbored BRCA1-mutations (out of 316 EOCs that underwent whole exome sequencing) while 51 tumors (out of 489 tumors with DNA promoter methylation data) harbored BRCA1 epigenetic silencing via promoter hypermethylation. All patients underwent surgery followed by platinum based chemotherapy. We evaluated the association between miR-622 expression and platinum response using various cut-offs for low versus high miR-622 expression. In all cases, we consistently found that tumors with higher miR-622 expression were associated with inferior response to first line platinum based chemotherapy and worse

survival. Specifically, using median miR-622 expression as a threshold to classify BRCA1-inactivated EOCs as exhibiting high versus low miR-622 expression, we found that BRCA1-inactivated tumors with high expression of miR-622 were associated with worse disease-free survival (DFS) (median DFS 14.7 vs 19.8 months respectively, log rank p = 0.03) and overall survival (OS) (median OS 39 vs 49.3 months respectively, log rank p = 0.03) compared with tumors with low miR-622 expression (Fig. 1C). Conversely, there was no association between miR-622 expression and outcome, DFS or OS in the remaining tumors in TCGA dataset, i.e. those without BRCA1 mutations and without BRCA1 promoter hypermethylation (data not shown). This trend was particularly evident in tumors with the highest miR-622 expression, i.e. those whose mir-622 expression was in the highest quintile. Specifically, BRCA1-inactivated tumors whose expression levels for miR-622 were in the highest quintile were associated with worse DFS (median DFS 13.7 vs 18.1 months respectively, log rank p = 0.005) and OS (median OS 35.3 vs 48.3 months respectively, log rank p = 0.001, Fig. 1D).

Furthermore, we compared tumors with the highest miR-622 expression versus those with the lowest miR-622 expression. Specifically, when comparing the top 5, 10 or 15 tumors with the highest miR-622 expression with the lowest 5, 10 or 15 tumors respectively, we consistently found that the tumors with the highest miR-622 expression were associated with inferior response to first line platinum chemotherapy, i.e. worse DFS and OS compared to the tumors with the lowest expression (Fig. 1E and Supp Fig. 1E).

Given the absence of other miRNA expression datasets with sizeable numbers of ovarian tumors with BRCA1-mutations or BRCA1 promoter hypermethylation, we explored the correlation between miR-622 and outcome in tumors with low BRCA1 expression in a different, clinically annotated ovarian cancer dataset (Shih et al., 2011). This dataset included miRNA and mRNA expression data from 60 patients with newly diagnosed FIGO stage III or IV tumors with serous histology, including 3 tumors with BRCA1 mutations. As shown in Supplement Figure 1F, we found similar correlation between high miR-622 expression and inferior outcome to first line platinum based chemotherapy.

miR-622 impacts NHEJ mediated repair of DSBs

The NHEJ pathway is composed of at least two branches: the well-studied classical NHEJ (C-NHEJ) and the poorly understood alternative end-joining (A-EJ)(Deriano and Roth, 2013). The molecular details and biological function of A-NHEJ remains largely unclear(Deriano and Roth, 2013). Loss or depletion of factors promoting C-NHEJ (such as 53BP1) or essential for C-NHEJ (such as Ku70) induces PARPi resistance in BRCA1-deficient mouse cells (Bunting et al., 2012; Bunting et al., 2010). To test whether miR-622 indeed impacts NHEJ, we assayed for C-NHEJ and A-NHEJ mediated repair of the yeast endonuclease, I-SceI-induced DSBs using the EJ5-GFP reporter and EJ2-GFP reporter, respectively. These are integrated fluorescence-based reporters (Bennardo et al., 2008) that allow for efficient quantification of the two distinct NHEJ pathways at targeted DSBs. We observed that miR-622 significantly impedes C-NHEJ (Fig. 2A), and enhances A-NHEJ (Fig. 2B). This is consistent with studies showing that depletion of C-NHEJ factors increases the frequency of A-NHEJ (Fattah et al., 2010). Depletion of 53BP1 and Ku70 induces

PARPi resistance in *BRCA1*-mutant cells by restoring HR-mediated repair of DSBs and significantly enhancing genomic stability after PARPi treatment (Bunting et al., 2012; Bunting et al., 2010). Consistent with its impact on NHEJ, we observe that expression of miR-622 in *BRCA1−/−MEFs* causes a significant decrease in the level of genomic instability (chromosomal aberrations) induced by olaparib treatment (Fig. 2C). To address the mechanism by which miR-622 promotes genome integrity in *BRCA1* mutant cells, we tested whether its expression could cause an increase in irradiation-induced Rad51 foci, a measure of the HR-pathway. We found that expression of miR-622 in UWB1.289 cells caused a statistically significant increase in Rad51 foci (Fig. 2D). Importantly, none of these effects are due to alterations in the cell cycle caused by the miR-622 mimics (Supp Fig. 2A).

miR-622 regulates expression of the Ku complex

To investigate the mechanism by which miR-622 influences NHEJ and impacts PARP inhibitor sensitivity we used a candidate-based approach whereby all genes implicated in NHEJ were screened for miRNA recognition elements (MREs) of miR-622 using the PITA algorithm. This algorithm is unique in allowing G:U wobbles or seed mismatches, and identifies base pairing beyond the 5'end of the miRNA, predicts the sites not restricted to the 3'UTR of mRNA and identifies non-canonical MREs for specific miRNA/mRNA combinations(Lal et al., 2009). Using this algorithm, miR-622 was predicted to target the transcripts of 53BP1, Ku70, Ku80, APTX and APLF (Supp Fig. 3). We assessed the impact of over-expressing miR-622 in UWB1.289 cells on the mRNA level of these genes and observed a significant reduction in the transcripts of 53BP1, Ku70 and Ku80 (Fig. 3A). Subsequently, we determined the impact of these miRNAs on the protein level of their putative targets. Over-expressing miR-622 reduces the protein levels of Ku70 and Ku80 in UWB1.289 cells. The basal expression of the Ku proteins is lower in MEFs, and the impact of miR-622 on Ku70 and Ku80 in *BRCA1−/−MEFs* is even more pronounced (Fig. 3B). On the contrary, there was no detectable impact of miR-622 on 53BP1 in the UWB1.289 cells. To test for association of miR-622 with the Ku70 and Ku80 transcripts we captured miRNA-mRNA complexes using streptavidin-coated beads from cells transfected with biotinylated forms of the miRNA mimics (Lal et al., 2011; Orom and Lund, 2007). The amount of Ku70, Ku80 and 53BP1 transcripts was measured in the pull-downs, and the enrichment was assessed relative to pull-down with biotinylated control mimic and also with GAPDH. Consistent with our previous results, miR-622 selectively pulled-down Ku70 and Ku80 transcripts but not the 53BP1 transcript (Fig. 3C). To verify further that Ku70 and Ku80 are targets of miR-622 and confirm that the interaction is mediated by the predicted MREs we used luciferase reporter assays. The predicted MREs (Fig. 3D) were cloned in the 3'UTR of the luciferase gene, and expression monitored in cells transfected with the miR-622 mimic (Fig. 3E). As anticipated, there was significant decrease in luciferase activity, and this was ‘rescued’ by point mutations that disrupt base pairing between miR-622 and their corresponding MREs in Ku70 and Ku80 (Fig. 3F). Together these results suggest that miR-622 regulates the expression of the Ku complex by direct interaction with Ku70 and Ku80 transcripts.

miR-622 causes resistance to PARP inhibitor and cisplatin by down-regulating expression of the Ku proteins

We examined the impact of Ku downregulation (using siRNAs) or inhibition (dominant negative Ku(He et al., 2007)) on olaparib and cisplatin sensitivity in parallel with miR-622 over-expression in UWB1.289 cells (Fig. 4A) and in *BRCA1−/−MEFs* (Fig. 4B). We observe that depletion/inhibition (efficacy of siRNAs shown in Supp. Fig. 4) of the Ku complex and over-expression of miR-622 have a comparable effect on de-sensitizing BRCA1-deficient cells to both olaparib and cisplatin. To determine whether the effect of miR-622 on olaparib and cisplatin sensitivity was indeed mediated via Ku suppression we utilized mouse Ku70 cDNA and rat Ku80 cDNA that lack miR-622 MREs. Next, UWB1.289 cells were co-transfected with miR-622 and mouse Ku70 cDNA or rat Ku80 cDNA. The Ku expression constructs lacking the miR-622 MREs 'rescued' the expression of these genes in the presence of miR-622 mimic further validating the predicted MREs (Fig. 4C, right panel). Furthermore, individual expression of the Ku proteins partially 'rescued' the impact of miR-622 on olaparib and cisplatin sensitivity (Fig. 4C, left panel).

Ku80 protein and mRNA expression levels are available in primary EOCs in the ovarian TCGA, and were correlated with miR-622 expression. Consistent with our results, there is statistically significant inverse correlation of miR-622 with both Ku80 protein and mRNA expression in *BRCA*-inactivated EOCs from the TCGA dataset. Specifically, among the 89 EOCs with either BRCA1 mutations (n=38) or BRCA1 promoter hypermethylation (n=51), miR-622 expression levels were statistically significantly inversely correlated with Ku80 RNA expression levels ($p = 0.019$) and Ku80 protein levels ($p=0.029$) as determined by reverse phase protein array (RPPA) in the TCGA dataset (Fig. 4D). This correlation was further confirmed in the independent cohort of EOC patients discussed above; specifically miR-622 expression levels were statistically significantly inversely correlated with Ku80 RNA expression levels ($p = 0.05$) (Fig. 4E). There was no Ku80 protein expression data in that dataset.

Physiological Relevance of miR-622 mediated suppression of the Ku complex

To explore the physiological relevance of the interactions of miR-622 with Ku70 and Ku80 transcripts we assessed their expression during cell cycle, specifically during the G1 to S transition. Synchronizing, UWB1.289 cells (profiles shown in Supp Fig. 5A) we observe that mRNA levels of Ku70 and Ku80 are reduced in the S-phase relative to the G1 phase (Fig. 5A). Interestingly, miR-622 inversely correlates with Ku70 and Ku80 transcripts, and is significantly up-regulated as cells move into the S-phase. Antagonizing miR-622 induces a specific increase in Ku70 and Ku80 transcripts (Fig. 5B) in the S-phase. To further confirm the cell cycle phase specificity of this phenotype avoiding the artifacts of synchronization, and in a diploid cell line with relatively few genomic abnormalities, we utilized the Fucci system(Sakaue-Sawano et al., 2008) to visualize the G1 phase (mKO2-CDT1-RFP) and S-phase (Geminin-GFP) in hTERT-immortalized retinal pigment epithelial cell line (RPE-1) cells. The G1 cells and S/G2 phases were separated and isolated using fluorescence-activated cell sorting (FACS) selection. Consistent with the previous results miR-622 expression inversely correlated with the Ku70 and Ku80 transcripts (Fig. 5C) and inhibition of miR-622 in RPE-1 caused a significant increase in Ku70 and Ku80 transcripts

in the S-phase (Fig. 5D). To further elucidate the cell-cycle based impact of miR-622 on the Ku proteins we utilized the luciferase assays (as in Fig. 3). We confirmed that antagonizing endogenous miR-622 in S-phase significantly increases luciferase activity of constructs with miR-622 recognition elements in the Ku70 and Ku80 transcripts, and this was negated by point mutations that disrupt base pairing between miR-622 and their corresponding binding sites in these transcripts (Supp Fig.5B).

Recruitment of the MRN (Mre11-Rad50-Nbs1) complex is the first step in HR. From the functional standpoint there is a competitive interplay between the Ku complex and MRN complex(Balestrini et al., 2013; Foster et al., 2011). Specifically the over-expression of Ku proteins reduces recruitment of Mre11 to DSBs in the S/G2 phase when HR is the preferred DSB repair pathway(Clerici et al., 2008). Therefore we examined the Mre11 foci in the S-phase of irradiated cells transfected with miR-622 antagomirs. Consistent with increased Ku levels antagonizing miR-622 causes a significant decrease in Mre11 foci (Fig. 5E). Furthermore the subsequent step in HR, which is resection of broken DNA ends and RPA2 foci formation is also reduced by antagonizing miR-622 (Fig. 5F). Importantly, antagonizing miR-622 does not impact the IR induced generation of DSBs (monitored by γ–H2AX, Fig. 5E and 5G). Together, these results strongly suggest that miR-622 plays a role in the optimal expression of the Ku complex during the cell cycle, and potentially facilitates the initiation of HR-mediated DSB repair in the S phase.

DISCUSSION

There is tight regulation of the DSB repair pathways during the cell cycle as HR is restricted to the S/G2 phase and NHEJ is pre-dominant in G1 but has moderate activity throughout the cell cycle. Importantly, the choice of DSB repair pathways during cell cycle is critical for maintaining genomic stability. A decisive factor in this choice is competition between DNA end protection (necessary for NHEJ) and DNA end resection (necessary for HR). Depletion of end protecting factors (such as 53BP1) allows DNA end resection in the G1 phase, thereby impairing NHEJ and causing genomic instability (Helmink et al., 2011),(Escribano-Diaz et al., 2013). Conversely ectopic expression of BRCA1 in the G1 phase via the inhibition/deletion of miRNAs suppressing BRCA1 also allows DSB end resection leading to unrepaired DSBs (Choi et al., 2014; Dimitrov et al., 2013). During the S/G2 phase of the cell cycle the relatively error-free HR pathway is preferred, and NHEJ needs to be restricted. The mechanism via which the NHEJ pathway is restricted in the S-phase remains unknown. Here, we uncover regulation of this step by miR-622. We find that miR-622 plays an important role in maintaining the balance between HR and NHEJ repair pathways during the cell cycle by regulating optimal expression of the Ku complex. The Ku complex is pivotal in pathway choice as it competes with the MRN complex to capture broken DSB ends, and divert it towards the C-NHEJ pathway. MiR-622 suppresses NHEJ through targeting of the Ku-complex during S phase, and enhances initiation of HR-mediated DSB repair in the S phase by facilitating the recruitment of Mre11. Therefore ectopic over-expression of miR-622 can limit NHEJ, and boost the HR pathway.

Another important finding of our study is that this role for miR-622 in maintaining balance between DSB repair pathways may mediate resistance to PARPis and platinum agents in

BRCA1-inactivated tumors. Elucidating mechanisms of platinum and PARPi resistance in BRCA-deficient EOCs is critical in order to identify approaches that suppress denovo and emerging resistant clones. Pharmacological effects that alter the cellular response to PARPis including increased expression of ABC transporters, such as the P-glycoprotein (PgP) efflux pump, have been associated with PARPi resistance in BRCA1-mutated breast and ovarian cancer, but their clinical relevance for platinum resistance remains unclear. Furthermore, although a number of resistance mechanisms have been described (Konstantinopoulos et al., 2015), only secondary *BRCA1/2* mutations restoring BRCA1/2 protein functionality have been validated in multiple EOC patient cohorts. It is noteworthy that most of these models systems have not investigated ovarian carcinomas thereby undermining their clinical relevance. In this regard, our study highlights a mechanism of PARPi resistance in BRCA1-deficient EOC patients involving miR-622 overexpression, and represents an extension of its physiological role in maintaining the balance of DSB repair pathways.

Importantly, unlike 53BP1 loss which confers only PARPi resistance, this resistance mechanism confers resistance to both platinum and PARPis. Although miRNA expression has been recently implicated in mediating HR deficiency and response to platinum and PARPis (Liu et al., 2015), here we implicate a miRNA in exactly the opposite, i.e. mediating PARPi and platinum resistance by rescuing HR deficiency. Strikingly, the clinical relevance of this resistance mechanism was evident in two different ovarian cancer datasets whereby overexpression of miR-622 was associated with inferior outcome after platinum chemotherapy in *BRCA1*-inactivated tumors. Of note, the expression of miR-622 was also inversely correlated with protein and mRNA expression levels of Ku80 thereby clinically validating our experimental observations that the association of miR-622 with worse outcome may indeed be related to its targeting of the Ku complex. In conclusion, our work suggests a role for miR-622 in regulating the balance between HR and NHEJ in cell cycle and highlights a potential role of this miRNA as a biomarker of responsiveness to platinum and PARPis in *BRCA1*-inactivated EOCs. Furthermore, miR-622 may be a promising target for augmenting PARPi and platinum response in *BRCA1*-inactivated EOCs.

MATERIALS AND METHODS

Viability Assay

Viability assays were done as previously described (Choi et al., 2014).

Ovarian Cancer datasets and statistical analysis

Association of miR-622 expression levels with outcome (OS and DFS) was assessed in two clinically annotated ovarian cancer datasets with miRNA expression data. First, we accessed expression data from the ovarian TCGA dataset which included 38 tumors with BRCA1-mutations (out of 316 EOCs that underwent whole exome sequencing) and 51 tumors (out of 489 tumors with DNA promoter methylation data) with BRCA1 epigenetic silencing via promoter hypermethylation. Promoter hypermethylation was assessed using the same criteria described in the ovarian TCGA dataset publication. The second dataset included expression data from 60 patients with newly diagnosed FIGO stage III or IV tumors, all with serous histology (Shih KK et al. Gynecol Oncol 2011). The t test and the Fisher exact test

were used to analyze the clinical and experimental data. Correlation between miR-622 and Ku80 expression levels was assessed using the Pearson's correlation coefficient. Significance was defined as a $p<0.05$; all reported p values are two sided. OS and DFS curves were generated by the Kaplan-Meier method, and statistical significance was assessed using the log-rank test.

Non-homologous End Joining Reporter Assay

NHEJ reporter assays were performed as the HR assays done previously (Choi et al., 2014) by using U2OS cells carrying a single copy of the recombination substrate with two tandem I-SceI sites.

Chromosome Breakage Analysis

Brca1−/− MEF cells were transfected with indicated miRNA mimics for 24 hours followed by treatment with or without the indicated concentrations of PARP inhibitor (Olaparib) for 24, 48 or 72 hours. Cells were exposed to 100 ng/ml colcemid for 2 hours followed by treatment with a hypotonic solution (0.075M KCl) for 20 minutes and fixed with 3:1 methanol/acetic acid solution. Slides were stained with Wright's stain and ≥50 metaphase spreads were scored for aberrations.

Immunofluorescence

Immunofluorescence in UWB1.289 and RPE1 Fucci cells were done as previously described (Lee et al., 2010) using RAD51 (Santa Cruz #sc-8349), γ-H2AX (Cell Signaling #9718S), RPA2 (Abcam #ab2175) and Mre11 (Novus Biologicals #NB100-142)

RNA Isolation and Quantitative Real-Time PCR

Total RNA was prepared and expression was analyzed by qRT-PCR as described previously (Moskwa et al., 2011).

Gene-specific primers used for qRT-PCR are as follows:

53BP1-F-1, GTCATTGAGCAGTTACCTCAG, R-1, GGGAATGTGTAGTATTGCCTG; 53BP1-F-2, ATGGTGGAGACCCATGATCC, R-2, GTCTTCTGGGGACTGGCAAC; KU70-F-1, GTTGATGCCTCCAAGGCTATG, R-2, GCACCTGGATTATCCAGCTC; KU70-F-2, AATTCAGGTGACTCCTCCAG, R-2, TGAAGTGCTGCTGCAGCAC; KU80-F-1, AAGCAAAATCCAACCAGGTTCT, R-1, GAATTGCAGGGAGATGTCACA; KU80-F-2, ACTCTGATCACCAAAGAGGAA, R-2, TGGCAGCTCTCTTAGATTCC; APTX-F, TGGAAGCAGTTGTGATTGGG, R, CACCATGTGGAGAACCTGG; APLF-F, GAAGCCAAATCTATGGTGCTA, R, CTTCATCAAGCACTTGACTGT

Immunoblots

The immunoblots were done as described previously (Lee et al., 2010; Moskwa et al., 2011) with 53BP1 (Cell Signaling Technology #4937), Ku70 (Santa Cruz #sc-1486), Ku80 (Thermo Scientific #PA5-17454) and α-tubulin (Sigma #T5168) antibodies.

Immunoprecipitation of miRNA Targets

Immunoprecipitation of miRNA target with biotinylated miR-622 was done with UWB1.289 cells as previously described (Choi et al. 2014).

Luciferase Assay

The wild type (WT) or mutant (Mt) miRNA recognition elements (MREs) of target genes were synthesized as oligonucleotide sequences, annealed and cloned in psiCHECK2 (Promega) downstream to *Renilla* luciferase. Luciferase assay in UWB1.289 cells using WT and Mt MRE constructs was done as described previously (Moskwa et al., 2011). The oligonucleotide sequences are as follows:

KU70-MRE1-F, TCGAAAGCAATGAATAAAAGACTGGGAAGAAGCAATGAATAAAAGACTGG, R, GGCCCCAGTCTTTTATTCATTGCTTCTTCCCAGTCTTTTATTCATTGCTT; KU70-MRE2-F, TCGAACCAAGCACTTCCAGGACTGAGAAGACCAAGCACTTCCAGGACTGA, R, GGCCTCAGTCCTGGAAGTGCTTGGTCTTCTCAGTCCTGGAAGTGCTTGGT; KU70-MRE1+2-F, TCGAAAGCAATGAATAAAAGACTGGGAAGACCAAGCACTTCCAGGACTGA, R, GGCCTCAGTCCTGGAAGTGCTTGGTCTTCCCAGTCTTTTATTCATTGCTT; KU80-MRE1-F, TCGAAGCTAAAAAATTAAAGACTGAGAAGAGCTAAAAAATTAAAGACTGA, R, GGCCTCAGTCTTTAATTTTTTAGCTCTTCTCAGTCTTTAATTTTTTAGCT; KU80-MRE2-F, TCGATTTATGAAGAGCATAGACTGCGAAGTTTATGAAGAGCATAGACTGC, R, GGCCGCAGTCTATGCTCTTCATAAACTTCGCAGTCTATGCTCTTCATAAA; KU80-MRE1+2-F, R, GGCCGCAGTCTATGCTCTTCATAAACTTCTCAGTCTTTAATTTTTTAGCT.

The oligonucleotides for mutant MREs are as follows:

Mt KU70-MRE1+2-F, TCGAAAGGTTGGAATAAATCTGACGGAAGAGGTAGCTGGAGCATCTGACA, R, GGCCTGTCAGATGCTCCAGCTACCTCTTCCGTCAGATTTATTCCAACCTT; Mt KU80-MRE1+2-F, TCGAACGAAATTAAAGTATCTGACAGAAGTTTATGAAGTCGATTCTGACC, R, GGCCGGTCAGAATCGACTTCATAAACTTCTGTCAGATACTTTAATTTCGT.

Cell Cycle Synchronization and Sorting

Cell synchronization was performed in UWB1.289 cells as previously described in *Choi et al*. (Choi et al., 2014). Cells transfected with miR-622 antagomir with rat Ku70 or moue Ku80 cDNA (gift from Andre Nussenzweig at National Cancer Institute) were similarly synchronized 48 hrs after transfection. RPE1 Fucci cells were sorted by using BD FACSAria based on fluorophore expression according to cell cycle (RFP-G1 phase, GFP-S/G2/M phase).

miRNA Target Prediction

We used a candidate-based prediction approach using PITA (http://genie.weizmann.ac.il/pubs/mir07/mir07_data.html), to analyze the Human DNA Repair Gene list (http://sciencepark.mdanderson.org/labs/wood/dna_repair_genes.html#Human%20DNA%20Repair%20Genes) which resulted in a list of DDR genes predicted as targets of miRNAs of our interest. Predicted targets are listed in Supplementary Figure 2 and further validated as explained in the manuscript.

Supplementary Material

Refer to Web version on PubMed Central for supplementary material.

ACKNOWLEDGEMENTS

DC is supported by R01 AI101897-01 (NIAID) and R01CA142698-07 (NCI), Basic Scholar Grant (American Cancer Society), Leukemia and Lymphoma Society Scholar Grant, Claudia Adams Barr Program for Innovative Cancer Research, Breast SPORE Pilot Award, First Fund Award and Mary Kay Foundation. PAK is supported by the Susan Smith Center for Women's Cancers, and the Department of Defense Ovarian Cancer Academy Award (W81XWH-10-1-0585). The BRCA1−/− MEFs were a gift from Andre Nussenzweig and NHEJ reporter construct was a gift from Jeremy Stark.

REFERENCES

Balestrini A, Ristic D, Dionne I, Liu XZ, Wyman C, Wellinger RJ, Petrini JH. The Ku heterodimer and the metabolism of single-ended DNA double-strand breaks. Cell reports. 2013; 3:2033–2045. [PubMed: 23770241]

Bennardo N, Cheng A, Huang N, Stark JM. Alternative-NHEJ is a mechanistically distinct pathway of mammalian chromosome break repair. PLoS Genet. 2008; 4:e1000110. [PubMed: 18584027]

Boersma V, Moatti N, Segura-Bayona S, Peuscher MH, van der Torre J, Wevers BA, Orthwein A, Durocher D, Jacobs JJ. MAD2L2 controls DNA repair at telomeres and DNA breaks by inhibiting 5′ end resection. Nature. 2015

Bouwman P, Aly A, Escandell JM, Pieterse M, Bartkova J, van der Gulden H, Hiddingh S, Thanasoula M, Kulkarni A, Yang Q, et al. 53BP1 loss rescues BRCA1 deficiency and is associated with triple-negative and BRCA-mutated breast cancers. Nature structural & molecular biology. 2010; 17:688–695.

Bunting SF, Callen E, Kozak ML, Kim JM, Wong N, Lopez-Contreras AJ, Ludwig T, Baer R, Faryabi RB, Malhowski A, et al. BRCA1 functions independently of homologous recombination in DNA interstrand crosslink repair. Molecular cell. 2012; 46:125–135. [PubMed: 22445484]

Bunting SF, Callen E, Wong N, Chen HT, Polato F, Gunn A, Bothmer A, Feldhahn N, Fernandez-Capetillo O, Cao L, et al. 53BP1 inhibits homologous recombination in Brca1-deficient cells by blocking resection of DNA breaks. Cell. 2010; 141:243–254. [PubMed: 20362325]

Chapman JR, Sossick AJ, Boulton SJ, Jackson SP. BRCA1-associated exclusion of 53BP1 from DNA damage sites underlies temporal control of DNA repair. Journal of cell science. 2012a; 125:3529–3534. [PubMed: 22553214]

Chapman JR, Tayloy GRM, Boulton SJ. Playing the End Game: DNA Double-Strand Break Repair Pathway Choice. Molecular cell. 2012b; 47:495–510. [PubMed: 22920290]

Choi YE, Pan Y, Park E, Konstantinopoulos P, De S, D'Andrea A, Chowdhury D. MicroRNAs down-regulate homologous recombination in the G1 phase of cycling cells to maintain genomic stability. eLife. 2014; 3:e02445. [PubMed: 24843000]

Ciccia A, Elledge SJ. The DNA damage response: making it safe to play with knives. Molecular cell. 2010; 40:179–204. [PubMed: 20965415]

Clerici M, Mantiero D, Guerini I, Lucchini G, Longhese MP. The Yku70-Yku80 complex contributes to regulate double-strand break processing and checkpoint activation during the cell cycle. EMBO reports. 2008; 9:810–818. [PubMed: 18600234]

Deriano L, Roth DB. Modernizing the Nonhomologous End-Joining Repertoire: Alternative and Classical NHEJ Share the Stage. Annu Rev Genet. 2013

Dimitrov SD, Lu D, Naetar N, Hu Y, Pathania S, Kanellopoulou C, Livingston DM. Physiological modulation of endogenous BRCA1 p220 abundance suppresses DNA damage during the cell cycle. Genes & development. 2013; 27:2274–2291. [PubMed: 24142877]

Escribano-Diaz C, Orthwein A, Fradet-Turcotte A, Xing M, Young JT, Tkac J, Cook MA, Rosebrock AP, Munro M, Canny MD, et al. A Cell Cycle-Dependent Regulatory Circuit Composed of 53BP1-RIF1 and BRCA1-CtIP Controls DNA Repair Pathway Choice. Molecular cell. 2013

Fattah F, Lee EH, Weisensel N, Wang Y, Lichter N, Hendrickson EA. Ku regulates the non-homologous end joining pathway choice of DNA double-strand break repair in human somatic cells. PLoS genetics. 2010; 6:e1000855. [PubMed: 20195511]

Fong PC, Boss DS, Yap TA, Tutt A, Wu P, Mergui-Roelvink M, Mortimer P, Swaisland H, Lau A, O'Connor MJ, et al. Inhibition of poly(ADP-ribose) polymerase in tumors from BRCA mutation carriers. N Engl J Med. 2009; 361:123–134. [PubMed: 19553641]

Foster SS, Balestrini A, Petrini JH. Functional interplay of the Mre11 nuclease and Ku in the response to replication-associated DNA damage. Molecular and cellular biology. 2011; 31:4379–4389. [PubMed: 21876003]

He F, Li L, Kim D, Wen B, Deng X, Gutin PH, Ling CC, Li GC. Adenovirus-mediated expression of a dominant negative Ku70 fragment radiosensitizes human tumor cells under aerobic and hypoxic conditions. Cancer research. 2007; 67:634–642. [PubMed: 17234773]

Helmink BA, Tubbs AT, Dorsett Y, Bednarski JJ, Walker LM, Feng Z, Sharma GG, McKinnon PJ, Zhang J, Bassing CH, et al. H2AX prevents CtIP-mediated DNA end resection and aberrant repair in G1-phase lymphocytes. Nature. 2011; 469:245–249. [PubMed: 21160476]

Konstantinopoulos PA, Ceccaldi R, Shapiro GI, D'Andrea AD. Homologous Recombination Deficiency: Exploiting the Fundamental Vulnerability of Ovarian Cancer. Cancer Discov. 2015

Lal A, Navarro F, Maher CA, Maliszewski LE, Yan N, O'Day E, Chowdhury D, Dykxhoorn DM, Tsai P, Hofmann O, et al. miR-24 Inhibits cell proliferation by targeting E2F2, MYC, and other cell-cycle genes via binding to “seedless” 3′UTR microRNA recognition elements. Molecular cell. 2009; 35:610–625. [PubMed: 19748357]

Lal A, Thomas MP, Altschuler G, Navarro F, O'Day E, Li XL, Concepcion C, Han YC, Thiery J, Rajani DK, et al. Capture of microRNA-bound mRNAs identifies the tumor suppressor miR-34a as a regulator of growth factor signaling. PLoS genetics. 2011; 7:e1002363. [PubMed: 22102825]

Lee DH, Pan Y, Kanner S, Sung P, Borowiec JA, Chowdhury D. A PP4 phosphatase complex dephosphorylates RPA2 to facilitate DNA repair via homologous recombination. Nature structural & molecular biology. 2010; 17:365–372.

Liu G, Yang D, Rupaimoole R, Pecot CV, Sun Y, Mangala LS, Li X, Ji P, Cogdell D, Hu L, et al. Augmentation of Response to Chemotherapy by microRNA-506 Through Regulation of RAD51 in Serous Ovarian Cancers. J Natl Cancer Inst. 2015; 107

Moskwa P, Buffa FM, Pan Y, Panchakshari R, Gottipati P, Muschel RJ, Beech J, Kulshrestha R, Abdelmohsen K, Weinstock DM, et al. miR-182-mediated downregulation of BRCA1 impacts DNA repair and sensitivity to PARP inhibitors. Molecular cell. 2011; 41:210–220. [PubMed: 21195000]

Norquist B, Wurz KA, Pennil CC, Garcia R, Gross J, Sakai W, Karlan BY, Taniguchi T, Swisher EM. Secondary somatic mutations restoring BRCA1/2 predict chemotherapy resistance in hereditary ovarian carcinomas. J Clin Oncol. 2011; 29:3008–3015. [PubMed: 21709188]

Orom UA, Lund AH. Isolation of microRNA targets using biotinylated synthetic microRNAs. Methods. 2007; 43:162–165. [PubMed: 17889804]

Sakaue-Sawano A, Kurokawa H, Morimura T, Hanyu A, Hama H, Osawa H, Kashiwagi S, Fukami K, Miyata T, Miyoshi H, et al. Visualizing spatiotemporal dynamics of multicellular cell-cycle progression. Cell. 2008; 132:487–498. [PubMed: 18267078]

Shih KK, Qin LX, Tanner EJ, Zhou Q, Bisogna M, Dao F, Olvera N, Viale A, Barakat RR, Levine DA. A microRNA survival signature (MiSS) for advanced ovarian cancer. Gynecologic oncology. 2011; 121:444–450. [PubMed: 21354599]

TCGA. Integrated genomic analyses of ovarian carcinoma. Nature. 2011; 474:609–615. [PubMed: 21720365]

Xu G, Chapman JR, Brandsma I, Yuan J, Mistrik M, Bouwman P, Bartkova J, Gogola E, Warmerdam D, Barazas M, et al. REV7 counteracts DNA double-strand break resection and affects PARP inhibition. Nature. 2015

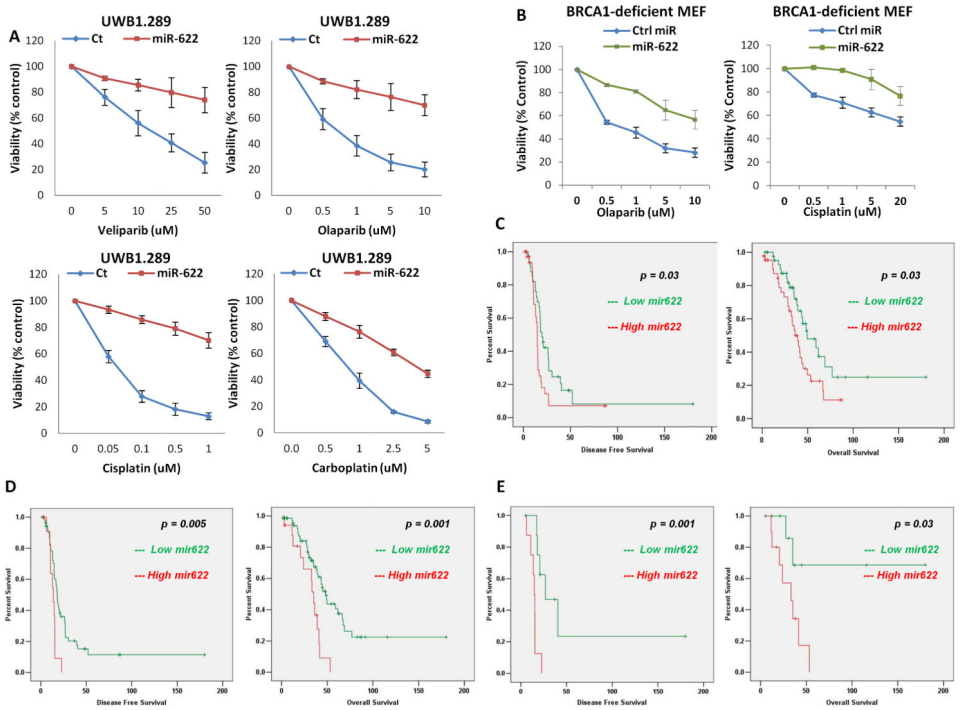

Figure 1. miRNA mediated resistance to PARP inhibitors and platinum in BRCA1 mutant cells

(A, B) Viability assays to examine the impact of miR-622 on drug sensitivity. BRCA1-null UWB1.289 cells (A) or BRCA1-deficient MEF cells (B) were transfected with control mimic or miR-622 mimic and treated with vehicle or indicated drug before measurement of viability by luminescence-based ATP quantification. Curves were generated from 3 independent experiments. **(C)** Association between miR-622 expression levels and DFS and OS in tumors with BRCA1 mutation and BRCA1 promoter hypermethylation in the TCGA dataset based on 50% cut-off. Tumors with BRCA1 mutations and BRCA1 promoter hypermethylation with above median expression levels of miR-622 were associated with worse DFS (left panel, log rank p = 0.03) and OS (right panel, log rank p = 0.03). **(D)** Association between miR-622 expression levels and DFS and OS in tumors with BRCA1 mutation and BRCA1 promoter hypermethylation in the TCGA dataset based on 20% cut-off. Tumors with BRCA1 mutations and BRCA1 promoter hypermethylation whose expression levels for miR-622 were in the highest quintile were associated with worse DFS (left panel, log rank p = 0.005) and OS (right panel, log rank p = 0.001). **(E)** DFS and OS in the 10 tumors with the highest mir-622 expression versus the 10 tumors with the lowest miR-622 expression in the TCGA dataset (tumors with BRCA1 mutation and BRCA1 promoter hypermethylation). The 10 tumors with the lowest mir-622 expression were associated with worse DFS (left panel, log rank p = 0.001) and OS (right panel, log rank p = 0.03) compared to the 10 tumors with the highest mir-622 expression.

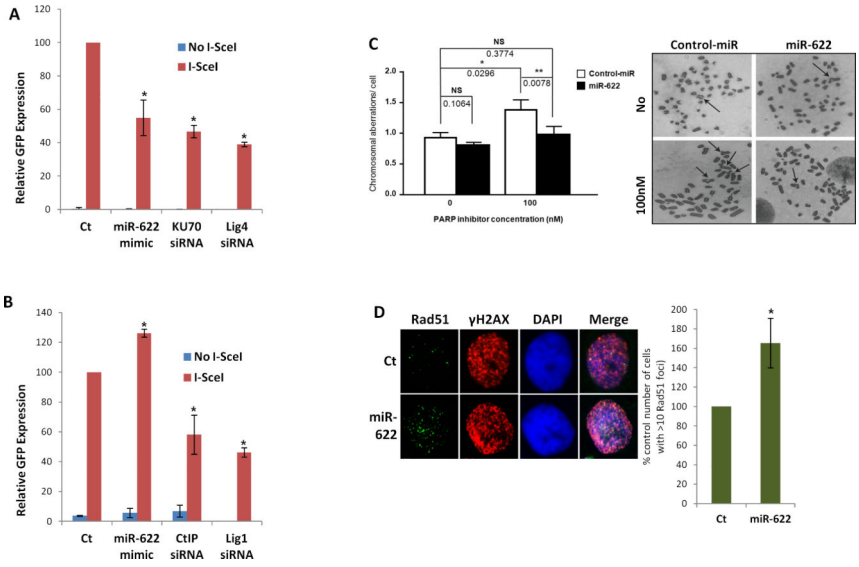

Figure 2. Impact of miR-622 on genome stability and NHEJ repair pathways

(A, B) Measurement of C-NHEJ (A) or A-NHEJ (B) mediated repair of I-SceI induced site specific DSBs. Cells carrying a single copy of the recombination substrate with two tandem I-SceI sites were transfected with control mimic, miR-622 mimic, Ku70 siRNA or Ligase4 siRNA before transfection with I-SceI or control vector. In 48 hrs, GFP positive cells were analyzed by flow cytometry. **(C)** Analysis of genomic instability in metaphases. BRCA1−/− MEF cells were transfected with control miRNA mimic or miR-622, treated with 100nM PARP inhibitor, and measured for abnormal chromosomes in metaphase. (n≥50 metaphases). **(D)** Analysis of HR-mediated repair by RAD51 focus formation. UWB1.289 cells were transfected with control miRNA mimic or miR-622, stained for RAD51 (green), γH2AX (red) and 4′,6-diamidino-2-phenylindole (DAPI) (blue) 6 hrs after exposure to 10Gy IR. The images were captured by fluorescence microscopy and RAD51 focus-positive cells (with > 20 foci) were quantified by comparing 100 cells

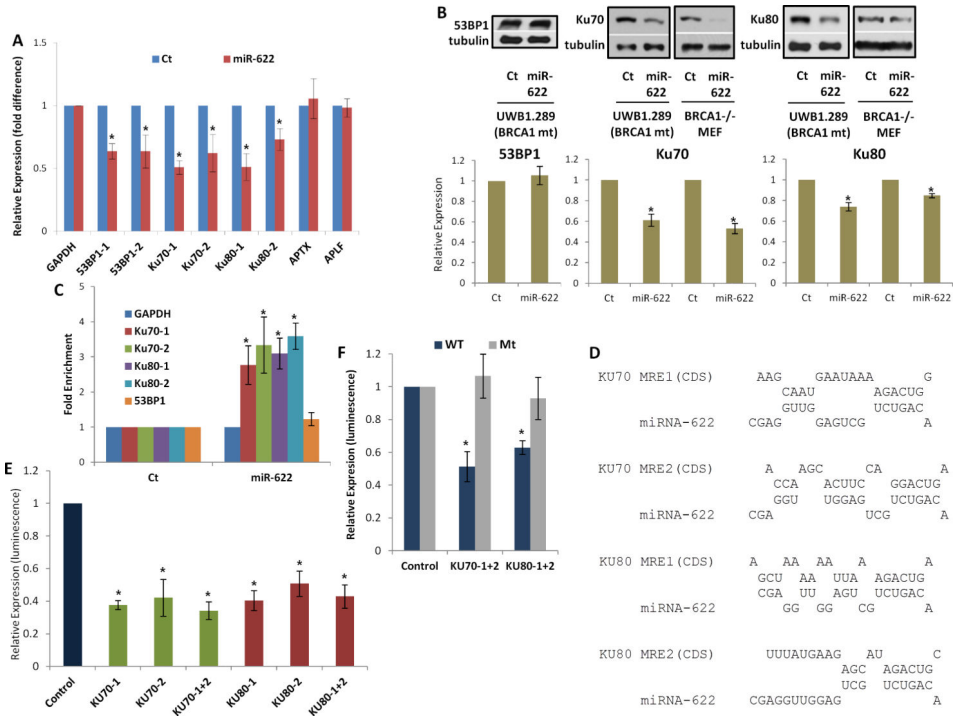

Figure 3. Identifying and validating targets of miR-622

(A-B) Expression of DDR genes is impacted by miR-622. UWB1.289 cells were transfected with control mimic or miR-622 mimic and mRNA levels of predicted DDR genes were analyzed by qRT-PCR using gene-specific primers and normalized to GAPDH (A). Cell lysates were then analyzed by immunoblot for factors which had statistically significant reduction in mRNA in cells transfected with miR-622 (B). Images were quantified by ImageJ software and the mean ± SD of 3 independent experiments is graphically shown. **(C)** Interaction of target transcripts with miR-622. UWB1.289 cells were transfected with biotinylated-control mimic or biotinylated miR-622 mimic. The immunoprecipitated RNA was analyzed by qRT-PCR using gene-specific primers and normalized to GAPDH. **(D)** Predicted MREs were obtained from PITA algorithm (http://genie.weizmann.ac.il/pubs/mir07/mir07_prediction.html) and their mutants were generated by mutating nucleotides providing complementarity to corresponding miRNAs. CDS (coding sequence) means the region in the gene where MRE is located. **(I)** Luciferase reporter assay to assess direct interaction of miR-622 with target genes. Individual or combinations of predicted miRNA recognition sites (MREs) for each putative target transcript of miR-622 were cloned into the luciferase reporter vector and transfected in UWB1.289 cells along with miR mimics. *Renilla* luciferase activity of the reporter was measured 48 h after transfection by normalization to an internal *firefly* luciferase control. **(J)** Luciferase reporter assay for wild-type or mutant MREs for miRNA-622 targets was performed in the same way as described in Figure 2I. (A-H) Mean ± SD of 3 independent experiments is shown and statistical significance is indicated by * ($p<0.05$).

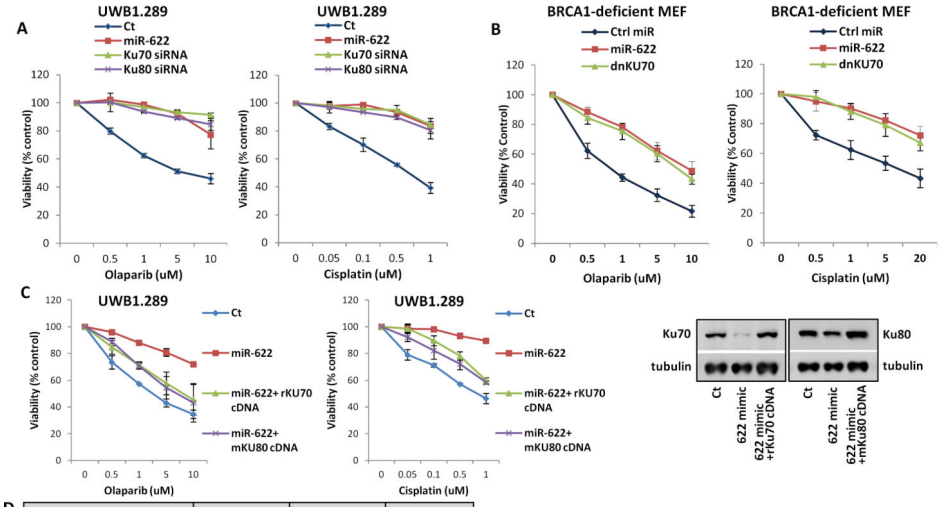

D

Relationship	Pearson Correlation	Covariance	P value (two sided)
miR622 expression levels / Ku80 RNA expression levels	-0.249	-0.354	0.019
miR622 expression levels / Ku80 protein levels (RPPA)	-0.273	-0.322	0.029

E

Relationship	Pearson Correlation	Covariance	P value (two sided)
miR622 expression levels / Ku80 RNA expression levels	-0.255	-0.24	0.05

Figure 4. Correlating the impact of miR-622 and its target, the Ku complex

(A, B) Viability assays to examine the impact of miR-622 on targets. Control mimic, miR-622 mimic, Ku70 siRNA, Ku80 siRNA or dominant negative Ku70 were introduced to UWB1.289 cells (A) or BRCA1-deficient MEF cells (B). Transfected cells were treated with vehicle or indicated drug before viability measurement as explained in Figure 1. **(C)** Impact of miR target rescue. UWB1.289 cells were transfected with control mimic or miR-622 mimic with or without rat Ku70 cDNA or mouse Ku80 cDNA and treated with vehicle or indicated drug before viability measurement as explained in Figure 1. Expression of introduced genes was examined by immunoblot. **(D)** Correlation between miR-622 expression levels and Ku80 RNA expression levels and Ku80 protein levels in the TCGA dataset. miR-622 expression levels were statistically significantly inversely correlated with Ku80 RNA expression levels ($p = 0.019$) and Ku80 protein levels ($p=0.029$). **(E)** Correlation between miR-622 expression levels and Ku80 RNA expression levels in a different ovarian cancer miRNA dataset. miR-622 expression levels were statistically significantly inversely correlated with Ku80 RNA expression levels ($p = 0.05$) in a different ovarian cancer dataset.

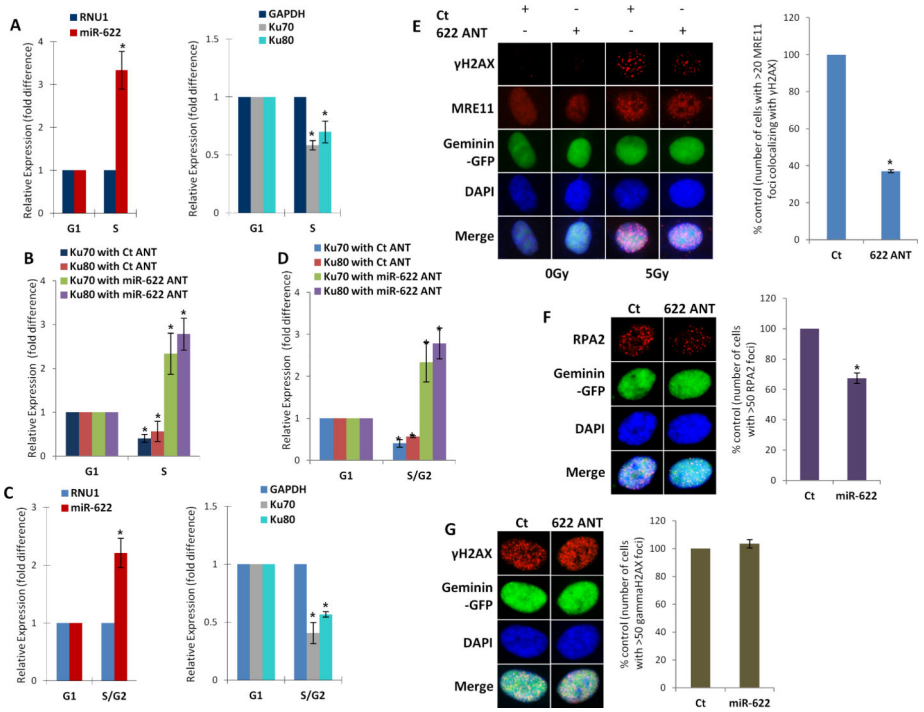

Figure 5. Impact of miR-622 on DSB repair during cell cycle

(A-D) Expression of miR and target transcripts in synchronized cells. (A) UWB1.289 cells were synchronized with mimosine and the relative amount of miR-622 or target mRNA for G1- or S-phase was determined by qRT-PCR (normalized to RNU1). (B) UWB1.289 cells were transfected with control ANT or miR-622 ANT and subsequently synchronized with mimosine. Expression of target mRNA was assessed by qRT-PCR in the G1 and S-phase (normalized to GAPDH). (C) RPE1 Fucci cells were sorted according to cell cycle-based fluorophore expression and the relative amount of miR-622 or target mRNA for G1- or S-phase was quantified by qRT-PC. (D) RPE1 Fucci cells were transfected with control ANT or miR-622 ANT and sorted for cell cycle. Expression of target mRNA was assessed by qRT-PCR in the G1 and S-phase. (A-D) Mean ± SD of 3 independent experiments is shown and statistical significance is indicated by * ($p<0.05$). **(E-G)** Impact of miR-622 inhibition on recruitment of DSB proteins. RPE1 Fucci cells were transfected with control ANT or miR-622 ANT and irradiated with 5 Gy (for γH2AX and Mre11, 3 hours after IR) or 10Gy (for RPA2, 4 hours after IR) IR. Cells were stained for Mre11 (red) (E), RPA2 (red) (F) or γH2AX (red) (G) and 4′,6-diamidino-2-phenylindole (blue). The images were captured by fluorescence microscopy and Mre11, RPA2 or γH2AX focus-positive cells (with > 20 foci or >50 foci) at S phase (green) were quantified by comparing 100 cells.